Critical Process Requirements for Membrane Desalination of Agricultural Drainage in the San Joaquin Valley

DRAFT

Final Project Report
Project Period: 9/01/04-8/31/07
Interagency Agreement 4600003343

submitted to the

Agricultural Drainage Program
California Department of Water Resources
3374 Sheilds Avenue
Fresno, California 93726

by

Yoram Cohen[1] and Brian McCool
Water Technology Research Center
and Chemical and Biomolecular Engineering Department
University of California, Los Angeles
Los Angeles, California 90095

Other UCLA Project Participants:
Julius Glater, Anditya Rahardianto and Eric Lyster

November 15, 2007

[1] Author to whom correspondence should be addressed. E-mail: yoram@ucla.edu; Phone: (310) 825-8766; Fax: (310) 477-3868.

TABLE OF CONTENTS

TABLE OF CONTENTS III

ABSTRACT IV

1. INTRODUCTION 5

2. BACKGROUND 6

2.1 REVERSE OSMOSIS 6

FIGURE 2-2. CUT-AWAY OF SPIRAL WOUND RO MEMBRANE MODULE [9]. 7

2.2 CONCENTRATION POLARIZATION 7
2.3 WATER QUALITY MEASUREMENTS 9
2.4 RO DESALTING RECOVERY LIMITS 10

3. ANALYSIS 11

3.1 FIELD WATER SITE SELECTION FOR SAMPLING AND ANALYSIS 11
3.2 RECOVERY LIMITS 12
3.3 DIAGNOSTIC FLUX DECLINE EXPERIMENTS 14
3.4 EQUIVALENT RECOVERY CALCULATIONS FOR DIAGNOSTIC EXPERIMENTS 14

4. EXPERIMENTAL 15

4.1 MATERIALS & REAGENTS 15
4.1.1 Laboratory Work *15*
4.1.2 Field Water Samples *15*
4.2 APPARATUS 15
4.3 DIAGNOSTIC PROCEDURE 17
4.3.1 Pretreatment *17*
4.3.2 Membrane Preparation *18*
4.3.3 Membrane Conditioning *18*
4.3.4 Flux Decline Run *18*
4.3.5 System Cleaning *19*
4.4 BIOFOULING POTENTIAL EXPERIMENTS 19
4.4.1 Protein Assay *19*
4.4.2 Cultures *19*

5. RESULTS AND DISCUSSION 20

5.1 VARIABILITY OF AGRICULTURAL BRACKISH WATER QUALITY (1999–2003; 2006–2007) 20
5.1.1 Field Water Site Selection for Sampling and Analysis *20*
5.1.2 Recent DWR Periodic Monitoring Data (1999–2003) *27*
5.1.3 Field Water Sample Data (2006–2007) *46*
5.2 DIAGNOSTIC FLUX DECLINE EXPERIMENTS 55
5.3 BIOFOULING POTENTIAL AND PARTICULATES 68

6. CONCLUSIONS AND RECOMMENDATIONS 69

6.1 CONCLUSIONS 69
6.2 RECOMMENDATIONS 70

7. REFERENCES 71

ABSTRACT

The use of reverse osmosis (RO) desalting for treating brackish agricultural drainage (AD) water in the San Joaquin Valley (SJV) was evaluated as a potential method for reducing the salinity of brackish drainage discharge and thus providing for reclamation and reuse of this water source. A systematic approach was developed using thermodynamic solubility analysis and diagnostic RO scaling experiments in a plate-and-frame RO system with a commercial low-pressure RO membrane to determine product water recovery limits with respect to the source water chemistry. Analysis of available SJV water quality monitoring data revealed substantial seasonal and spatial water quality variations. Water sources in a number of locations were nearly saturated with respect to gypsum. Theoretical analysis of RO recovery limits due to mineral scaling of sparingly soluble salts (e.g. calcite, gypsum, silica) suggested that RO recovery would be limited to about 54% - 68% (assuming the use of standard scale mitigation strategies such as pH adjustment and antiscalant dosing). The analysis also revealed that, If limitations due to mineral scaling could be alleviated, recovery limits imposed by osmotic pressure would range from about 70% to 94% for 600 psi RO vessels and from about 81% to 96% for 1000 psi RO vessels. The above analysis was supplemented by comparative diagnostic flux decline experiments using field water samples from five different locations in the SJV. These locations were selected to be representative of the range of water compositions throughout the San Joaquin Valley. Membrane RO desalination tests were carried using a plate-and-frame module geometry. These tests were conducted such that the average initial gypsum saturation indices at the membrane surface that ranged from 0.28 to 2.1. Equivalent recoveries (based on estimation of concentration polarization and observed salt rejection), for the non-scaling diagnostic tests, were in reasonable agreement with recovery limits estimated through thermodynamic solubility analysis. RO desalination is a feasible technology for desalting SJV drainage water. However, given the spatial and temporal water quality in the San Joaquin Valley, a distributed system of desalination facilities would be the most appropriate approach for field-scale deployment of RO desalination. Such systems would require effective feed quality monitoring along with monitoring of membrane scaling/fouling along with effective self-initiated scaling/fouling mitigation technologies. Pilot field studies, utilizing advanced concepts in scaling and fouling mitigation, would be necessary in order to evaluate self-adaptive RO operation paradigm and assess the ability to operate at reasonably recoveries and handle temporally variable feed water quality.

1. Introduction

Rising salinity of agricultural drainage water and groundwater in the San Joaquin Valley (SJV) is a problem of growing concern [1-3]. Decades of irrigation and evapotranspiration combined with a shallow water table and naturally saline soil have led to the rise in groundwater salinity. When the salinity tolerances of the crops are exceeded, the land is often retired, progressively diminishing the productivity of the SJV [1-4]. In order to reduce further buildup of salt in the soil, beginning in the late 1940s, surface and subsurface drains were installed throughout the valley to collect the brackish agricultural drainage (AD) water to be sent to evaporation ponds or other discharge sites and by 1965 more than 1000 miles of drains had been built [2]. Construction of a master drain discharging to the Sacramento-San Joaquin River Delta was stopped in 1983 after the drainage from a preliminary portion of the drain that had been discharging into the Kesterson Reservoir was discovered to contain high levels of [2, 3, 5]. The northern portion of the SJV has historically provided natural drainage in the northern area of the SJV (see Figs 5-1 – 5-5). However, where natural drainage does not typically exist (e.g. Tulare Lakebed and Kern Lakebed in the southern area), AD runoff is sent to evaporation ponds and other discharge sites, but concerns over bioaccumulation of selenium remains a major concern [2, 3, 5].

A possible solution to the high salinity AD water problem is to employ reverse osmosis (RO) desalination to reduce the salinity of AD water, and thus produce reusable fresh water for irrigation, while reducing the volume of concentrate (brine) to be disposed. As the recovery of the RO system is increased, the volume of fresh water produced is increased and the volume of brine discharge is decreased. However, the achievable RO recovery may be limited by a number of factors including: mineral salt scaling, osmotic pressure, biofouling, and cost.

In order to evaluate the technical feasibility of RO desalting of SJV brackish water, one must first characterize the drainage waters with respect to composition, mineral salt saturation levels, and geographic and temporal variability. One of the complicating factors is the significant variation in drainage water quality found throughout the valley [2]. Then, based on RO operating limitations (e.g. scaling), the achievable recoveries at different locations can be estimated. After the drainage waters have been characterized, representative field drainage water samples can be obtained for laboratory scale diagnostic testing. This work outlines a general approach for assessing recovery limitations and provides specific examples for selected location in the SJV.

2. Background

2.1 Reverse Osmosis

The flux that is achieved by reverse osmosis membrane desalination can be described by the following expression:

$$J_W = L_P(\Delta p - \sigma \cdot \Delta\pi) \quad (2\text{-}1)$$

where J_W is the water flux through the membrane, L_P is the membrane water permeability, $\Delta p = p_f - p_m$, where p_f and p_m are the feed and permeate pressures, respectively, σ is the salt reflection coefficient, and $\Delta\pi$ is the osmotic pressure difference between the feed and permeate sides. RO desalination is typically carried out in a cross-flow scheme in which the pressurized saline feed water enters the membrane channel and flows tangentially across the membrane surface (Figure 2-1). The permeate is collected on the permeate side and the feed stream exits the membrane channel as a concentrate stream. Commercial RO membrane modules are typically arranged in a spiral-wound configuration (Figure 2-2) in order to provide for a large membrane surface area to volume ratio [6-8]. Brackish water desalination is often carried out in a 2:1 RO configuration as illustrated in Figure 2-3. Prior to desalting the feed has to be pretreated to remove particulate matter, as well as to adjust the feed pH and possible add antiscalants to reduce fouling and scaling propensity of the RO membranes.

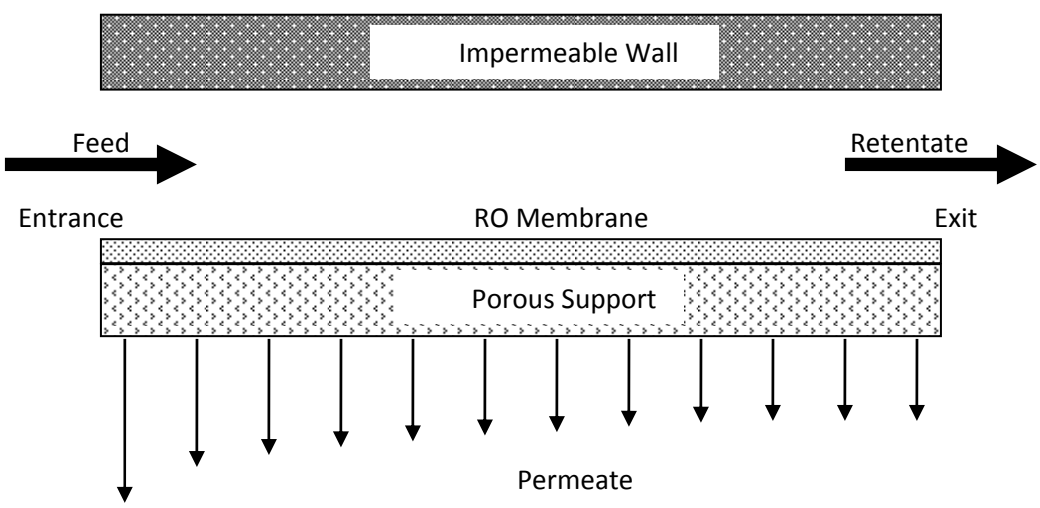

Figure 2-1. Schematic of cross-flow plate-and-frame RO system.

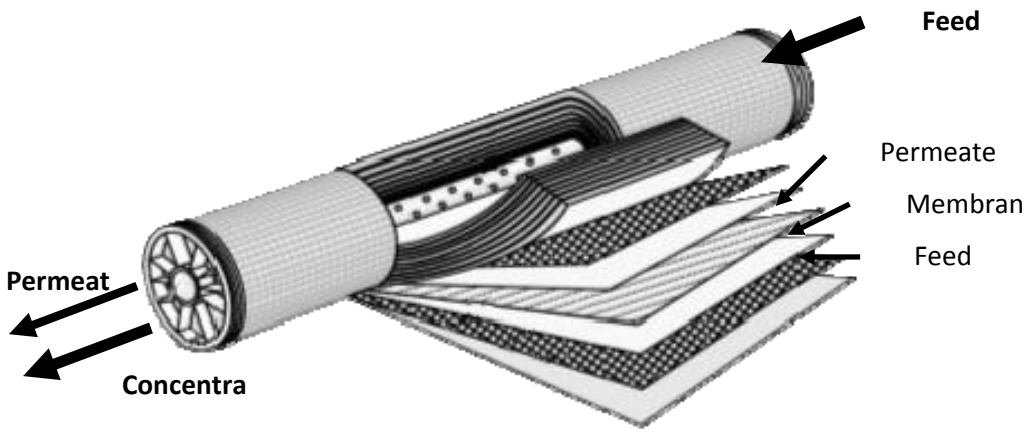

Figure 2-2. Cut-away of spiral wound RO membrane module [9].

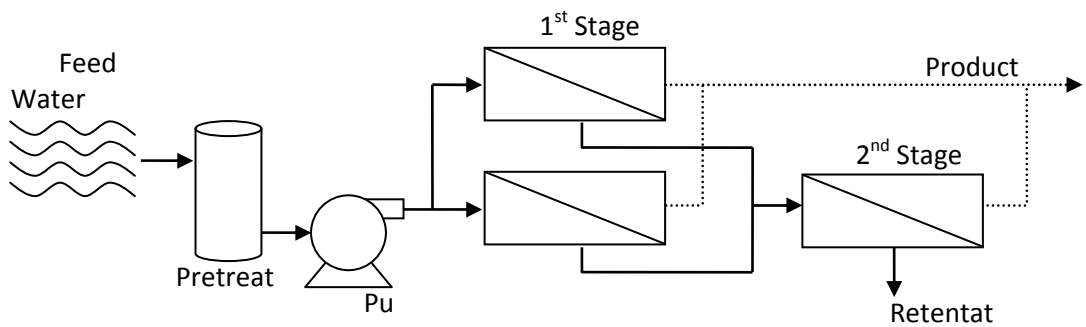

Figure 2-3. Schematic of typical two stage (2:1) RO desalination.

2.2 Concentration Polarization

As water permeates across an RO membrane, rejected salt ions accumulate near the membrane surface resulting in the formation of a concentration boundary layer. The concentration of the salts at the membrane surface can be approximate using the simple film model:

$$CP = \frac{C_m - C_p}{C_b - C_p} = \exp\left(\frac{J}{k}\right) \qquad (2\text{-}3)$$

where C_m, C_b, and C_p are the concentrations of the solute at the membrane surface, in the bulk, and in the permeate, respectively, J is the permeate flux and k is the solute feed-side mass transfer coefficient. CP increases along the RO membrane channel, reaching its highest value at the channel exit [10]. As the concentration and osmotic pressure at the membrane surface gradually increase, from the entrance to the exit, the effective net driving force for permeation decreases, thus, the permeate flux decreases towards the exit region as illustrated in Figure 2-4.

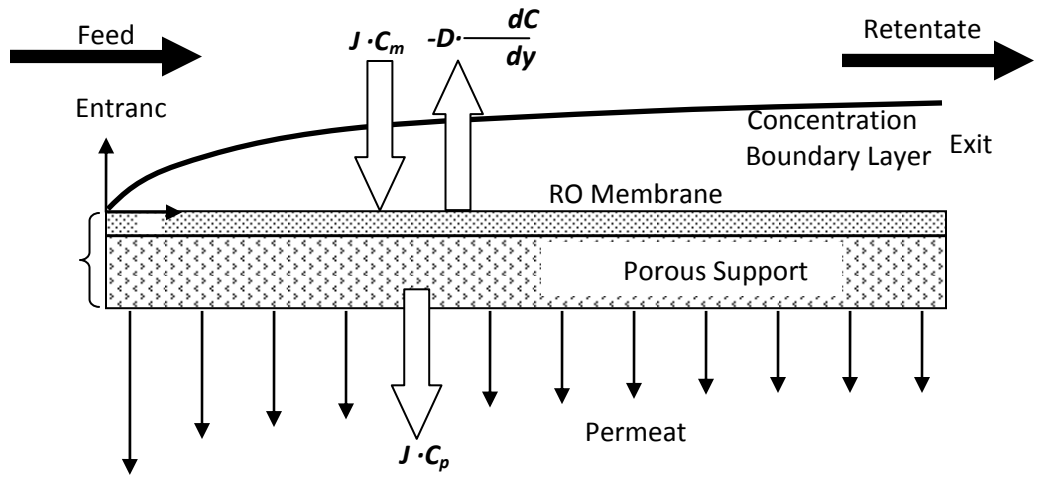

Figure 2-4. Schematic of cross-flow plate-and-frame RO system showing the formation of a concentration boundary layer. Block arrow represent solute fluxes. *J* is the water flux, C_m and C_p are the respective concentrations at the membrane surface and in the permeate, *D* is the solute diffusivity, and *dC/dy* is the solute concentration gradient in the y-direction.

The observed salt rejection for an RO membrane, R_S, is defined as:

$$R_S = 1 - \frac{C_P}{C_F} \tag{2-4}$$

where C_P is the concentration of the permeate and C_F are the concentrations of the feed and permeate streams, respectively. Permeate productivity is measured in terms of the fractional recovery, R_W, defined as:

$$R_W = \frac{Q_P}{Q_F} = 1 - \frac{Q_R}{Q_F} \tag{2-5}$$

where Q_P, Q_F, and Q_R are the permeate, feed, and retentate volumetric flow rates, respectively. As an RO process is pushed to higher recoveries, the retentate stream becomes more concentrated and the degree of concentration is typically expressed in terms of a concentration factor, *CF*, defined as:

$$CF = \frac{C_C}{C_F} = \frac{1 - R_W(1 - R_S)}{1 - R_W} \tag{2-6}$$

where C_C and C_F are the respective concentrate and feed concentrations. Equation (2-6) can be rearranged such that the recovery can be found as a function of the concentration factor and the salt rejection:

$$R_W = \frac{CF - 1}{CF - 1 + R_S} \tag{2-7}$$

where R_W is the fractional product water recovery, CF is the concentration factor, and R_S is the observed fractional salt rejection.

2.3 Water quality measurements

Measures of water quality that are particularly relevant to membrane RO desalting include total dissolved solids (TDS), electrical conductivity, total alkalinity, silt density index (SDI), turbidity and biofouling potential. TDS is a measure of all ionic species present and is typically reported in milligrams per liter (mg/L). The TDS is often reported based on an equivalent salt concentration for a measured electrical conductivity of the solution. Natural waters can typically be classified into four different categories by their salinity: fresh water (<1000 mg/L), low salinity brackish water (1000 – 3000 mg/L), high salinity brackish water (3000 — 35,000 mg/L), and seawater (35,000 mg/L).

Electrical Conductivity (EC) measures the ability of a solution to conduct electricity and is an indirect measure of the salinity of the solution. By comparing the EC of the feed in an RO system to that of the permeate, the EC-based salt rejection can be calculated:

$$R_S = 1 - \frac{EC_P}{EC_F} \tag{2-8}$$

where EC_P and EC_F denote the permeate and feed conductivities, respectively.

Total alkalinity is a measure of the water's ability to neutralize acid and is usually measured in mg/L as calcium carbonate ($CaCO_3$). Carbonate (CO_3^{2-}) and bicarbonate (HCO_3^-) ions are in equilibrium with carbonic acid (H_2CO_3) and dissolved carbon dioxide (CO_2) according to the following reactions:

$H_2CO_3 \leftrightarrow HCO_3^- + H^+$, $pK_{a1} = 3.60$ (25 ºC)

$HCO_3^- \leftrightarrow CO_3^{2-} + H^+$, $pK_{a2} = 10.25$ (25 ºC)

$CO_2 + H_2O \leftrightarrow HCO_3^- + H^+$, $pK_a = 6.36$ (25ºC)

The relative amounts of the above species depend primarily on pH, temperature, and carbon dioxide partial pressure. The bicarbonate ion typically has the greatest contribution to total alkalinity in natural waters, although other species can also contribute including phosphate, nitrate, silicates, borate, ammonia, sulfide, hydroxide, and conjugate bases of organic acids. The bicarbonate concentration can be estimated where analytical data are unavailable by assuming that all other contributors to total alkalinity are negligible. Brackish water in the SJV typically has a total alkalinity in the range of 100 to 700 mg/L as $CaCO_3$ [11].

The Silt Density Index (SDI) is a measure of the particulates present in natural waters that are rejected by a 0.45 µm filter. The SDI is calculated by comparing the length of time required to collect a

designated volume of permeate initially and after a certain length of time in dead-end filtration. The SDI is defined by the ASTM Standard Test Method D4189-07 [12]:

$$SDI_T = \frac{\%P_{30}}{T} = \frac{\left[1 - \frac{t_i}{t_f}\right]100}{T} \qquad (2\text{-}9)$$

where $\%P_{30}$ is the plugging factor at a trans-membrane pressure of 30 psi, T is the time between sample collections (min), and t_i and t_f are the times (min) to collect initial and final permeate samples, respectively. Prefiltration is generally recommended for water having an SDI_{15} greater than 5.0 to prevent particulates from plugging the RO membrane [13].

2.4 RO Desalting Recovery Limits

Mineral salt scaling and osmotic pressure are the two major factors that can limit product water recovery in RO desalination of agricultural drainage water [14-20]. Mineral salt scaling is the process by which sparingly soluble salts crystallize on RO membranes obstructing permeate flow through the membrane. Crystallization can occur in the bulk solution (homogeneous crystallization) and then deposit onto the membrane where crystals may continue to grow. Crystallization can also occur directly on the membrane surface itself (heterogeneous crystallization). Crystallization may occur when the saturation of any particular sparingly soluble salt is exceeded. The degree to which the saturation is exceeded for a given salt is measured by the saturation index which is the ratio of the ion activity product (*IAP*) to the solubility product (K_{SP}): $SI = \frac{IAP}{K_{SP}}$

(2-10)

For example, the SIs for gypsum, SI_G, calcite, SI_C, and barite, SI_B, are defined as:

$$SI_G = \frac{(Ca^{2+})(SO_4^{2-})}{K_{SP,G}}, \quad SI_C = \frac{(Ca^{2+})(CO_3^{2-})}{K_{SP,C}}, \quad SI_B = \frac{(Ba^{2+})(SO_4^{2+})}{K_{SP,B}} \qquad (2\text{-}11)$$

where (Ca^{2+}), (Ba^{2+}), (SO_4^{2-}), and (CO_3^{2-}) are the calcium, barium, sulfate, and carbonate ion activities, respectively, and $K_{SP,G}$, $K_{SP,C}$, and $K_{SP,B}$ are the gypsum, calcite, and barite solubility products, respectfully. A saturation index greater than unity implies a tendency for a salt to crystallize. However, the kinetics of crystallization must also be considered when evaluating scale formation.

The Langelier Saturation Index (LSI) is commonly used for predicting calcite scale solubility and is defined as the difference between the measured pH of the solution and the pH at which the solution would be saturation with respect to calcite:

$$LSI = pH - pH_s \quad (2\text{-}12)$$

where pH and pH_s are the measured pH and the saturation pH, respectively. Solutions with a negative LSI are undersaturated and will dissolve calcite, solutions with a positive LSI are oversaturated and have the potential to precipitate calcite, and solutions with LSI near zero are close to calcite saturation and small changes in temperature or pH may lead to under- or over-saturated solutions [21].

The osmotic pressure of the retentate limits the recovery by reducing the effective pressure driving force available for permeate production (Eq 2-3). The retentate concentration increases with increasing recovery which in turn increases the osmotic pressure; eventually the permeate flux will vanish when the osmotic pressure reaches the applied pressure. In general, recovery is ultimately limited by the available pumping power and/or maximum operating pressure of the membrane pressure vessels.

Biofouling due to adherence and growth of bacteria or other microorganisms onto the membrane surface reduce water permeation through the membrane and reduce the membrane useful lifetime. Often the microbes will form a biofilm which can be difficult and costly to remove. Pretreatment of the feed is required to retard biofouling for source water rich in microbes [22, 23].

3. ANALYSIS

3.1 Field Water Site Selection for Sampling and Analysis

The first step in studying the feasibility of desalination of AD water in the San Joaquin Valley consisted of performing thermodynamic solubility analyses based on compositional data of water samples taken from different locations in the valley. The analyses were divided into two parts based on two data sets: recent California Department of Water Resources (DWR) periodic monitoring data, collected from 1999 to 2003 for [11] and field water sample data collected by DWR during 2006 – 2007 specifically for the UCLA study. The first data set was analyzed to select field water sampling locations, to determine recovery limits, and to assess water quality variability. While the data from the DWR drainage monitoring reports contained sufficient information for selecting sampling locations, determining recovery limits, and measuring water quality variability, there were some limitations to the

data set, including the lack of information on the concentrations of bicarbonate, carbonate, hydroxide, and silica. However, the DWR drainage monitoring report data set did contain total alkalinity monitoring data which can be used as an indirect measure of bicarbonate concentration assuming that all other alkalinity contributors (e.g. carbonate) are negligible. Solubility analysis was performed with the OLI Systems Lab Analyzer 3.0 thermodynamic simulator based on water composition data provided by DWR. This simulator predicts thermodynamic properties of mixed electrolyte aqueous systems, including dissolved mineral salts' saturation indices which provide a measure of scaling tendencies.

In order to perform a meaningful evaluation of the feasibility of RO Desalination in the San Joaquin Valley (SJV), it is essential to have a thorough water quality analysis of up to date water samples from the SJV. Complete water quality analysis is essential in order to estimate the effects of all constituents, including those which can have a large effect even at trace concentrations. Bench scale experiments must also be performed with real water samples because analyses performed with model solutions may not exhibit the range of problems that may occur in real waters (e.g. interactions caused by organics, particulates, and unknown constituents).

The first data set used in the present study was developed by DWR based on sampling of 55 different agricultural drainage water sites spread throughout the SJV listed in Table 5-1. A representative selection of specific sampling locations were chosen for further study based on the following selection criteria: 1) The sites should be spread throughout the valley to help form a complete picture of the range of water chemistries present; 2) The sites should provide data covering a reasonable range of TDS, gypsum saturation index, and ratio of total carbonate to sulfate; and 3) The sites must be active and readily accessible for sampling for use in the second phase of the study.

3.2 Recovery Limits

Recovery limits were calculated with respect to mineral salt scaling and osmotic pressure. The scaling propensity of mineral salts found in AD water were determined from thermodynamic solubility analysis. The OLI Systems Stream Analyzer 2.0 was used to calculate saturation indices and osmotic pressure for multi-electrolyte solutions. Mineral salts prone to crystallization have SIs greater than unity. Calcite solubility increases substantially as the pH of the solution is lowered. Therefore, in RO processes, scaling by calcite can be mitigated by pH adjustment. Gypsum and barite saturation indices, however, are relatively pH insensitive and scaling by these salts cannot be managed by pH adjustment. Gypsum and barite precipitation can be inhibited when antiscalants are added to the RO feed. Antiscalants are generally proprietary chemicals consisting of mixtures of water soluble polymers with multiple charged groups. Scaling can generally be controlled for gypsum up to SI = 2.3 and for barite up to SI = 90 by using

appropriate antiscalants [24]. Control of silica scaling is more difficult because of its speciation, formation of colloids, and potential polymerization in solution. Silica scaling can generally be controlled when the feed or retentate concentrations are in the range of 160 – 240 ppm [25].

The RO recovery limits based on scaling were determined by calculating the recoveries at which the concentrations of sparingly soluble salts (e.g. calcite, gypsum, barite) reached their maximum controllable (i.e. non-scaling) saturation levels. Because of concentration polarization (CP), concentrations at the membrane surface can be significantly greater than those in the bulk. The SIs at the membrane surface were determined by multiplying the bulk ion concentrations by the average CP along the membrane and then calculating SIs at these new, higher, concentrations. This approach accounts for the changes in both ion concentrations and activities and assumes the CP is the same for all ions as shown in Equation 3-1,

$$SI_{m,i} = f\left(CP_{avg} \cdot \sum C_{b,j}\right) = \frac{IAP_{m,i}}{K_{SP}} \tag{3-1}$$

where $SI_{m,i}$ is the saturation index at the membrane surface for the sparingly soluble salt, i, CP_{avg} is the average concentration polarization along the membrane surface, $C_{b,j}$ is the bulk concentration of ion, j, and $IAP_{m,i}$ is the ion activity product at the membrane surface for sparingly soluble salt, i. CP_{avg} was estimated by the finite element numerical model developed by Lyster and Cohen [26] which considers the fully coupled governing equations for fluid dynamics and mass transfer.

Calcite scaling can be inhibited up to an SI of one, while gypsum and barite scaling can be controlled with antiscalants up to SIs of 2.3 and 90, respectively, with antiscalant use. The SIs for calcite, gypsum, barite, and silica were calculated for a range of concentration factors (CF: Eq. 2-6) for to determine recovery limits. The calculated SIs were then plotted versus recovery by converting the CFs to equivalent recoveries using Equation 2-7,

$$R_W = \frac{CF - 1}{CF - 1 + R_S} \tag{2-7}$$

where R_W is the fractional product water recovery, CF is the concentration factor, and R_S is the nominal fractional salt rejection (assumed to be 0.98 for the LFC-1 membrane used in the present study [27]). These calculations were performed first at a constant pH of 7.5 and then 6.0; the pH levels were maintained via addition of sodium hydroxide or hydrochloric acid, both of which were accounted for in thermodynamic solubility calculations. The field water samples had natural pHs ranging from 7.1 to 8.1. Therefore, analysis at a pH of 7.5 was deemed reasonable for assessing the impact on RO desalting, while a pH of 6.0 was taken as typical of the low pH limit to control calcite scaling.

Based on analytical data provided by the California DWR [2] and the present analysis, the mineral salts prone to scaling membranes in the San Joaquin Valley are calcite, gypsum, silica, and barite. However, given that barium is found at very low concentrations (less than 0.25 – 1.0 mg/L) and because barite tends to remain in solution even at very high supersaturation levels (up to SI = 4.9 without antiscalants and up to SI = 90 with antiscalants [24, 28]), barite is not likely to scale the membrane during the relatively short residence times encountered in RO desalting. It is noted that the reported barium concentrations are at detection limits and thus the actual barium concentrations are likely well below the detection limits for this study.

Two possible osmotic pressure recovery limits were calculated as the recoveries at which the retentate osmotic pressure equals 600 and 1000 psi—these two limits are the common maximum operating pressures for RO pressure vessels for brackish water and seawater, respectively.

3.3 Diagnostic Flux Decline Experiments

The flux decline for each run was quantified by plotting the relative flux (the flux at a given time divided by the initial flux) versus time. The average SIs of calcite, gypsum, and silica at the membrane surface were calculated by first estimating the average CP for each run and then calculating the SIs at the new concentration by using the average CP as a concentration factor (see Eq. 3-1).

3.4 Equivalent Recovery Calculations for Diagnostic Experiments

Equivalent recoveries can be calculated for each diagnostic experiment by using Equation 2-7, substituting CP_{avg} for CF. This yields an estimate of the recovery at which the RO module would experience an average concentration in its exit region equivalent to that at the membrane surface in the plate-and-frame system as expressed in Equation 3-2,

$$R_{W,eqv} = \frac{CP_{avg} - 1}{CP_{avg} - 1 + R_S} \tag{3-2}$$

where $R_{W,eqv}$ is the equivalent product water recovery, CP_{avg} is the average concentration polarization along the membrane surface, and R_s is the observed salt rejection of a particular experiment, ranging from 0.96 to 0.99.

4. EXPERIMENTAL

4.1 Materials & Reagents

4.1.1 Laboratory Work

The aromatic polyamide RO membrane, LFC-1 (Hydranautics, Oceanside, CA) was selected for the scaling tests because of its low biofouling potential, high permeability, and high salt rejection [29]. The LFC-1 membrane has a permeability of 9.8 ± 0.3 x 10^7 m $bar^{-1}s^{-1}$, a nominal salt rejection of 98 %, and a root-mean-square (RMS) surface roughness of 65.5 nm [27]. Membrane compaction/conditioning was accomplished using solutions of sodium sulfate (certified A.C.S anhydrous, Fisher Scientific, Pittsburgh, PA). Hydrochloric acid (Technical 22º Baume, Fisher Scientific, Pittsburgh, PA) and Sodium hydroxide pellets (certified ACS, Mallinckrodt Baker, Inc., Phillipsburg, NJ) were used to make 2.0 N HCl and 0.10 N NaOH solutions, respectively, for pH adjustments. PermaTreat PC-504 (Nalco Company, Naperville, IL) was the selected antiscalant because of its strong inhibition of calcium sulfate scaling in bulk crystallization [30, 31].

4.1.2 Field Water Samples

Collection and delivery of AD water field samples from each of the five selected locations in the SJV were scheduled with the California Department of Water Resources (DWR) [32]. Upon delivery the field water samples were refrigerated and maintained at 5 ºC prior to use. The alkalinity and SDI of water samples were measured using the HACH model AL-DT alkalinity test kit (Loveland, CO) and the Simple SDI Portable Auto SDI Tester (Applied Membranes, Inc., Vista, CA), respectively. The pH and electrical conductivity (EC) of the various waters were measured with an Oakton 110 Series pH meter with and an Oakton 110 Series conductivity meter (Vernon Hills, IL), respectively.

4.2 Apparatus

The diagnostic RO desalting system consisted of four main elements: a feed tank, a pump, two plate-and-frame reverse osmosis cells in parallel, and a microfiltration cartridge as shown in Figure 4-1. A five-gallon cylindrical polyethylene reservoir served as the feed tank for the water sample with temperature control provided through a stand-alone refrigerated recirculator (model 625, Fisher Scientific, Pittsburgh, PA) that circulated water through quarter-inch stainless steel tubing coiled into 10 eight-inch diameter loops. The tank was placed on a stir plate with a three-inch Teflon-coated stir bar

placed inside the tank to keep the sample well mixed. The water sample was fed through a nozzle at the bottom of the tank via 1.25 inch tubing leading to the feed pump.

A three-quarter horsepower electric motor (Dayton Electric Mfg. Co., Niles, IL) powered a three-stroke positive displacement pump (Hydra-Cell, Wanner Engineering, Minneapolis, MN). The pressurized water stream exited the pump through half-inch high-pressure tubing which connected to half-inch stainless steel piping. A bypass valve allowed regulation of the feed flow rate to the reverse osmosis cells. Recycled water was returned to the holding tank through half-inch plastic tubing connected to the bypass valve.

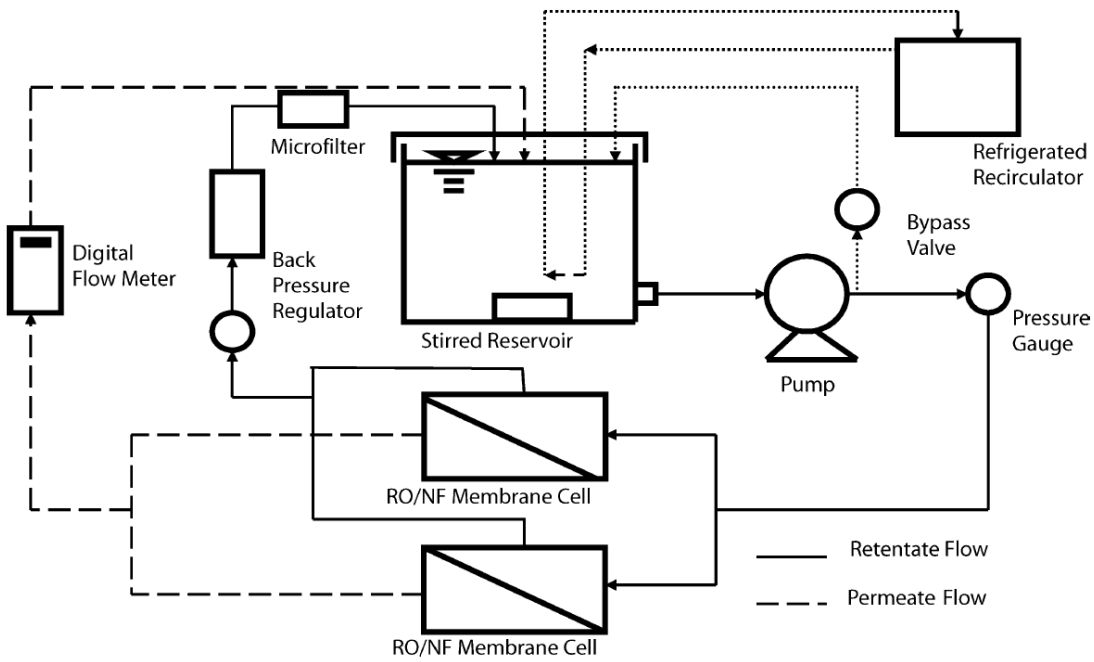

Fig. 4-1. Schematic of laboratory reverse osmosis system [33]

After passing through the bypass valve the pressurized feed water was split into two streams and fed in parallel to the two plate-and-frame reverse osmosis cells each having an effective membrane surface area of 19.8 cm^2 (2.6 cm x 7.6 cm). The permeate streams from both cells were combined and the flow rate was measured using a digital flow meter (model 1000, Fisher Scientific, Pittsburgh, PA). Subsequently, the permeate stream was either returned to the feed reservoir (total recycle) or collected separately (permeate withdrawal). The pressure in the cells was regulated by a backpressure valve (US Paraplate, Auburn, CA) placed following the recombination of the retentate streams. A rotameter (Blue-White Industries, Huntington Beach, CA) measured the flow rate of the retentate which was then passed through a 10 inch 0.2 μm Nylon filter cartridge (Cole-Parmer Instrument Company, Vernon Hills, IL)

within a transparent styrene acrylonitrile housing (Cole-Parmer Instrument Company, Vernon Hills, IL) before being diverted back to the holding tank.

4.3 Diagnostic Procedure

Diagnostic flux decline experiments were performed on field water samples from the five selected locations in the San Joaquin Valley to assess their relative feasibility for RO desalination. The diagnostic experiments were performed for field water samples rather than model solutions to more closely represent conditions found in actual RO desalination plants with respect to organics, microbes, and other unknown species that may be present in field water. Three distinct experiments were performed for each field water sample (except for LNW field water source for which only two of the experiments conducted are reported) by changing the initial conditions of the sample water, while leaving the operating conditions unchanged. The samples were run at the natural pH without any adjustment (pH 7.42 to pH 8.02), with adjustment to a low target of pH 6.0 (in practice the adjusted pH ranged from 5.27 to 6.48), and with adjustment to a low target of pH 6.0 with antiscalant addition (0.20 ppm PC-504). The antiscalant concentration was chosen such that it would be high enough to retard scaling to some extent but not so high as to completely inhibit scaling and make difficult a comparison between different gypsum saturation indices.

The flux decline for each run was measured by plotting the relative flux (the flux at a given time divided by the initial flux) versus time. Although most of the runs were started at nearly the same initial flux (within 2%), and considering that in some cases the final flux decline was small (< 10%), the above flux measurements were normalized for comparisons among all of the runs.

4.3.1 Pretreatment

Prior to performing the mineral scale diagnostic flux decline tests each field water sample was filtered successively through a 5 µm gradient density polypropylene filter cartridge and a 0.2 µm pleated Nylon filter cartridge (Cole-Parmer Instrument Company, Vernon Hills, IL) to remove suspended particles. For the flux decline tests carried out at a reduced pH (~ 6), the pH of the sample water was adjusted by addition of HCl. If the pH was inadvertently adjusted below the desired level, NaOH was added to readjust the pH to the desired level. In order to reduce pH drift during the experiments the dissolved carbon dioxide in solution needed to be in equilibrium with the atmosphere. Therefore, carbon dioxide exchange was increased by bubbling air through the water during pH adjustment to reduce the time required to reach equilibrium with respect to carbon dioxide. RO desalting performance

improvement with AS addition was evaluated in diagnostic flux decline experiments in which the AS was added just prior to the start of the 24 hour run in which it was needed.

4.3.2 Membrane Preparation

Membrane coupons were prepared prior to flux decline runs by cutting two 5 cm by 10 cm rectangles from the stock membrane roll. The coupons were rinsed for five to ten seconds under running DI tap water to remove dirt and dust. Then the membrane coupons were hydrated by soaking them in DI water for at least two hours in the refrigerator prior to placement in the RO cells.

4.3.3 Membrane Conditioning

The membrane coupons were placed inside the parallel plate-and-frame RO cells and conditioned by running the system with a sodium sulfate solution having approximately the same osmotic pressure as the field sample water. This was achieved by preparing a solution having an electrical conductivity (EC) about 20 % greater than that of the field water sample. The 20 % EC discrepancy was determined empirically during preliminary experimentation and accounts for composition differences between the field water and the compaction solution. Sodium sulfate was used for the compaction solution because it is non-scaling and sodium and sulfate were the most abundant ions found in the field water samples [2]. Detailed analytical reports for field water and compositions of the conditioning solutions are provided in Appendices A and C. The RO system was operated at a retentate flow rate of about 4.5 L/min for an hour and then for 3 hours at retentate and permeate flow rates equal to the rates desired for the subsequent flux decline run. After a total of 4 hours of membrane conditioning the system was shut down and the sodium sulfate solution was drained from the system.

4.3.4 Flux Decline Run

After membrane conditioning, each flux decline run was started at the desired conditions (cross flow rate, permeate flow rate, pressure) with the pretreated water sample. The system was closely monitored for the first 30 minutes to ensure that the cross flow and permeate flow rates stabilized. After the initial stabilization period, adjustments were made terminated after 24 hours and the membrane coupons were then removed and saved for later analysis.

4.3.5 System Cleaning

At the end of the 24 hour flux decline run the system was cleaned to remove residue that could interfere with any subsequent runs. Sacrificial LFC-1 membrane coupons designated for the cleaning procedure were placed in the RO cells and the system was thoroughly rinsed with DI water. Subsequently, the system was run with water at pH 10 followed by DI water containing about 0.1% v/v Micro-90, a concentrated detergent (International Products Corporation, Burlington, NJ). Finally, the system was thoroughly rinsed with DI water to remove any soap residue, the sacrificial membranes were then removed, and the system was left to dry with the valves and the RO cells open.

4.4 Biofouling Potential Experiments

Biofouling is the process by which bacteria or other microorganisms adhere to and grow on the membrane surface and reduce water permeation through the membrane. Often the microbes will form a biofilm which can be difficult and costly to remove. In the present study a series of simple assays were evaluated to assess the potential for biofouling.

4.4.1 Protein Assay

The amount concentration of bacteria in a field water sample is one way to measure the biofouling potential of the water. Measuring the concentration of a particular protein in the water provides an indirect measure of the bacteria concentration. Accordingly, in the present study protein concentration was measured by preparing a series of standards with known concentrations of a representative protein (BSA) and then measuring the absorbance of these samples with a UV/Vis spectrometer. A standard curve of absorbance versus protein concentration was constructed. The absorbance was subsequently measured for the field water samples and the concentrations were determined using a calibration curve.

4.4.2 Cultures

One method to determine if active microorganisms are present in a water sample is to culture a sample, incubate it, and then count any visible colonies. Samples of the field water were placed in Petri dishes and incubated for 24 hours at 30ºC.

5. RESULTS AND DISCUSSION

5.1 Variability of Agricultural Brackish Water Quality (1999–2003; 2006–2007)

The first step in studying the feasibility of desalination of AD water in the San Joaquin Valley consisted of performing thermodynamic solubility analyses based on compositional data of water samples taken from different locations in the valley. These analyses were split into two parts based on two data sets: Recent DWR periodic monitoring data, collected from 1999–2003 for drainage monitoring reports (§5.1.2) [11] and field water sample data collected by DWR during 2006–2007 specifically for the UCLA study (§5.1.3). The first data set from the 1999–2003 sampling period was studied to select field water sampling locations, to determine recovery limits, and to measure water quality variability. The data from the DWR drainage monitoring reports contained sufficient information for selecting sampling locations, determining recovery limits, and measuring water quality variability. However, the data set did not contain information on the concentrations of bicarbonate, carbonate, hydroxide, and silica. The DWR drainage monitoring report data set did contain the total alkalinity which provided an indirect measure of bicarbonate concentration assuming that all other alkalinity contributors (e.g. carbonate) were negligible. The second data set from the 2006–2007 sampling period contains more detailed analytical data along with field water samples.

5.1.1 Field Water Site Selection for Sampling and Analysis

In order to perform a meaningful evaluation of the feasibility of RO Desalination in the San Joaquin Valley (SJV), it is essential to have a complete water quality analysis of up to date water samples from the SJV. Complete water quality analysis is essential in order to estimate the effects of all constituents, including those which may be present in trace. Bench scale experiments must also be performed on real water samples because analyses performed with model solutions may not exhibit the range of problems that may occur in real waters (e.g. interactions caused by organics, particulates, and unknown constituents).

The first data set used in the present study was developed by the California Department of Water Resources (DWR) based on sampling of 55 different agricultural drainage water sites during the period of 1999 – 2003 spread throughout the SJV listed in Table 5-1.

Table 5-1. Agricultural drainage water monitoring sites in the San Joaquin Valley

Drainage Site	Location	Drainage Site	Location	Drainage Site	Location
CCN 3550	LC	SFD 2727	LC	CTL 3728	C
CNR 0801	KL	SFD 2944	LC	DPS 1016	C
COC 4126	KL	SFD 3027	LC	DPS 1367	C
COC 5329	KL	STC 3505	LHS	DPS 2535	C
COC 8221	KL	STC 5436	LHS	DPS 3465	C
COC 8252	KL	STC 5843	LHS	DPS 4616	C
ERR 6705	LC	VGD 3906	LC	FBH 5056	C
ERR 7525	LC	VGD 4406	LC	FBH 2016	C
ERR 8429	LC	VGD 4806	LC	FBH 3236	C
ERR 8641	LC	VGD 5409	LC	FBH 4045	C
GSY 0855	LC	VGD 5412	LC	FBH 5056	C
GSY 0935	LC	VGD 5509	LC	FBH 8061	C
HCH 7439	LHS	BVS 6001	C	HMH 7016	C
HCH 7841	LHS	BVS 6016	C	HMH 7516	C
LME 7569	LC	BVS 7007	C	OAS 0364	C
LNW 5454	LHS	BVS 7402	C	OAS 2548	C
LNW 5467	LHS	BVS 8003	C	CTL 4504	C
LNW 6459	LHS	BVS 8110	C	DPS 3235	C
LNW 6467	LHS				

Note: LC—Lemoore/Corcoran, LHS—Lost Hills/Semitropic, KL—Kern Lakebed, C—Central.

Sampling locations were chosen for further study based on the following three selection criteria: 1) The sites should be spread throughout the valley to help form a valley-wide assessment of the range of water chemistries present; 2) The sites should provide data covering a reasonable range of TDS, gypsum saturation index (SI_G), and ratio of total carbonate to sulfate; and 3) The sites must be active and readily accessible for sampling for use in the second phase of the study. With these three criteria in mind, five locations were selected (Table 5-2; see Figs 5-2 through 5-5). The second analytical data set was obtained for the UCLA study for the sites selected for sampling and experimental evaluation as listed in Table 5-2. The saturation indices for silica are not included in this table due to limitations in the first data set explained above.

Table 5-2: Site selections and selection criteria

Name	Location	TDS†, mg/L	[Total Carbonate] / $[SO_4^{2-}]$†, mol/mol	SI_G† (20ºC)
CNR 0801	Southern Area, Kern Lakebed	6,987	0.1130	0.758
LNW 6467	Southern Area, Lost Hills	11,944	0.0534	0.987
OAS 2548	Central Area	7,999	0.0967	0.748
VGD 4406	Southern Area, Lemoore	23,480	0.0483	0.844
ERR 8429	Southern Area, Corcoran	4,690	--	--

†Values are one year averages (2003 – 2004), -- data were insufficient.

Mineral scaling of RO membranes by sparingly soluble mineral salts is the primary limitation encountered in AD water desalination. Based on preliminary water quality analysis, some of the most problematic mineral scalants found in AD water include, but are not limited to calcite, barite, and gypsum. Typically, calcite scaling does not dictate the ultimate recovery limit because its solubility is readily controlled by adjusting the feed water pH (as long as pH adjustment is not prohibitively costly). Also, barite scaling is not expected to be a major problem because barium in the SJV is found at very low concentrations (often at the method detection limit) [2]. However, barite concentrations above saturation can be problematic. Gypsum scaling is a major concern because gypsum is generally present at high saturation indices and its solubility is nearly independent of pH. Therefore, the saturation index of gypsum sets the primary recovery limit of water in the SJV.

The osmotic pressure of the feed, concentrate, and permeate streams is primarily a functions of TDS. Because all the brackish waters in the SJV in the present study have the same major contributors to TDS and are composed largely of sodium sulfate, the osmotic pressure can be assumed to be dictated largely by the TDS. The TDS is an important criteria to consider because the associated osmotic pressure for the given water source determines the required pumping power to achieve reasonable fluxes and the ultimate recovery limit for RO desalination (assuming that scaling problems can be overcome).

The ratio of total carbonate to sulfate is known to affect the kinetics of membrane crystallization [18, 30, 34]. Brackish water oversaturated with gypsum and having a low carbonate to sulfate ratio are likely to form gypsum scale, while those having higher ratios are likely to exhibit coprecipitation of calcite and gypsum with relatively slower crystallization kinetics and longer induction periods [30].

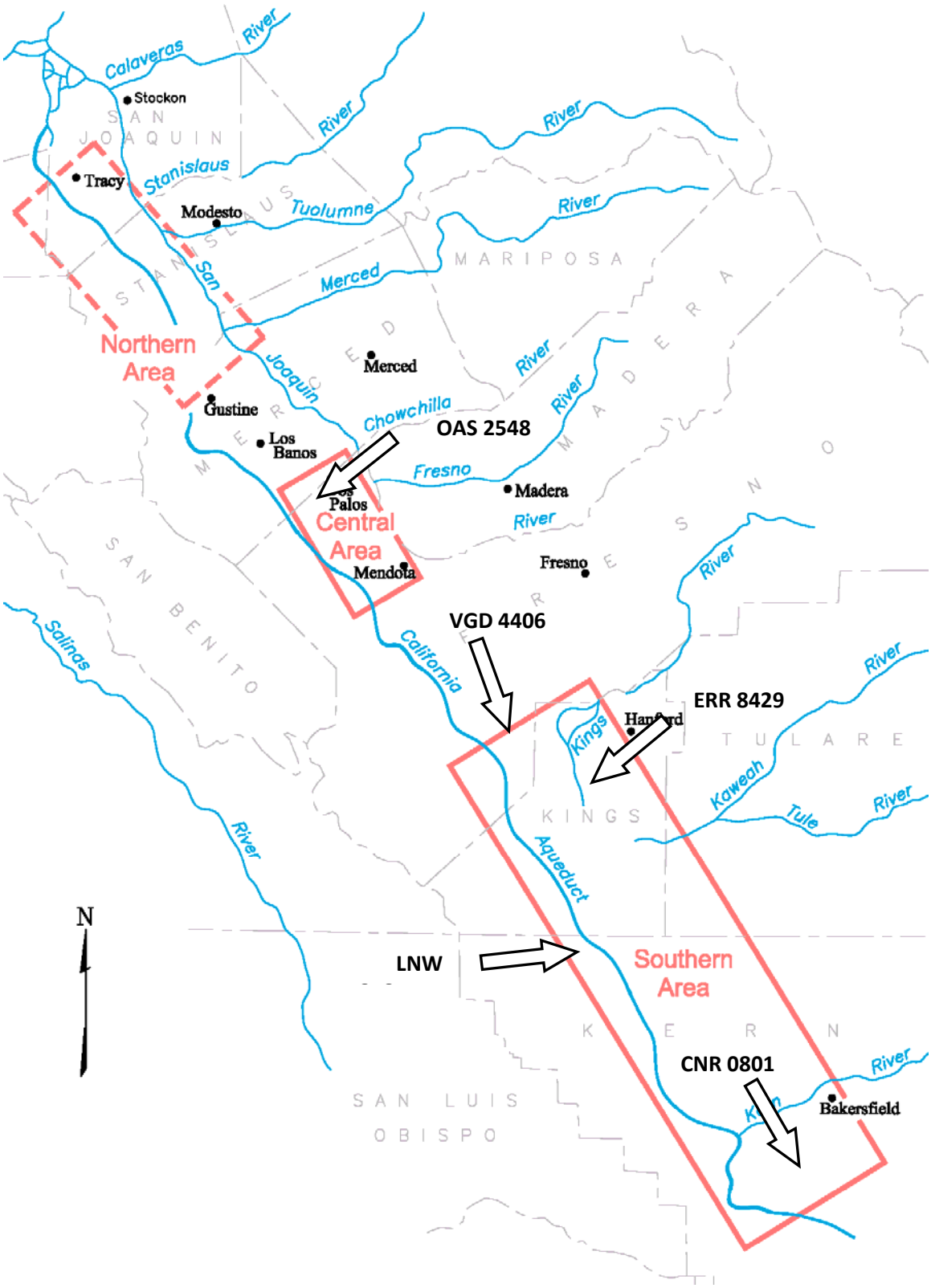

Figure 5-1: Overview of sampling area locations [2]

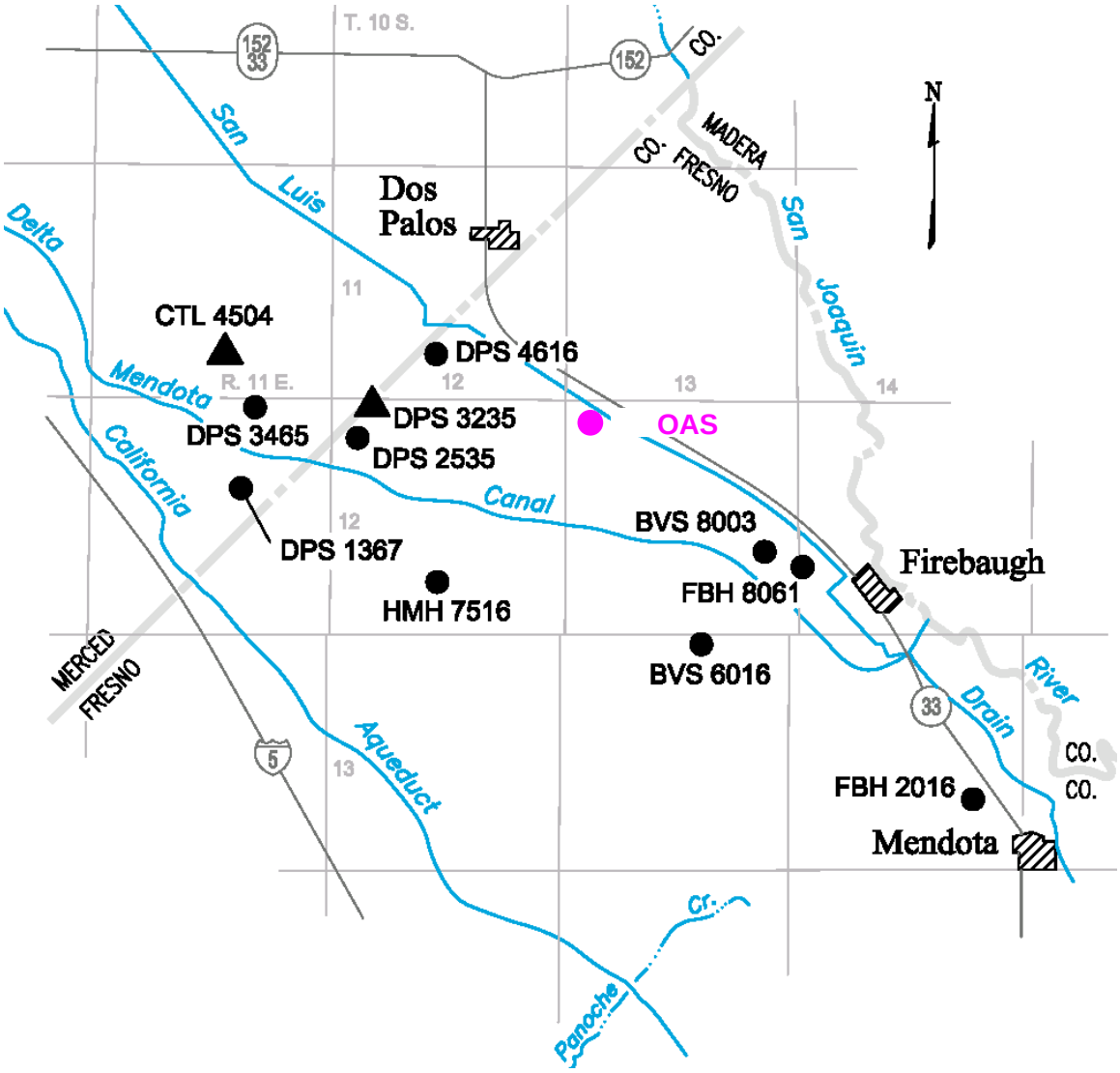

Figure 5-2: Central area drain locations [2]

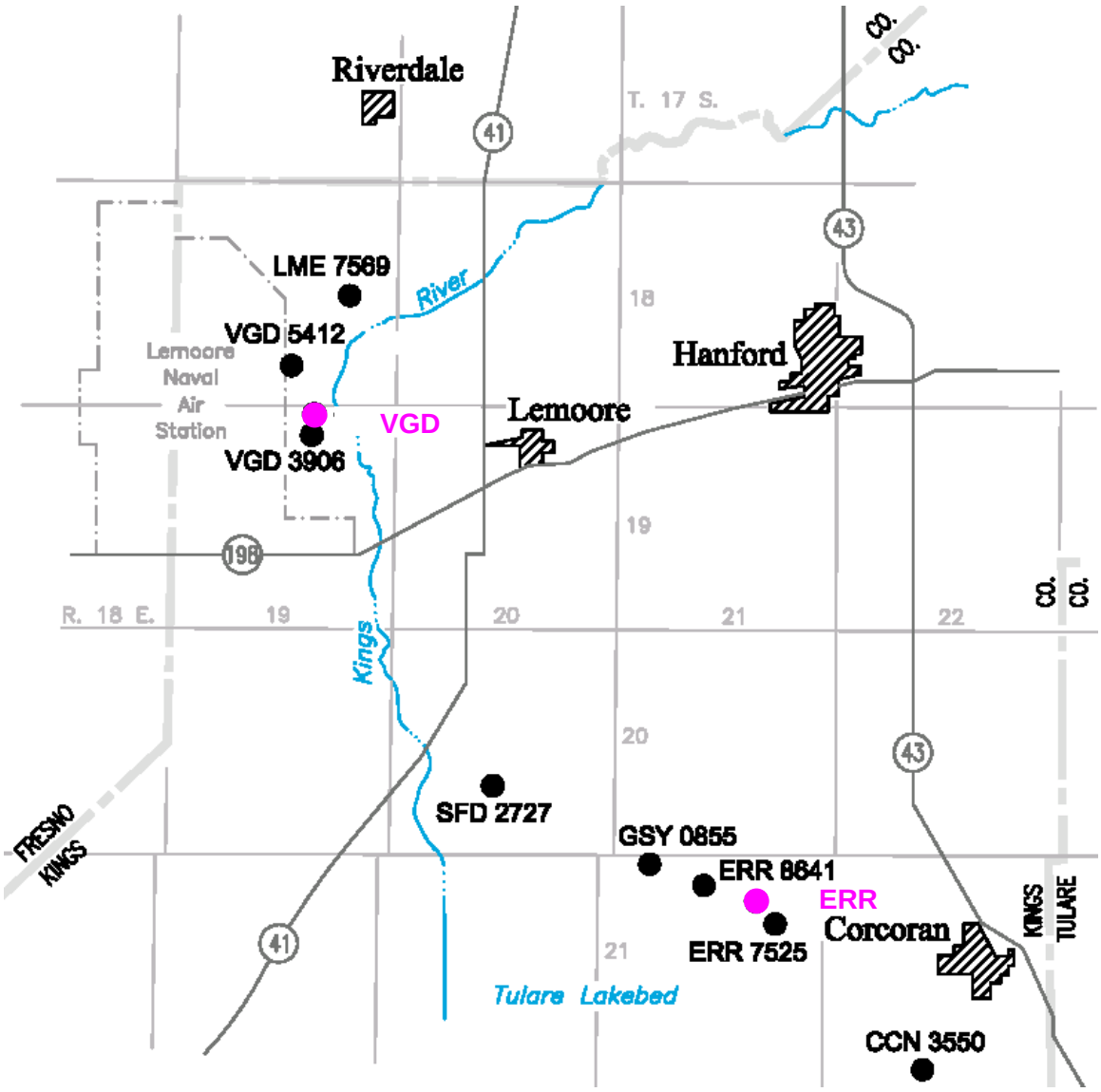

Figure 5-3: Southern area drain locations—Lemoore/Corcoran stations [2]

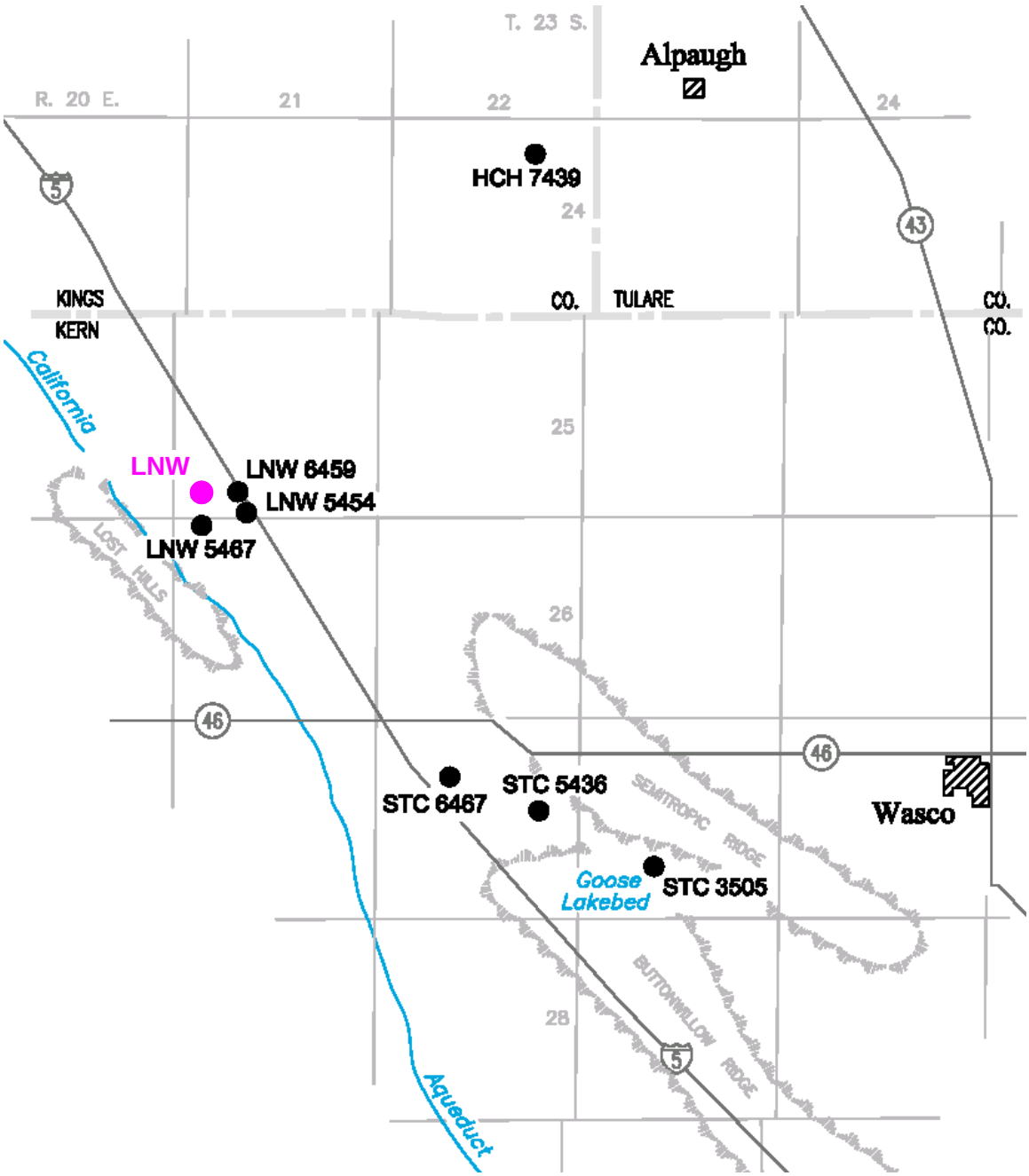

Figure 5-4: Southern Area Drain Locations—Lost Hills/Semitropic Stations [2]

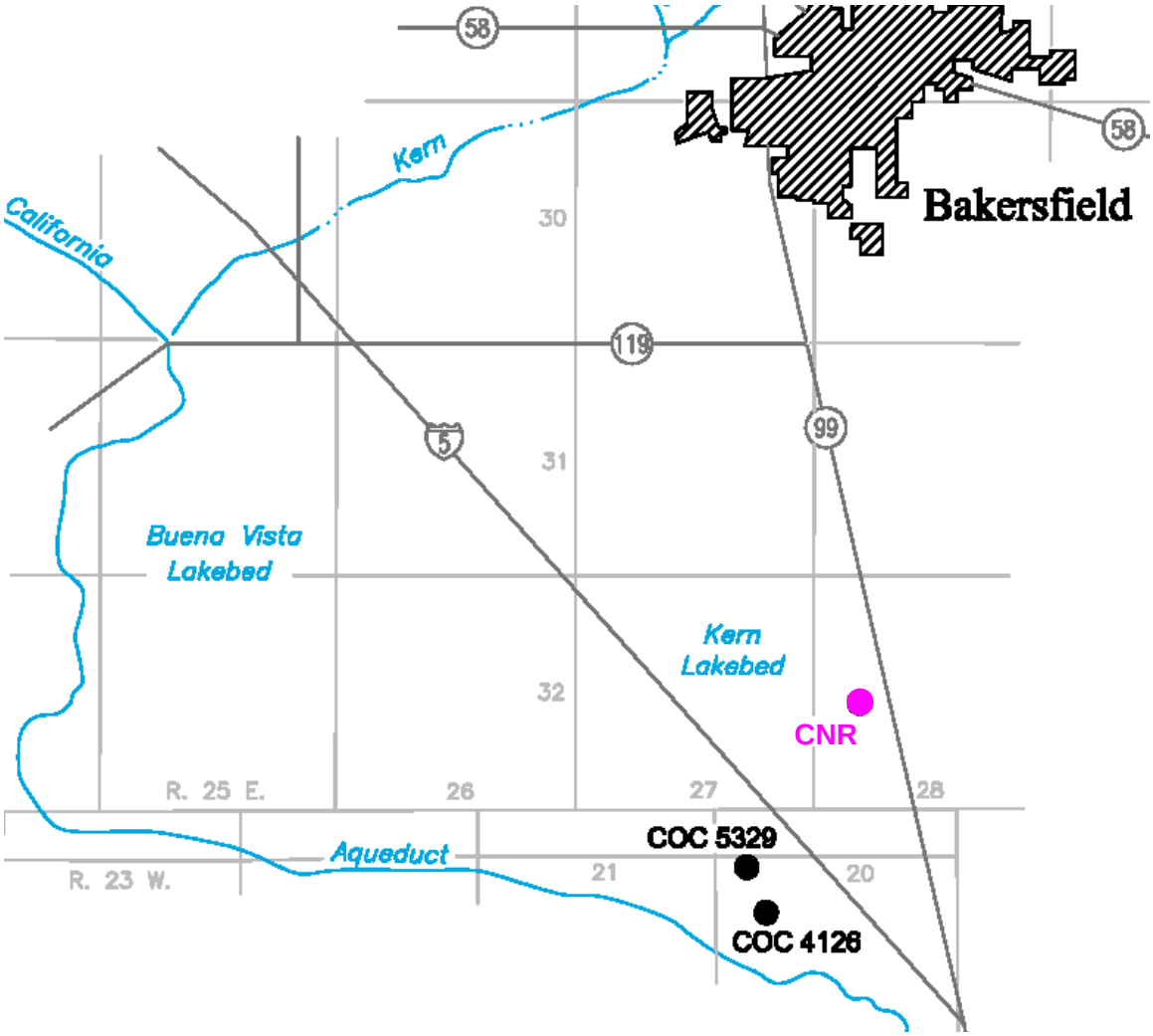

Figure 5-5: Southern area drain locations—Kern Lakebed stations [2]

5.1.2 Recent DWR Periodic Monitoring Data (1999–2003)

The 1999–2003 DWR periodic monitoring data were analyzed in order to assess seasonal and geographic variations in water quality and to determine potential recovery limitations for different locations throughout the SJV. Five sample locations (CNR 0801, LNW 6467, OAS 2548, and VGD 4406) were selected for further study (i.e thermodynamic solubility analysis and diagnostic flux decline experiments of field water samples). It is noted that the data provided did not contain measurements of bicarbonate, carbonate, and silica concentrations. The analysis was limited to the latest year of available data for each location because the most recent data are more likely to represent the current state of water quality in the SJV. Information regarding the selected sites is summarized in Table 5-3 below. It is noted that while the calcite saturation index (SI_C) is included in Table 5-3, it was not used as a site

selection criterion because SI_C is strongly dependant on pH which varies significantly among the sampling dates and locations. Changes in SI_C can largely be attributed to pH variations while changes in SI_G are largely due to changes in water composition (e.g. changes in calcium or sulfate concentrations). Instead, as shown later in this section, solubility analyses were performed for all locations at two standardized pH values of 7.5 (near the natural pH of most of the water samples) and 6.0 (a sufficiently low pH level for suppressing calcite scaling).

Table 5-3. Summary of average water quality for the most recent year of data (2003–2004)†

Name	Location	TDS, mg/L	pH	[Total Carbonate]‡ / [SO_4^{2-}], mol/mol	SI_C (20ºC)	SI_G (20ºC)
CNR 0801	Southern Area, Kern Lake Bed	6,987	7.7	0.1130	5.05	0.758
LNW 6467	Southern Area, Lost Hills	11,944	7.5	0.0534	2.31	0.987
OAS 2548	Central Area	7,999	7.7	0.0967	3.89	0.748
VGD 4406	Southern Area, Lemoore	23,480	7.9	0.0483	5.29	0.844
ERR 8429	Southern Area, Corcoran	4,690	--	--	--	--

† TDS, pH, and [SO_4^{2-}] were obtained from analytical reports, while SI_C and SI_G were calculated based on the water composition, ‡ [Total Carbonate] was calculated assuming HCO_3^- was the only species contributing to the total alkalinity, -- insufficient data available for calculation

5.1.2.1 Seasonal Variability of Water Quality

The variation of SI_G was plotted versus sample date over the latest year of data along with TDS, total alkalinity, Calcium ion, and Sulfate ion. The temporal variability of water quality is illustrated in Figures 5-6 through 5-9 in plots of percent deviation of water quality indicators and SI_G from the respective annual average values versus time over the latest year of available data for each location.

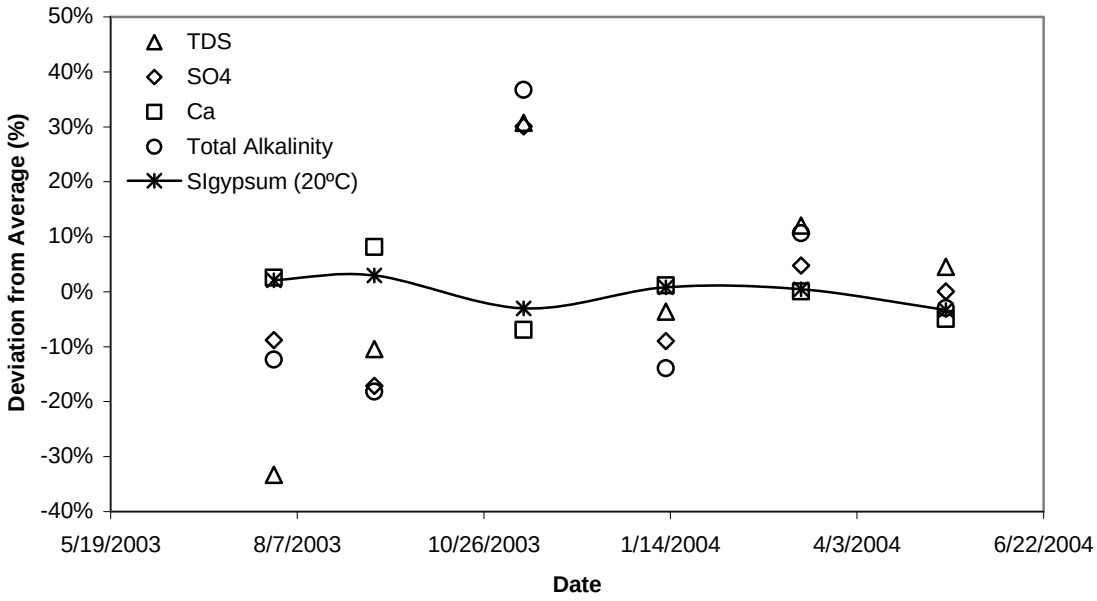

Figure 5-6. CNR seasonal variability of water quality

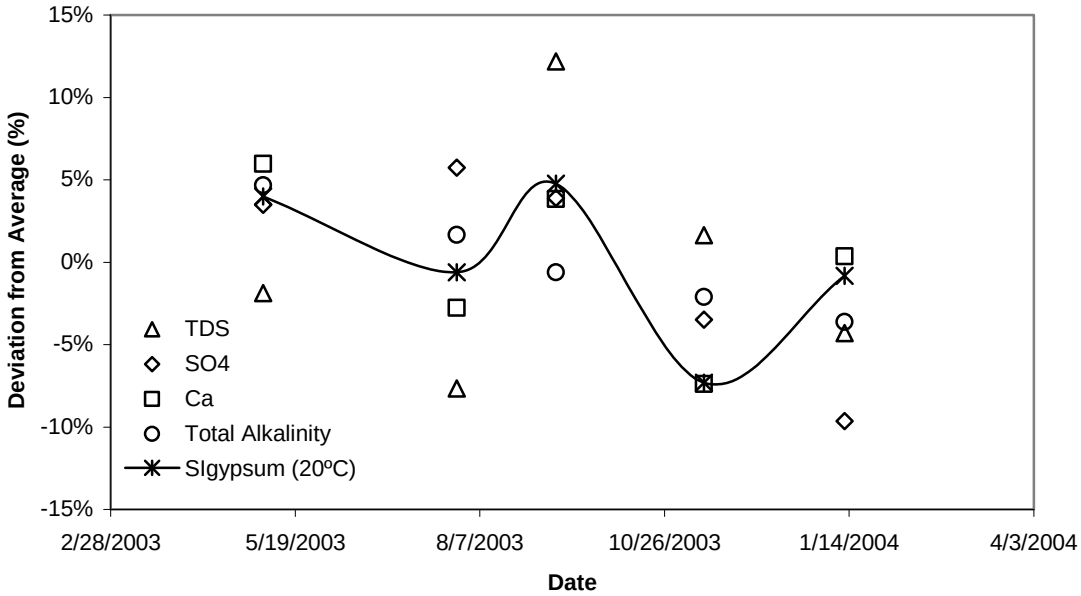

Figure 5-7. LNW seasonal variability of water quality

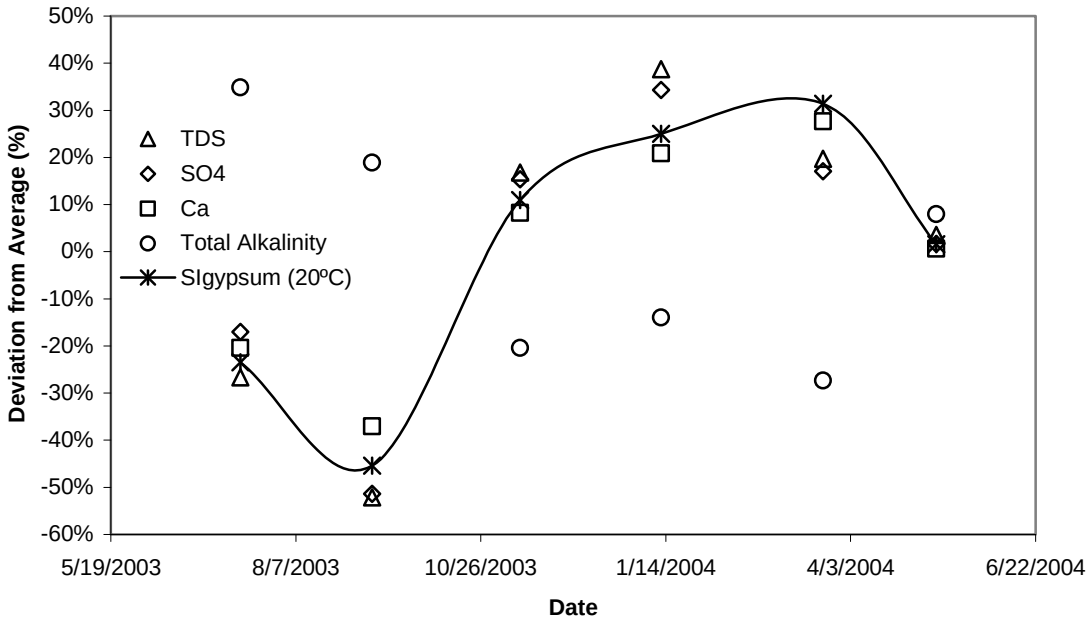

Figure 5-8. OAS seasonal variability of water **quality**

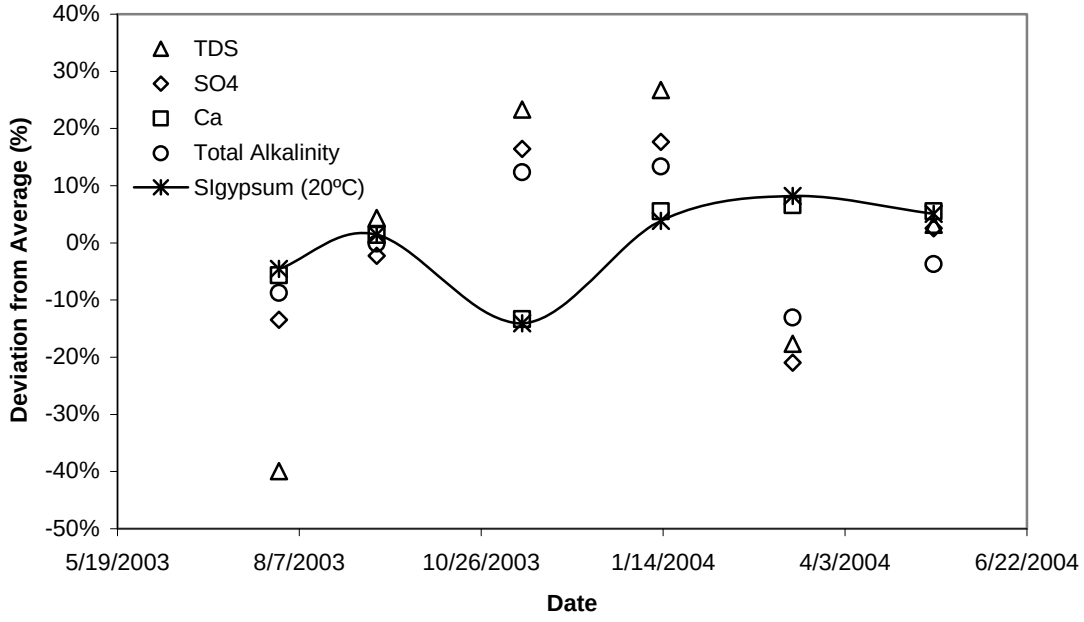

Figure 5-9. VGD seasonal variability of water quality

As illustrated in Figures 5-6 through 5-9, the brackish water quality varied significantly over the course of a year for each of the selected location in the SJV both seasonally and geographically. One might expect SI_G to increase with TDS, calcium concentration, and/or sulfate concentration. No consistent seasonal variations were found across the sample locations and no consistent correlation between SI_G and TDS was found for any of the locations. However, the variation of SI_G appears to closely match the variation in calcium concentration. The average TDS for the selected locations ranged from 6987 mg/L to 23,480 mg/L for CNR and VGD, respectively, while the maximum absolute percent deviation of TDS from the average values ranged from 12% to 52% for LNW and OAS, respectively. The average calcium ion concentrations ranged from 356 mg/L to 606 mg/L for OAS and LNW, respectively, and do not correlate with the low and high average TDS values. The maximum absolute percent deviation of calcium ion concentration from the average values ranged from 7.4% to 37% for LNW and OAS, respectively. SI_G varied from 0.75 to 0.99 (OAS and LNW, respectively), neither of which corresponds to the low or high measured TDS. The maximum absolute percent deviation of SI_G from the average values ranged from 5.2% to 45% for CNR and OAS, respectively. The lack of correspondence between SI_G and TDS illustrates the variability in water chemistry over time at each location. The low and high values for average sulfate ion concentration, 4880 mg/L and 16,062 mg/L (LNW and VGD, respectively) do, however, correspond with the low and high average TDS values. This correspondence is reasonable even for waters of varying composition because the sulfate ion is the largest single contributor to TDS for each location, contributing to it by a large majority (from 60% to 68%) for all locations except for LNW (41%). The maximum absolute percent deviation of sulfate ion concentration from the average values ranged from 9.6% to 51% for LNW and OAS, respectively. Overall, OAS exhibits the most variability in water quality of the selected sites, while LNW exhibits the least variability.

5.1.2.2 pH Dependence of Saturation Indices

The relationship between pH and saturation indices for gypsum, calcite, and barite are shown in Figures 5-12 through 5-19 for each of the four selected locations for both the high and low annual TDS conditions listed in Table 5-2. The values for barite are provided for illustrative purposes only because the barium concentrations were reported at or below the detection limits which vary between 0.25 to 1.0 mg/L. The actual barium concentrations may be much lower, thus, the calculated barite saturation indices are upper limits that may not reflect the recovery limits.

As illustrated in Figures 5-12 through 5-19, the saturation index of calcite is highly pH dependant, increasing by several orders of magnitude over the pH range shown (pH 4 to 6), while the

gypsum saturation index decreases by less than 14% over the same range and the barite saturation index changes by less than 5% over the same pH range except for the CNR location at the high TDS condition and OAS at the low TDS condition for which the decreases in gypsum saturation index were 18% and 22%, respectively. Because the saturation indices of gypsum, calcite, and barite vary to different degrees, different strategies must be used to manage their scaling. Calcite scaling can generally be managed by reducing the pH of the feed water, while barite and gypsum are relatively pH insensitive and can be partially managed with antiscalant use.

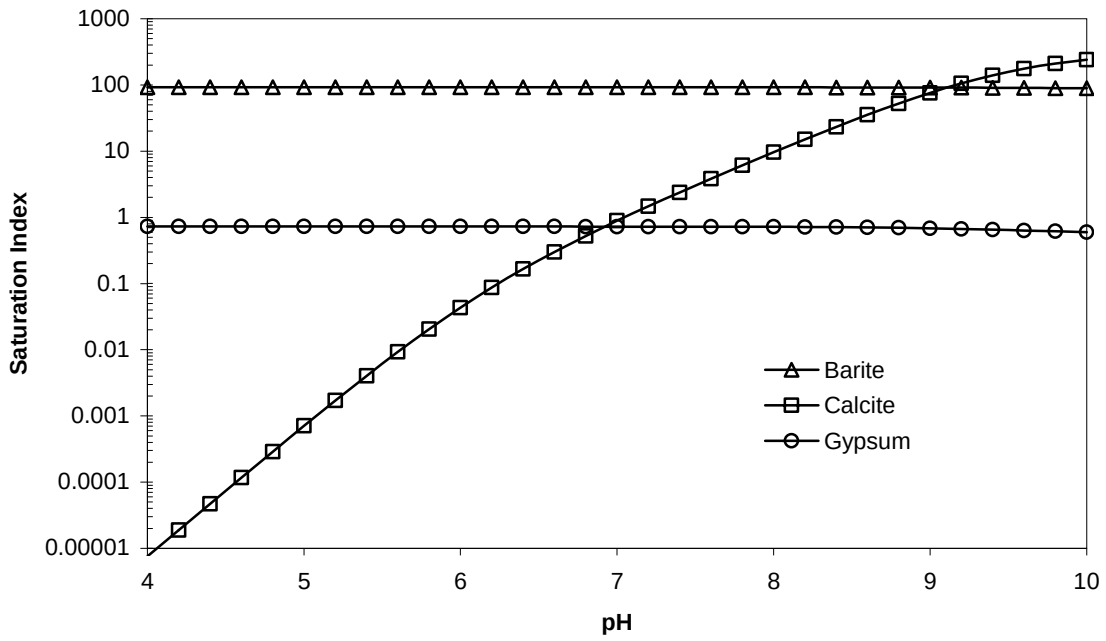

Figure 5-10. Mineral salt solubility dependence on pH for CNR for the high TDS condition (9163 mg/L, 11/12/2003)

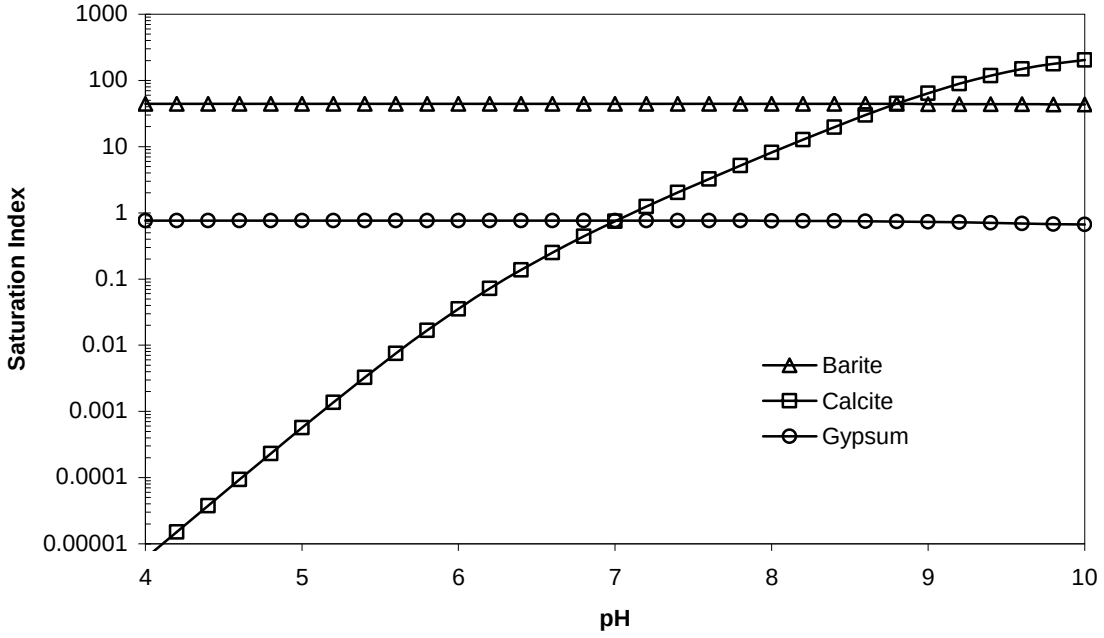

Figure 5-11. Mineral salt solubility dependence on pH for CNR for the low TDS condition (4660 mg/L, 7/28/2003)

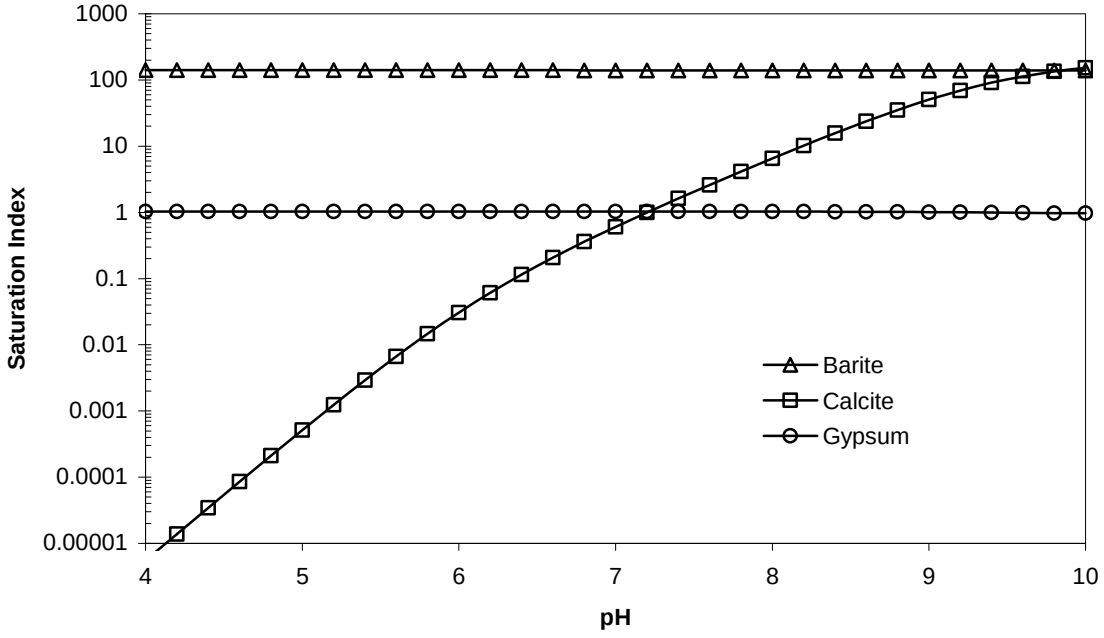

Figure 5-12. Mineral salt solubility dependence on pH for LNW for the high TDS condition (13,400 mg/L, 9/9/2003)

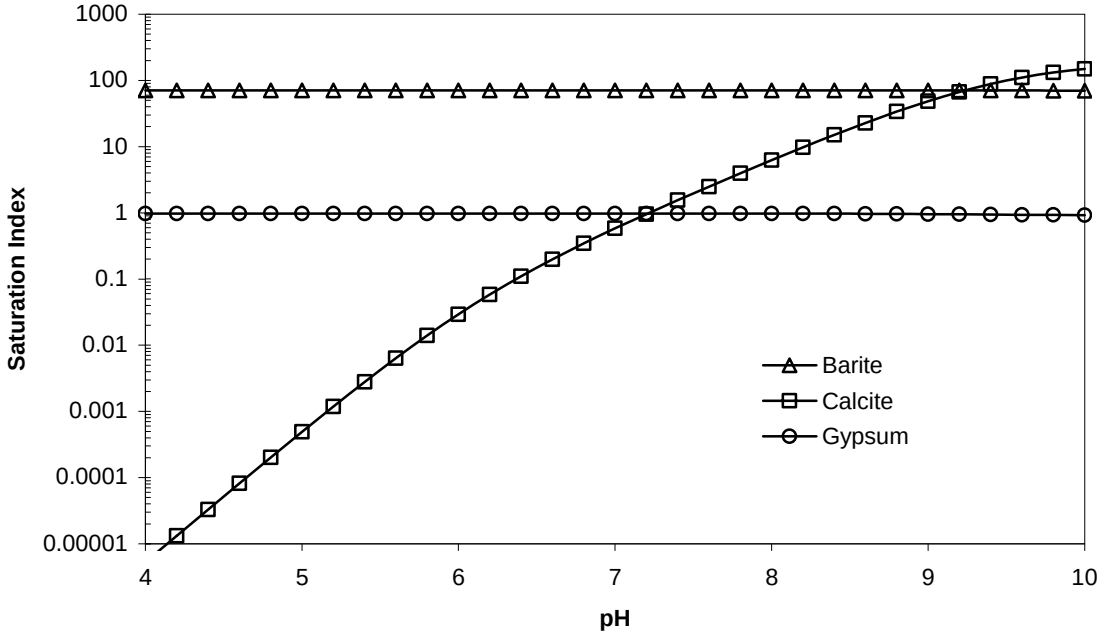

Figure 5-13. Mineral salt solubility dependence on pH for LNW for the low TDS condition (11,030 mg/L, 7/28/2003)

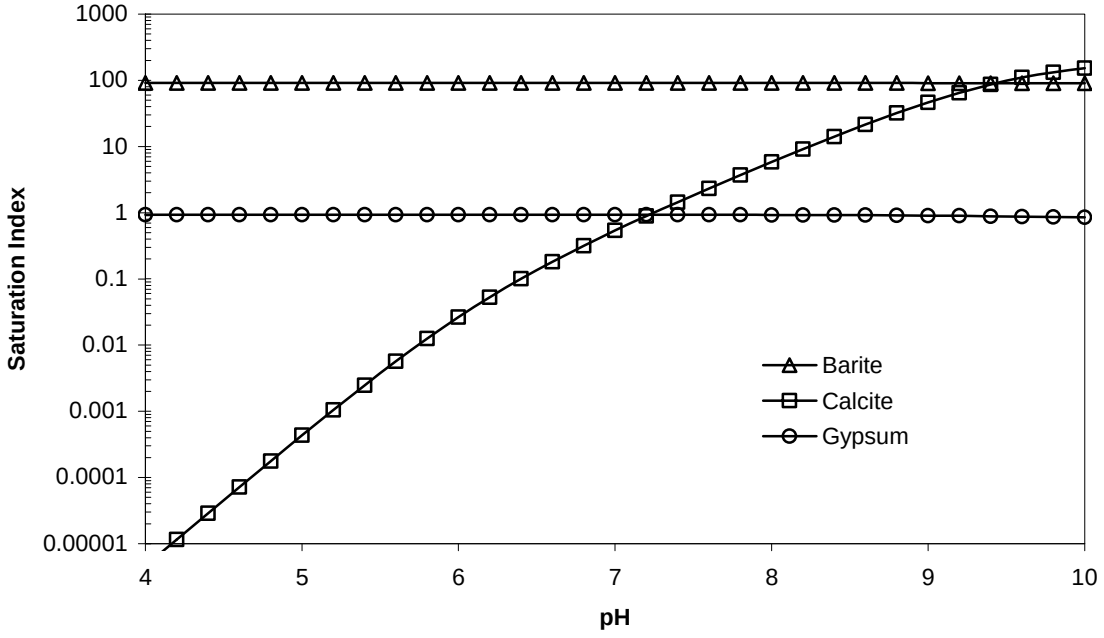

Figure 5-14. Mineral salt solubility dependence on pH for OAS for the high TDS condition (11,100 mg/L, 1/12/2004)

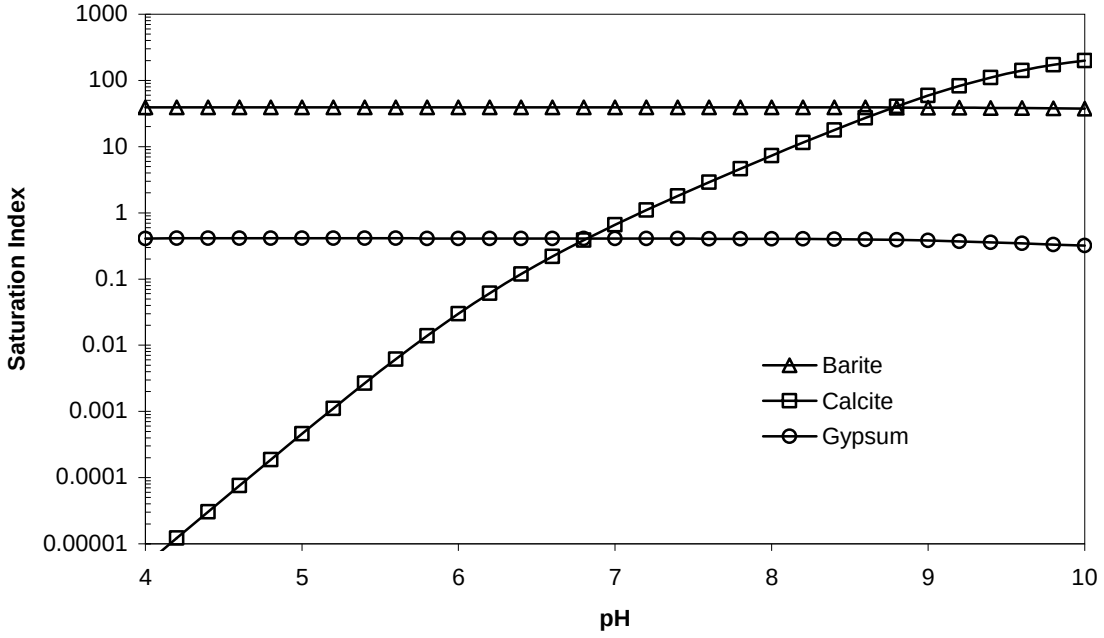

Figure 5-15. Mineral salt solubility dependence on pH for OAS for the low TDS condition (3828 mg/L, 9/9/2003)

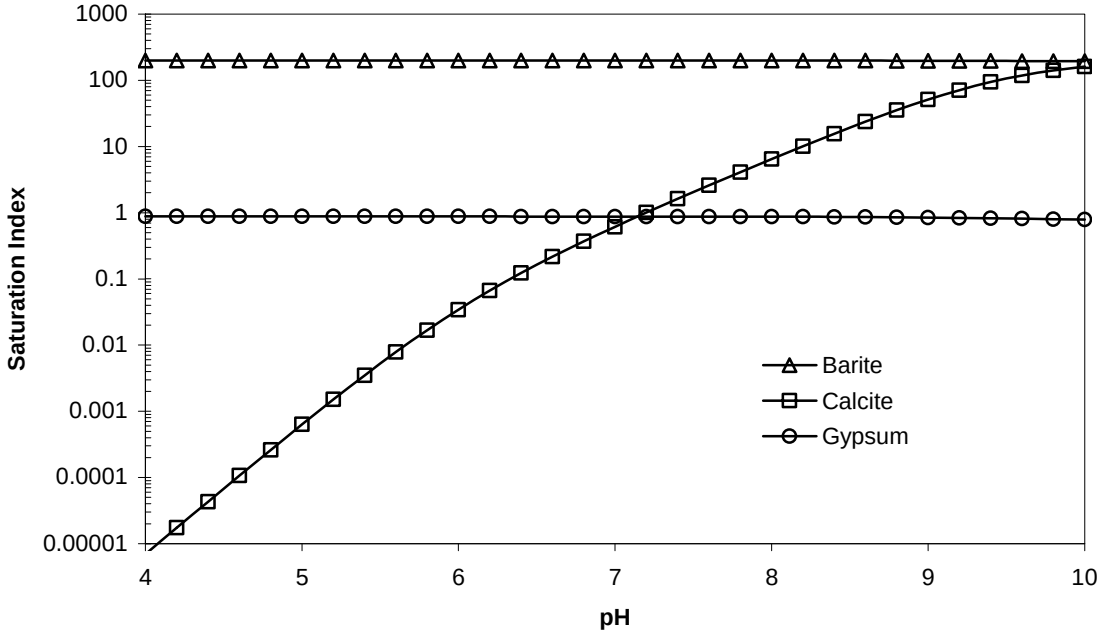

Figure 5-16. Mineral salt solubility dependence on pH for VGD for the high TDS condition (29,760 mg/L, 1/13/2004)

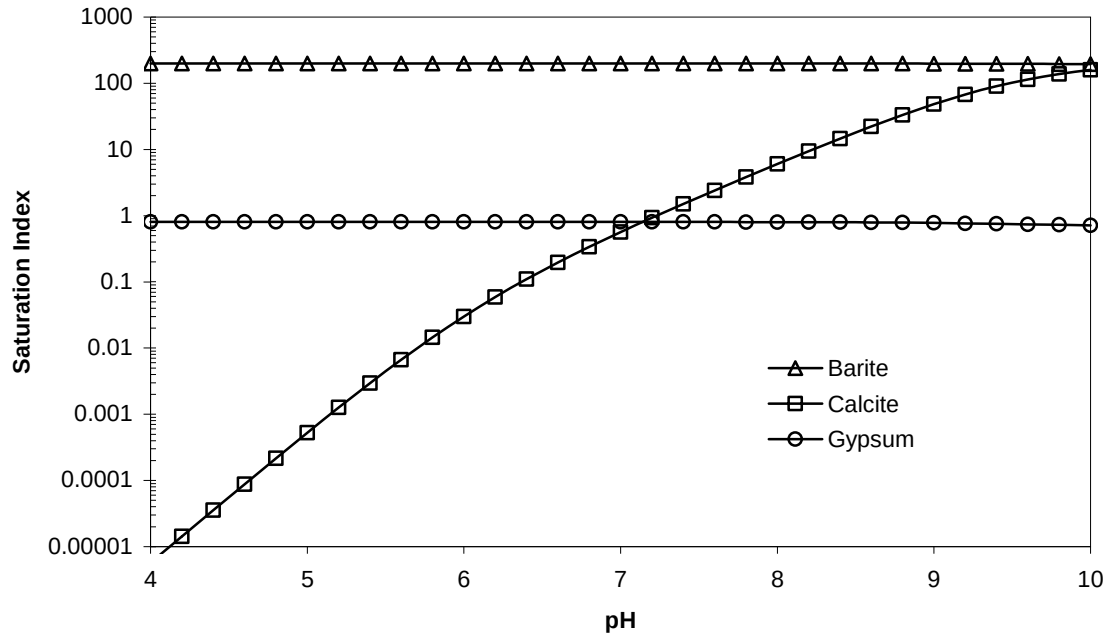

Figure 5-17. Mineral salt solubility dependence on pH for VGD for the low TDS condition (14,110 mg/L, 7/29/2003)

5.1.2.3 Recovery Limits

RO recovery limits based on scaling were determined by calculating the recoveries at which the concentrations of sparingly soluble salts (e.g. calcite, gypsum, barite) reach their maximum controllable (i.e. non-scaling) saturation levels. Calcite scaling can be controlled by pH adjustment to saturation or below and thus SI_C equal to unity was set as the upper limit. Gypsum and barite scaling can be controlled up to SIs of 2.3 and 90, respectively, with antiscalant use. SI_C, SI_G, and SI_B were calculated for a range of concentration factors (CF; see Eq. 2-6) for the five selected locations (except for ERR for which there was insufficient data; Table 5-2) to determine recovery limits. The change in SI with recovery was then calculated and plotted by converting the CF values to equivalent recoveries using Equation 2-7,

$$R_W = \frac{CF - 1}{CF - 1 + R_S} \qquad (2\text{-}7)$$

where R_W is the fractional product water recovery, *CF* is the concentration factor, and R_S is the fractional salt rejection. The results of the above analysis are summarized in Figures 5-18 through 5-33 where the pH was held constant first at 7.5 and then at 6.0 by addition of sodium hydroxide or hydrochloric acid. Because all of the water samples had a natural pH in the range 7.1–8.1, an average pH of 7.5 was selected as a reasonable value for an “untreated” water and a pH of 6.0 was selected as an adjusted feed pH representative of the condition for controlling calcite scaling.

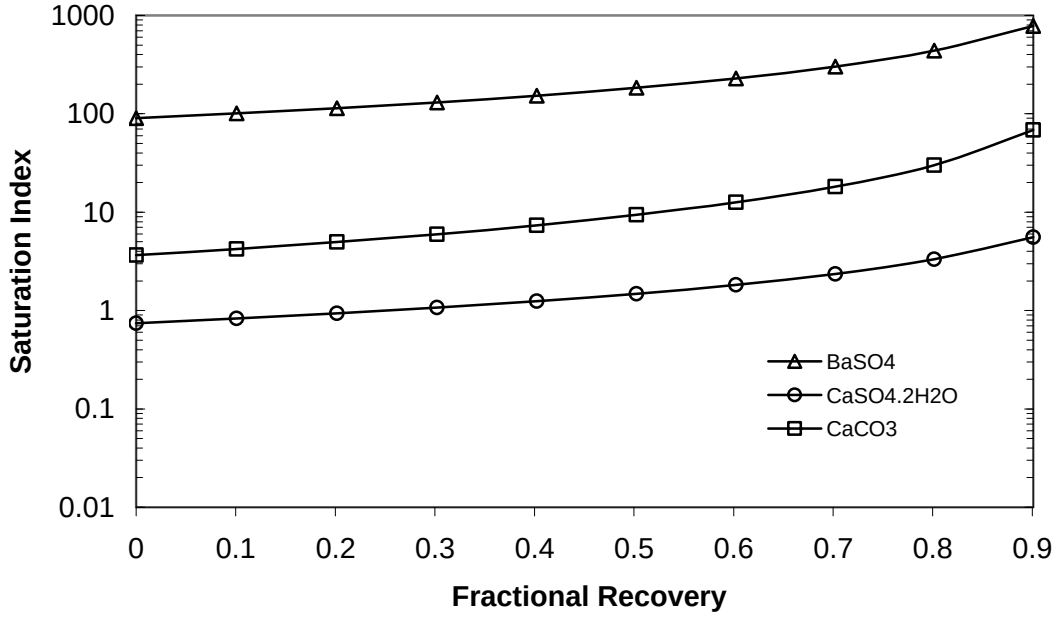

Figure 5-18. Saturation indices vs recovery (CNR, TDS 9136, pH 7.5)

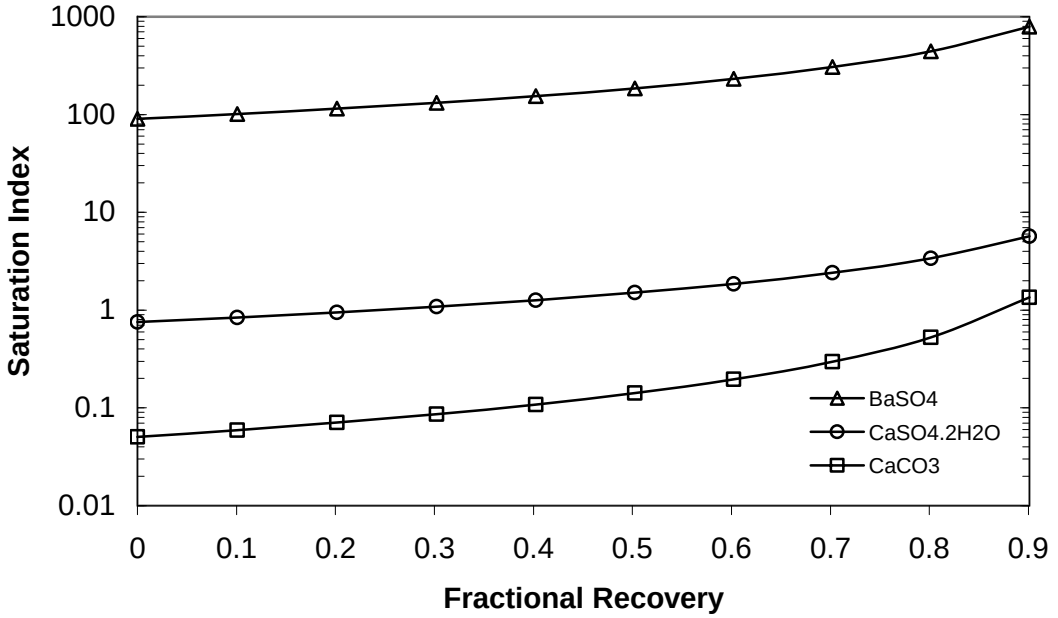

Figure 5-19. Saturation indices vs recovery (CNR, TDS 9136, pH 6.0)

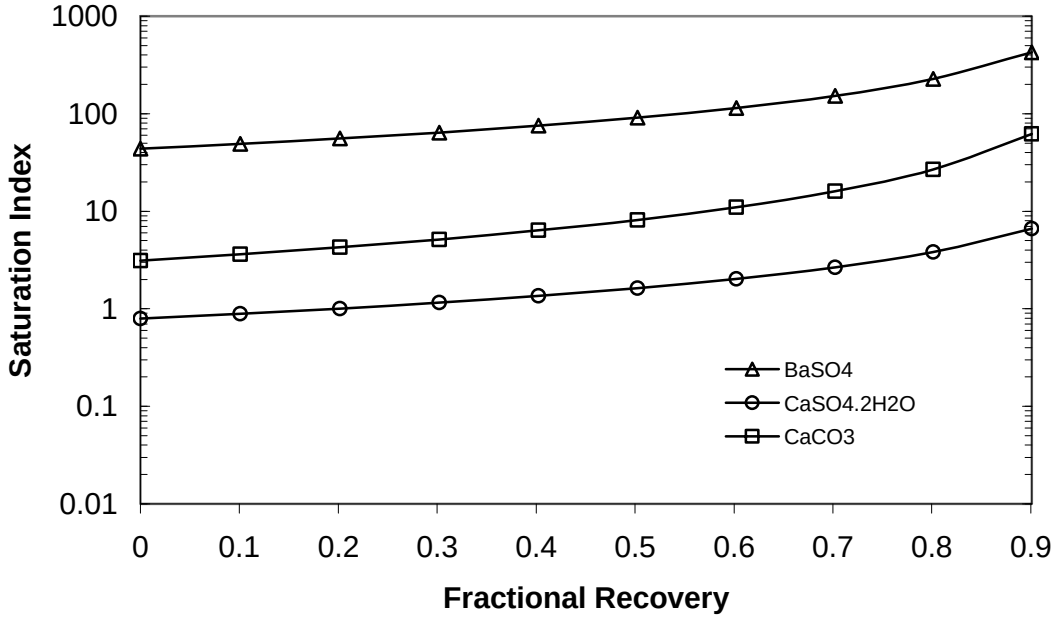

Figure 5-20. Saturation indices vs recovery (CNR, TDS 4660, pH 7.5)

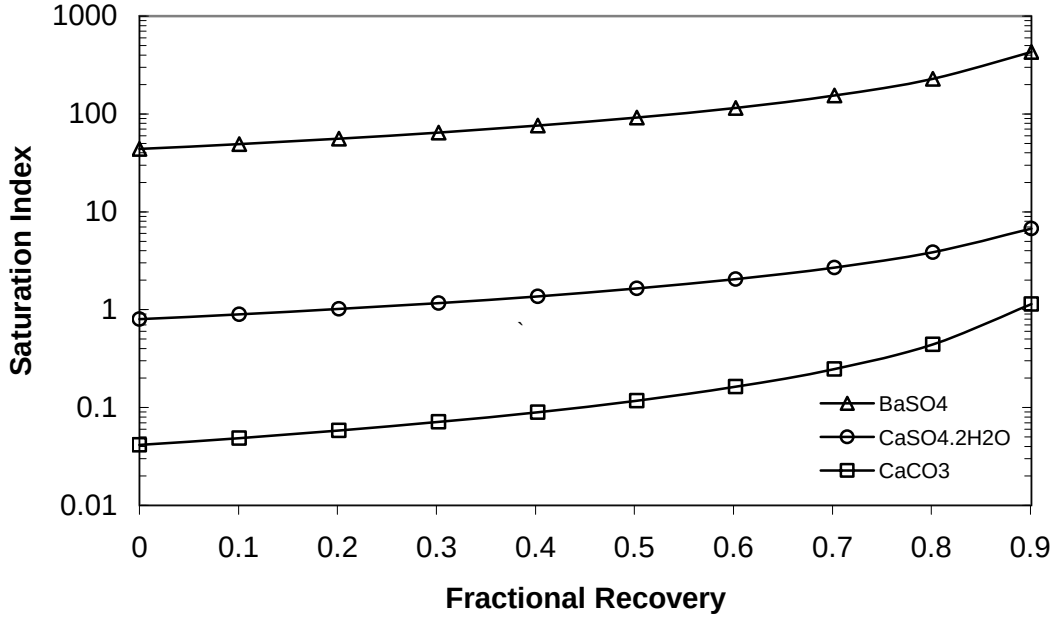

Figure 5-21. Saturation indices vs recovery (CNR, TDS 4660, pH 6.0)

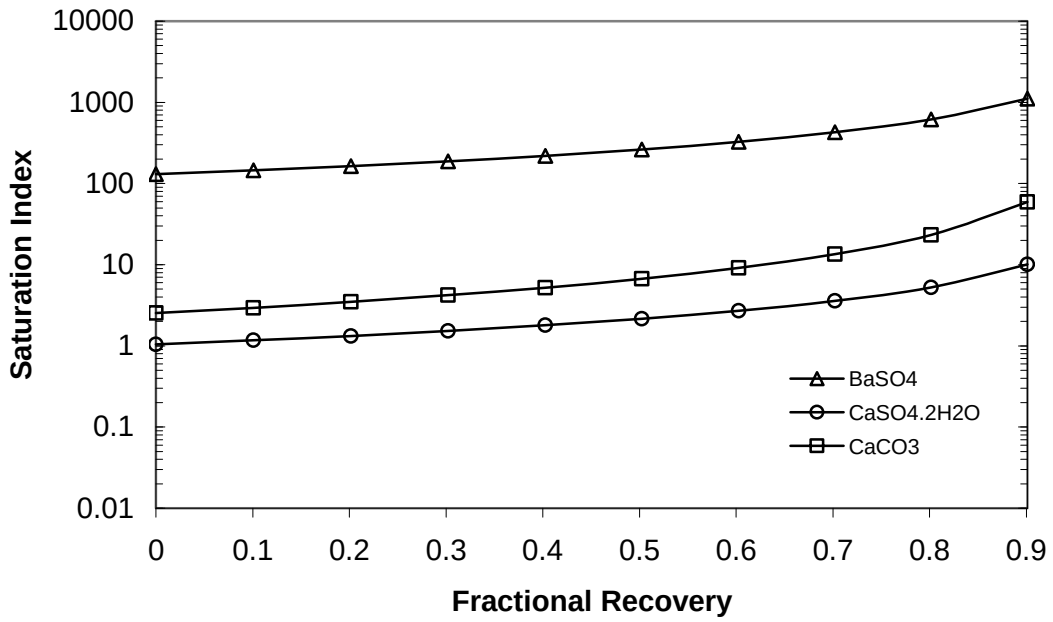

Figure 5-22. Saturation indices vs recovery (LNW, TDS 13400, pH 7.5)

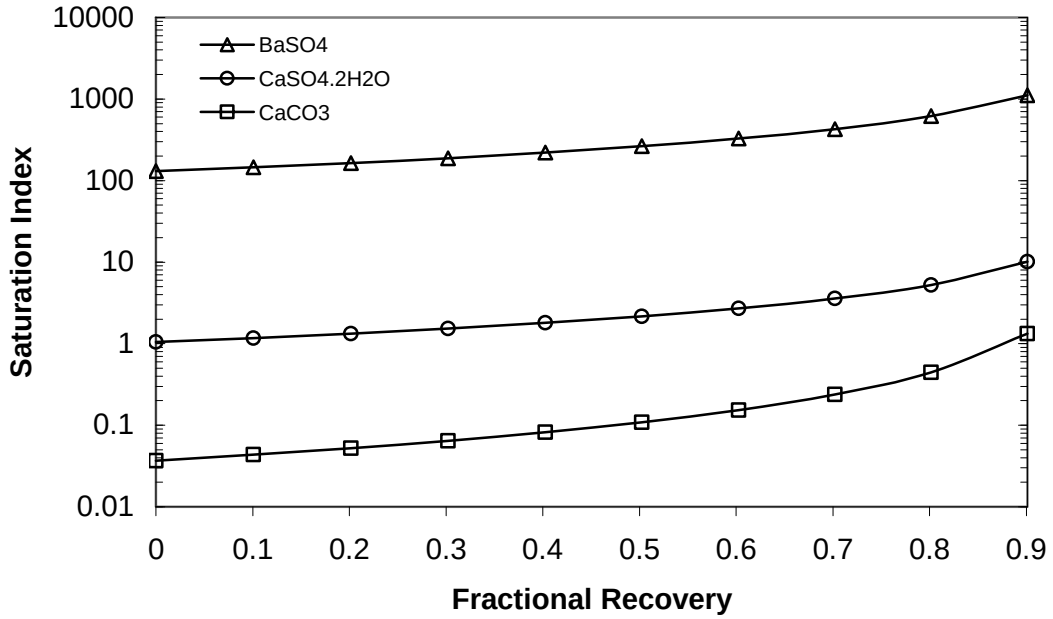

Figure 5-23. Saturation indices vs recovery (LNW, TDS 13400, pH 6.0)

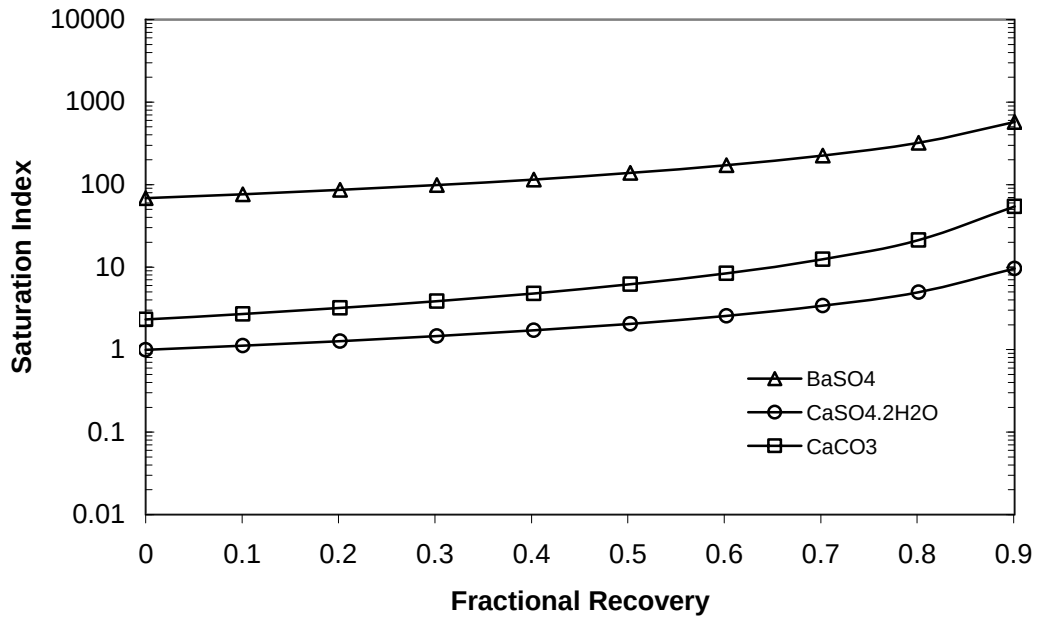

Figure 5-24. Saturation indices vs recovery (LNW, TDS 11030, pH 7.5)

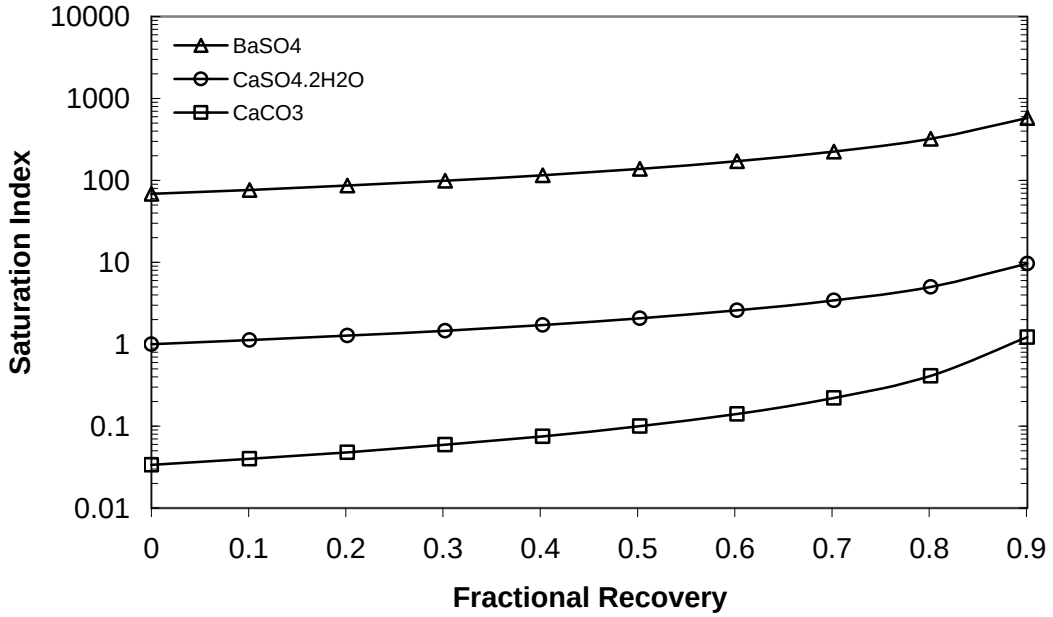

Figure 5-25. Saturation indices vs recovery (LNW, TDS 11030, pH 6.0)

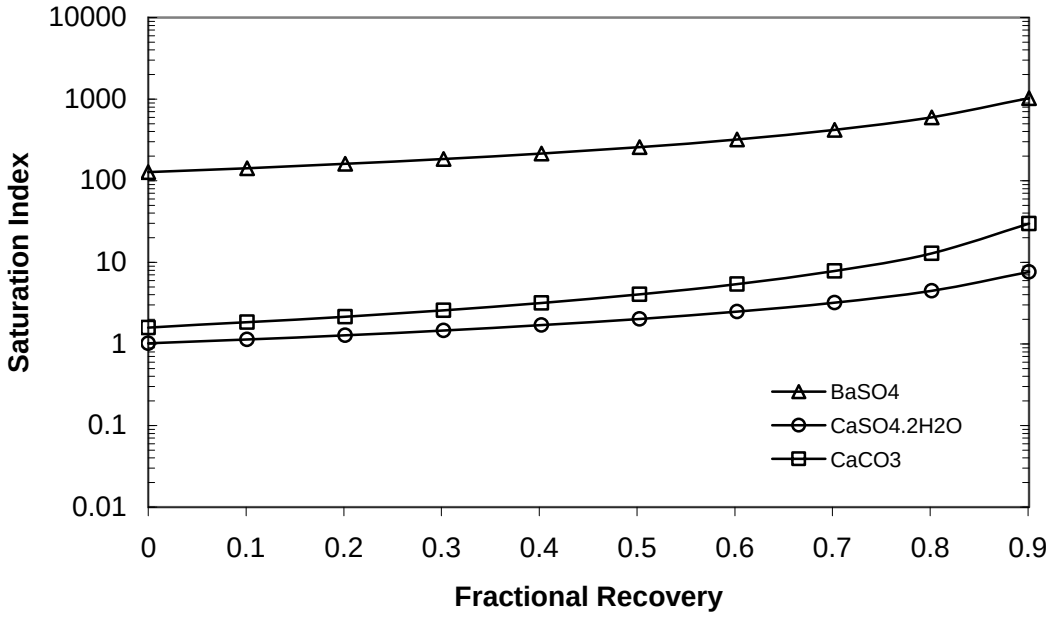

Figure 5-26. Saturation indices vs recovery (OAS, TDS 11100, pH 7.5)

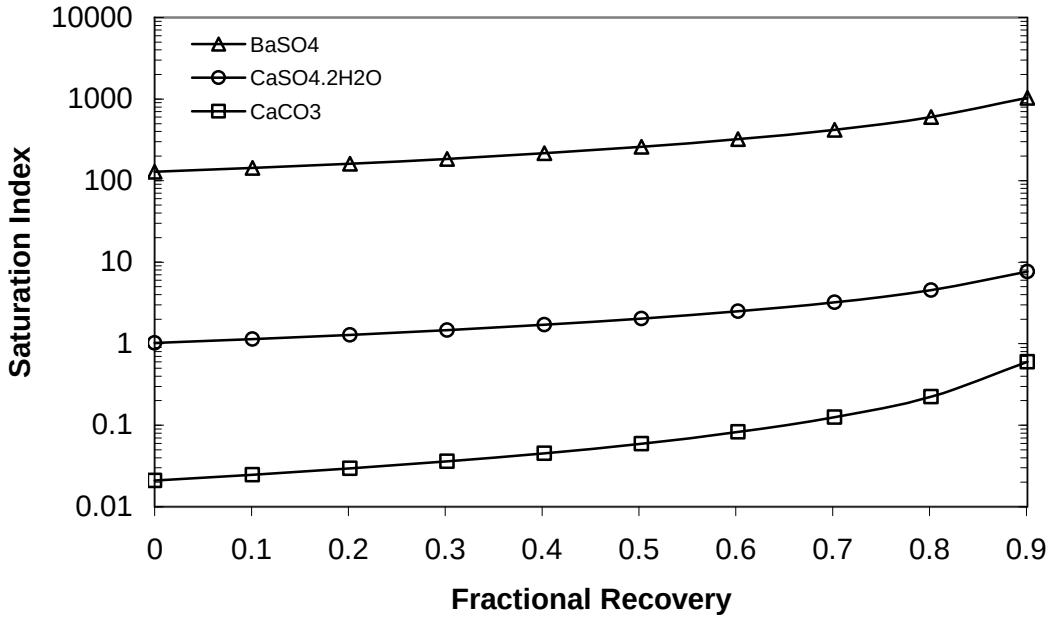

Figure 5-27. Saturation indices vs recovery (OAS, TDS 11100, pH 6.0)

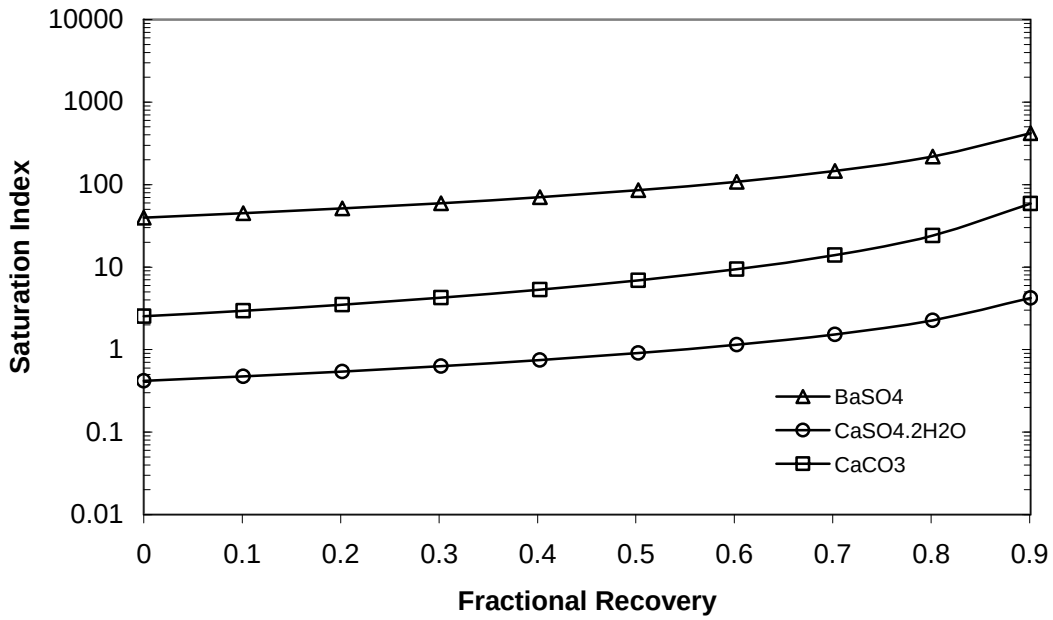

Figure 5-28. Saturation indices vs recovery (OAS, TDS 3828, pH 7.5)

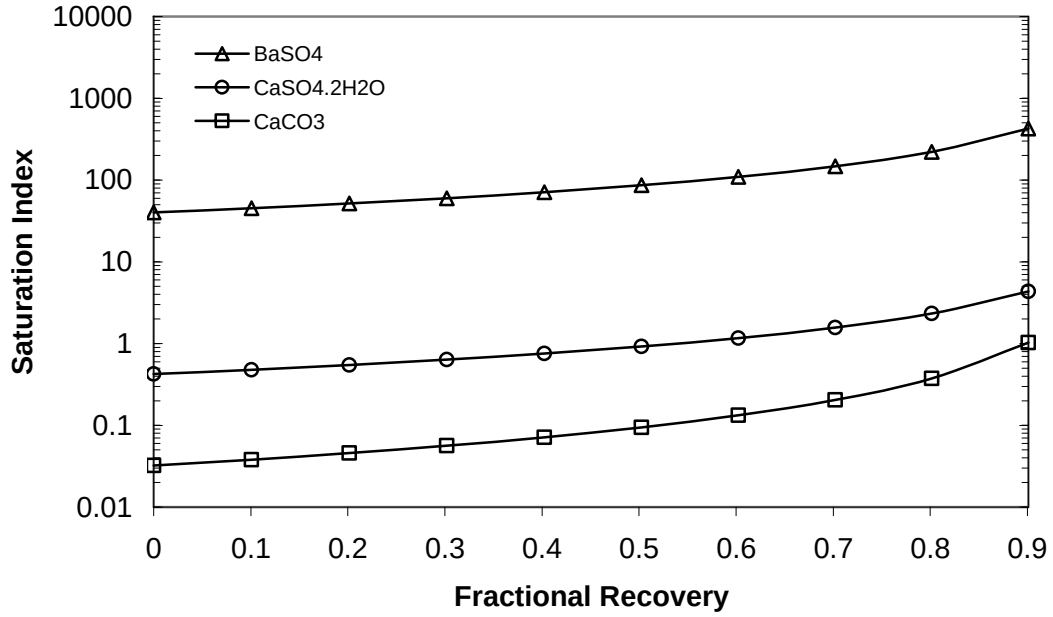

Figure 5-29. Saturation indices vs recovery (OAS, TDS 3828, pH 6.0)

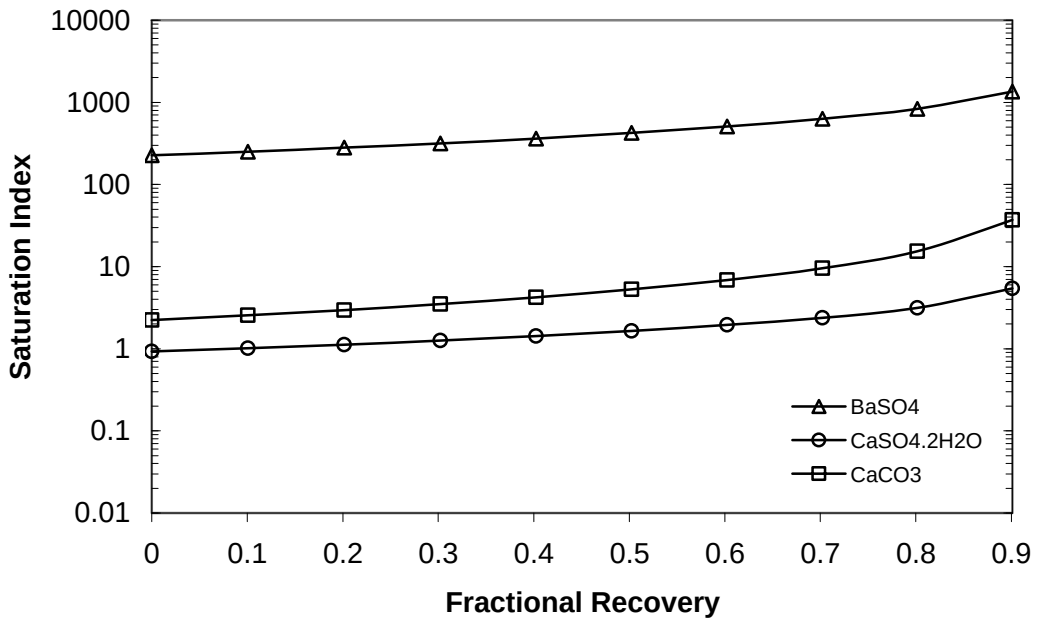

Figure 5-30. Saturation indices vs recovery (VGD, TDS 29760, pH 7.5)

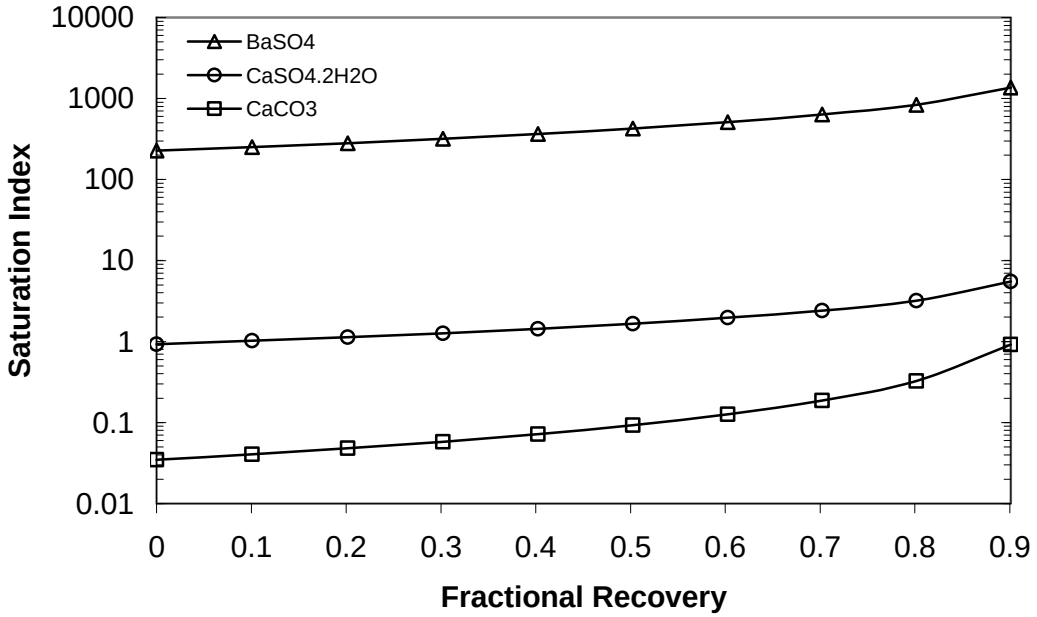

Figure 5-31. Saturation indices vs recovery (VGD, TDS 29760, pH 6.0)

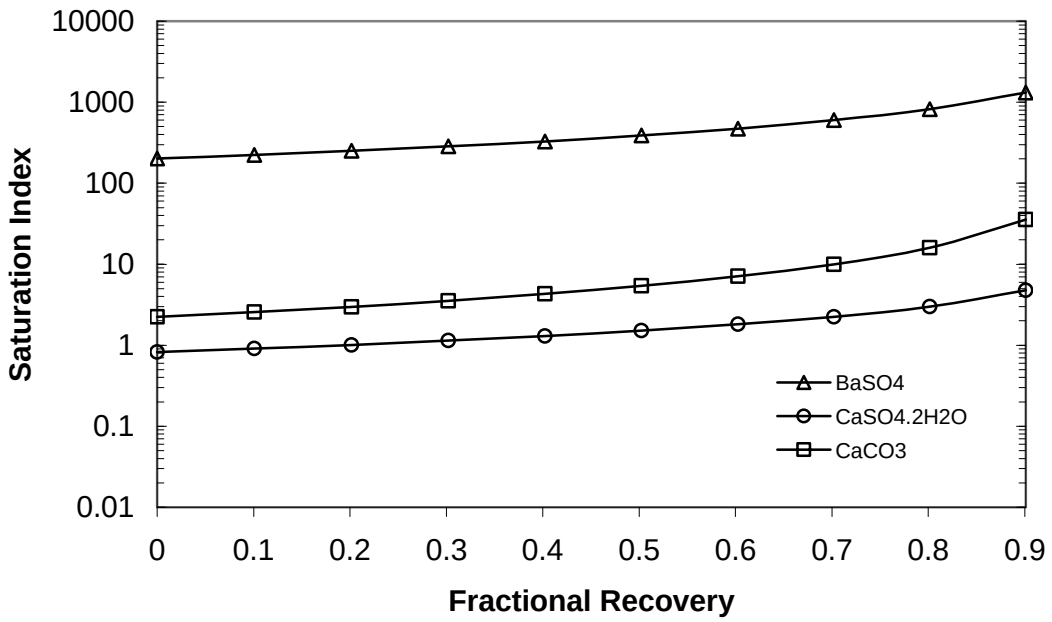

Figure 5-32. Saturation indices vs recovery (VGD, TDS 14110, pH 7.5)

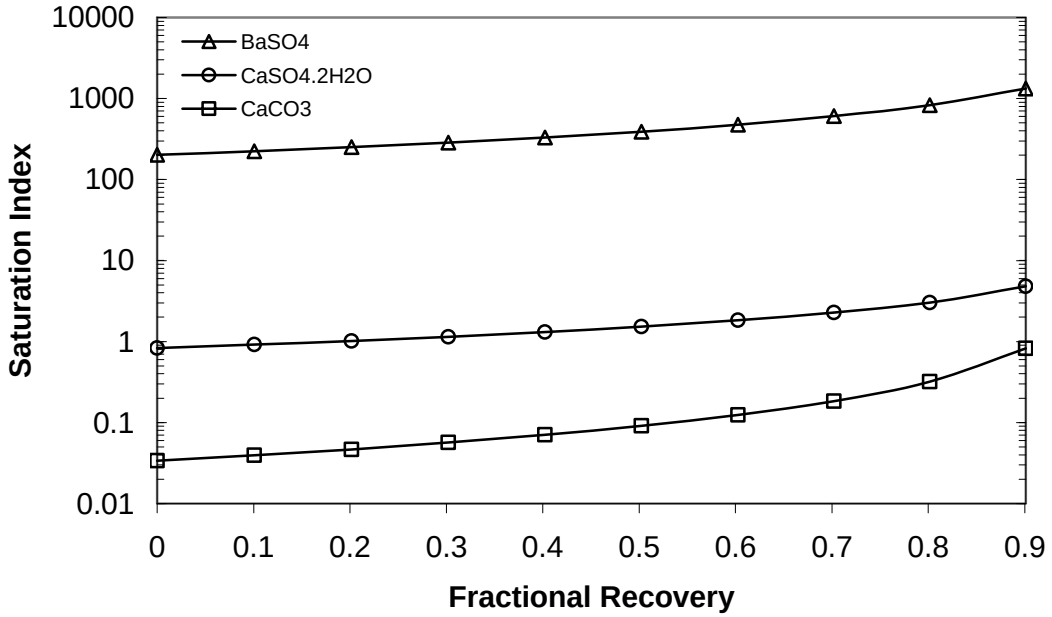

Figure 5-33. Saturation indices vs recovery (VGD, TDS 14110, pH 6.0)

As illustrated in Figures 5-18 through 5-33, SI_B, SI_C, and SI_G all increase with increasing recovery as would be expected. When comparing the SI values at pH 7.5 to those at pH 6.0, it is apparent that SI_G and SI_B do not vary significantly with pH (increasing less than 3 % and 1.5 % for SI_G and SI_B, respectively,

at 90 % recovery), while SI_C changes by nearly two orders of magnitude (decreasing by at least a factor of 40 at 90 % recovery) over the pH range of 7.5 to 6.0. It is noteworthy that at high recoveries the SIs for all scalants increase rapidly with increasing recovery. The SIs increase by about the same factor from between zero and 65 % recovery as they do from between 65 % and 90 % recovery.

The product water recovery limits were calculated with respect to gypsum and calcite for each of the four sample locations for both the samples having the highest TDS during the latest year of available data and for the samples having the lowest TDS over the same period. Both high and low TDS conditions were selected to illustrate the impact of seasonal variability on the recovery limits that are likely to be encountered for RO desalting of inland brackish water in the SJV. Recovery limits were calculated at a pH of 7.5 and 6.0 for comparison as shown in Table 5-4. Note that because there is no direct correlation between TDS and SI (i.e. water having the highest TDS does not necessarily have the highest SI), Table 5-4 may not necessarily contain the best and worst case recovery limits for each site. Nonetheless, TDS was selected as the basis for comparison of high and low recovery limits in the present study because TDS can be quickly and easily measured in field RO desalting operations, while SI calculations require complete water composition which can take weeks to acquire.

Table 5-4. Recovery limits (SI = 1) with respect to gypsum and calcite at pH = 7.5 and 6.0 for water samples having the max and min TDS observed during the latest year of reported data [11].

			Recovery Limits			
			pH =7.5		**pH = 6.0**	
Site	**Sample Date**	**TDS**	**gypsum**	**calcite**	**gypsum**	**calcite**
CNR 0801	11/12/2003	9136	25%	0%	24%	86%
CNR 0801	7/28/2003	4660	20%	0%	19%	88%
LNW 6467	9/9/2003	13400	0%	0%	0%	86%
LNW 6467	7/28/2003	11030	0.33%	0%	0.002%	87%
OAS 2548	1/12/2004	11100	0%	0%	0%	93%
OAS 2548	9/9/2003	3828	54%	0%	53%	90%
VGD 4406	1/13/2004	29760	8.5%	0%	7.6%	91%
VGD 4406	7/29/2003	14110	19%	0%	18%	92%

All water samples are saturated or near saturated with gypsum and oversaturated with calcite and barite at a pH of 7.5 (near the natural pH of the water samples), thus calcite scaling would limit the water recovery for each location. When the pH is lowered to 6.0, gypsum becomes the limiting scalant with respect to recovery. Barite scaling is not expected to be a limiting factor because, even though the water is oversaturated in barite, Barium is present at very low concentrations at or below detection limits and the total mass of barite that could scale is very small. Also, experience shows that because of the slow kinetics of barium sulfate, precipitation is not a problem at the residence times typically

observed in RO desalination units [20, 28, 35]. The recovery limits with respect to scaling for each water sample location are summarized below.

i. CNR 0801 (2003 –2004)

The percent recovery limit (i.e. at SI_G = 1.0) at this location is 24 % for the highest observed TDS (9136 mg/L) and 19 % for the lowest TDS (4660 mg/L) at a pH of 6.0. It is noteworthy that the percent recovery limit imposed by gypsum is actually higher at the higher TDS because of variations in water composition between the samples.

ii. LNW 6467 (2003 –2004)

Of the four locations analyzed, the lowest recovery limit would be expected at this location based on gypsum scaling (highest average SI_G of all locations was 0.99) with SI_G ranging from 0.91 to 1.03 over the course of a year. The water sample with the highest TDS observed over the latest year (13,400 mg/L) is oversaturated in gypsum (SI_G = 1.03), thus RO desalting would not be feasible without scale mitigation. At the lowest TDS, RO desalting at this site would be limited to a recovery of 0.002 %. Water from this location would require pretreatment and/or antiscalants to achieve any reasonable product water recovery.

iii. OAS 2548 (2003 –2004)

This location had the largest range of recovery limits based on gypsum scaling from zero % at the high TDS (11,100 mg/L) to 53 % at the low TDS (3828 mg/L), corresponding to both the highest and lowest recoveries observed at all four locations.

iv. VGD 4406 (2003 –2004)

This location had the highest observed TDS (29,760 mg/L) of all four sample locations, even its minimum TDS (14,110 mg/L) during the latest year of available data is higher than the maximum TDS seen at any of the other three locations (13,400 mg/L at LNW). However, when compared to the recoveries at each location's high TDS value, the recovery limit at this location is 7.6% which is greater than two of the other locations, LNW and OAS, which have TDS values less than half of VGD's value. Also, at VGD's low TDS, the recovery limit is 18%, which is higher than the recovery limit at LNW (0.002%) and nearly as high as the CNR (19%).

5.1.3 Field Water Sample Data (2006–2007)

The more recent water quality data was provided by DWR in 25-gallon water samples for each of the five chosen sites for analysis. A summary of the data and the detailed water quality analyses for the five locations and are shown in Tables 5-5 and 5-6, respectively.

Table 5-5. Field sample water quality and SI summary (2006–2007)

Name	Sample Date	Location	TDS, mg/L	pH	Total Alk, mg/L as $CaCO_3$	SI_C	SI_G	SI_S
CNR 0801	7/31/2006	Southern Area, Kern Lakebed	6372	7.5	230	2.70	0.704	0.222
LNW 6467	2/15/2006	Southern Area, Lost Hills	11270	7.6	128	2.72	1.03	0.345
OAS 2548	4/10/2006	Central Area	11020	7.6	213	3.02	0.985	0.287
VGD 4406	11/13/2006	Southern Area, Lemoore	28780	7.6	368	2.18	0.953	0.377
ERR 8429	1/29/2007	Southern Area, Corcoran	4115	8.0	706	9.50	0.120	0.339

Note: Values are those measured on the sampling date.

Table 5-6. Detailed water quality analyses (2006–2007)

Measurement	Units	Location				
		CNR	**LNW**	**OAS**	**VGD**	**ERR**
Conductance	µS/cm	7111	14430	12620	26070	5580
pH	pH units	7.5	7.6	7.6	7.6	8
UV Absorbance (254 nm)	absorbance/cm	0.126	0.094	0.13	0.178	0.587
Dissolved Measurements						
Bicarbonate	mg/L as $CaCO_3$	229	128	212	367	699
Boron	mg/L	13.5	17.5	23.5	43.4	2.6
Calcium	mg/L	350	625	462	422	88
Carbonate	mg/L as $CaCO_3$	1*	1*	1*	1*	7
Chloride	mg/L	324	3020	1060	1910	632
Fluoride	mg/L	5*	10*	10*	5*	5*
Hydroxide	mg/L as $CaCO_3$	1*	1*	1*	1*	1*
Magnesium	mg/L	236	198	284	962	59
Nitrate	mg/L	344	155	46.7	51.9	51.3
DOC	mg/L as C	4.2	4.6	5.1	6.2	15.8
Potassium	mg/L	46.7	5*	5*	7.8	3.5
Selenium	mg/L	0.032	0.223	0.184	0.05*	0.011
Silica	mg/L	23.5	37.9	31.4	43.2	38
Sodium	mg/L	1250	2820	2780	9270	1250
Sulfate	mg/L	3700	4520	6360	21400	1570
Total Measurements						
Total Alkalinity	mg/L as $CaCO_3$	230	128	213	368	706
Aluminum	mg/L	0.1*	0.1*	0.05*	0.5*	0.102
Arsenic	mg/L	0.01*	0.014	0.006	0.05*	0.089
Barium	mg/L	0.5*	0.5*	0.25*	2.5*	0.5*
TDS	mg/L	6372	11270	11020	28780	4115
Iron	mg/L	0.174	0.152	0.045	1.41	0.279
Manganese	mg/L	0.05*	0.05*	0.025*	1.55	0.595
TOC	mg/L as C	4.5	3.4	5.1	6.2	16.7
Phosphorus	mg/L	0.01*	0.03	0.08	0.12	1.96
Selenium	mg/L	0.034	0.235	0.195	0.05*	0.013
Strontium	mg/L	17.2	9.96	5.5	9.6	0.898
TSS	mg/L	1*	4	4	2	4

***** Measured value is at or below reporting limit.

5.1.3.1 pH Dependence of Saturation Indices

The saturation indices of sparingly soluble salts depend on pH to varying degrees. The relationship between pH and SI (at 20 ºC) is shown in Figs 5-36 through 5-40 for gypsum, calcite, barite, and silica for field water samples from each of the locations listed in Table 5-5. The values for barite are provided for illustrative purposes only because the barium concentration is known only to be at or below the detection limits which vary between 0.25 to 1.0 mg/L. The actual barium concentrations may be much lower.

As illustrated previously in Figures 4-11 through 4-18 for the recent water quality data (2003–2004), Figures 5-36 through 5-40 illustrate, for the field water sample data (2006–2007), that SI_C is pH sensitive, increasing by several orders of magnitude over the pH range shown (4 to 10), while SI_G decreases by less than 15% and SI_B changes by less than 3% over the same pH range of 4 to 10 (except for water from ERR where the SI_G and SI_B decrease by 58% and 22%, respectively). The silica saturation index (SI_S) at each location decreases by more than one order of magnitude over the same pH range of 4 to 10.

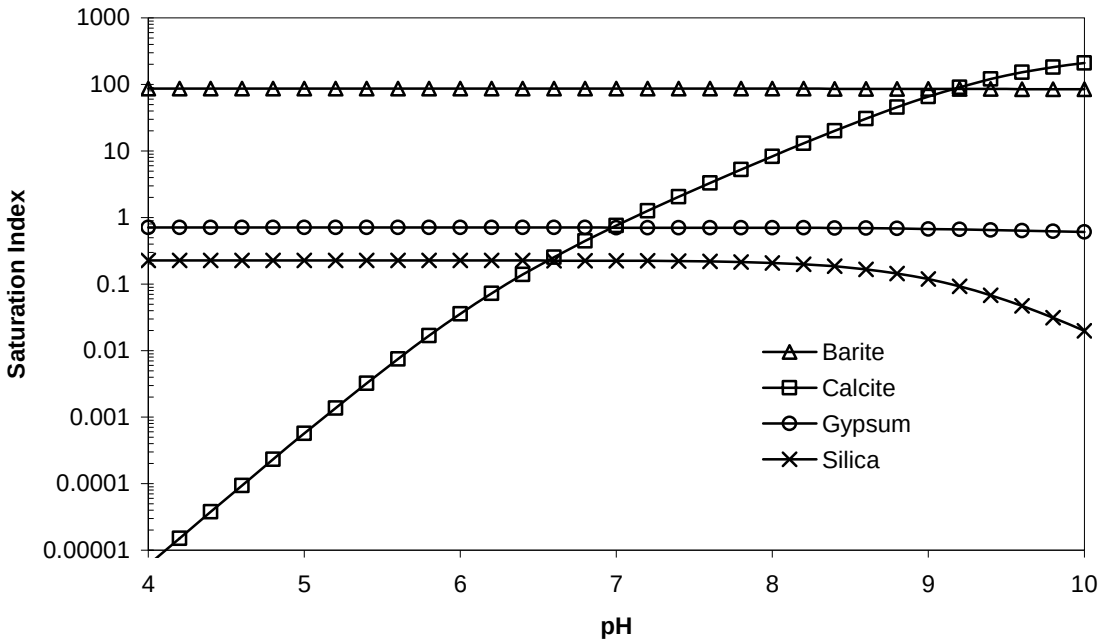

Figure 5-36. Mineral salt solubility dependence on pH for CNR field water sample (see Table 5-6)

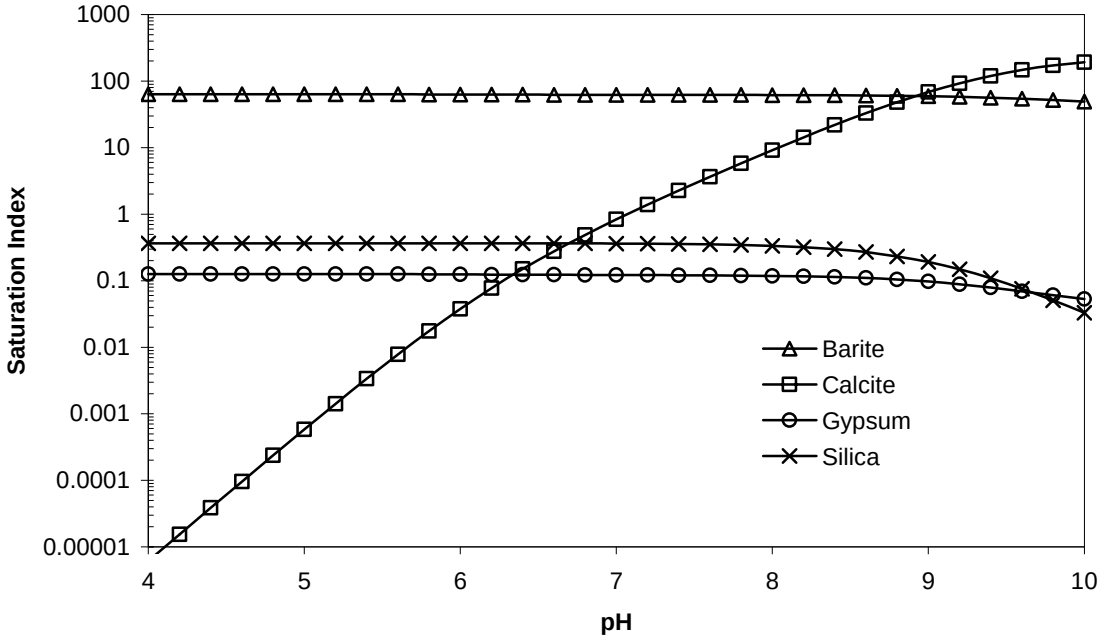

Figure 5-37. Mineral salt solubility dependence on pH for ERR field water sample (see Table 5-6)

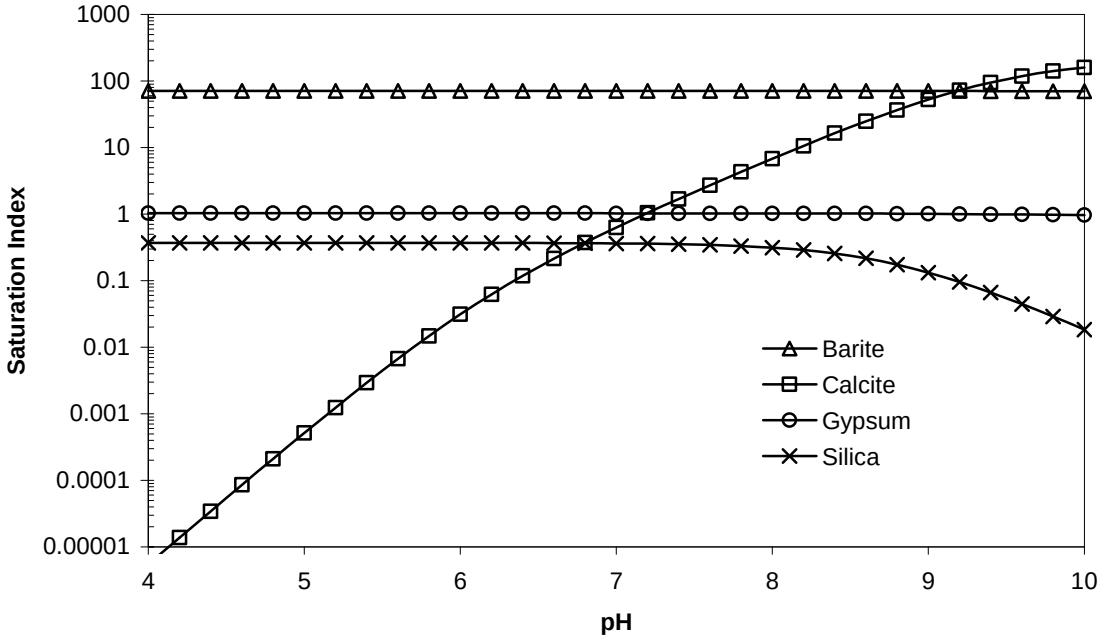

Figure 5-38. Mineral salt solubility dependence on pH for LNW field water sample (see Table 5-6)

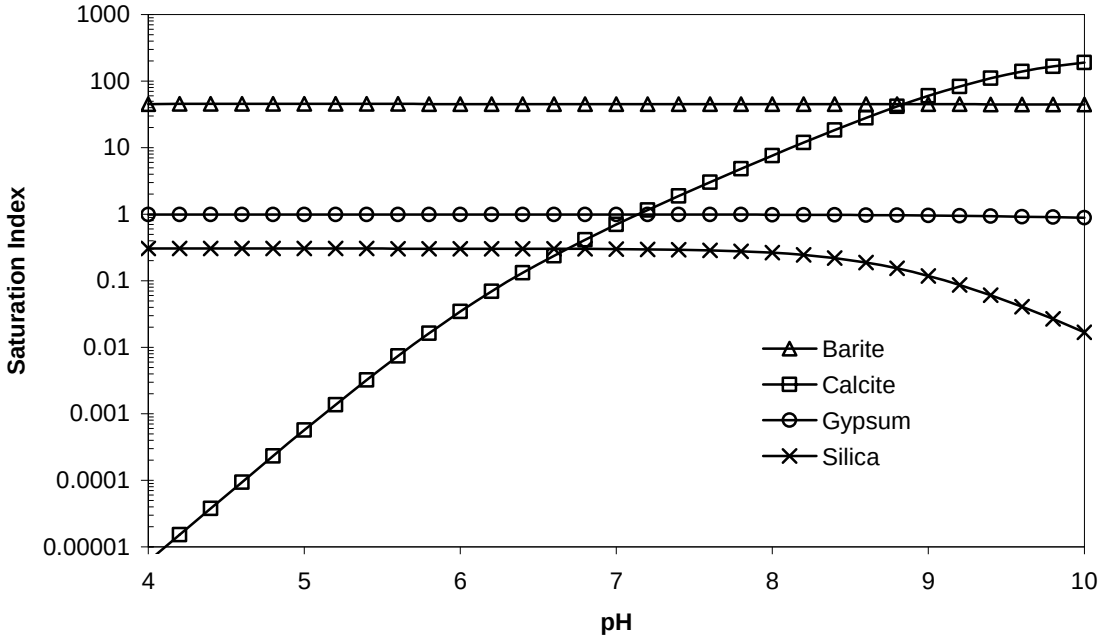

Figure 5-39. Mineral salt solubility dependence on pH for OAS field water sample (see Table 5-6)

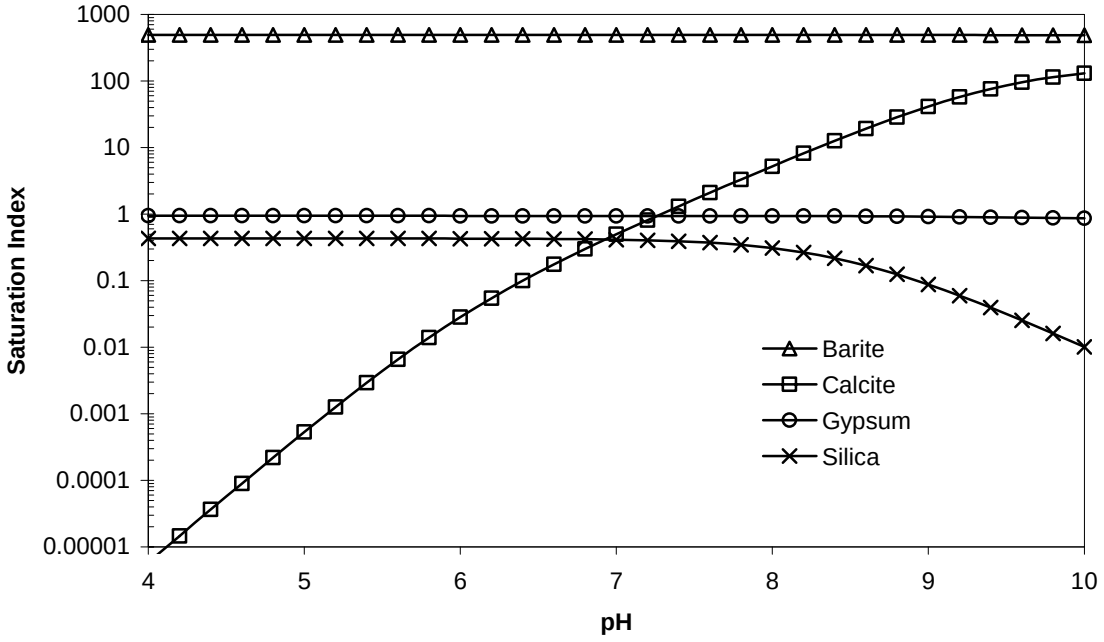

Figure 5-40. Mineral salt solubility dependence on pH for VGD field water sample (see Table 5-6)

5.1.3.2 Recovery Limits

SI_C, SI_G, and SI_S were calculated as a function of the product water recoveries. The analysis was carried out by holding the pH constant first at the water's natural pH and then at 6.0 by addition of sodium hydroxide or hydrochloric acid as needed. The above pH conditions were chosen for each location to illustrate the effectiveness of pH reduction on increasing the recovery limits with respect to calcite as is the common practice in RO desalination plants.

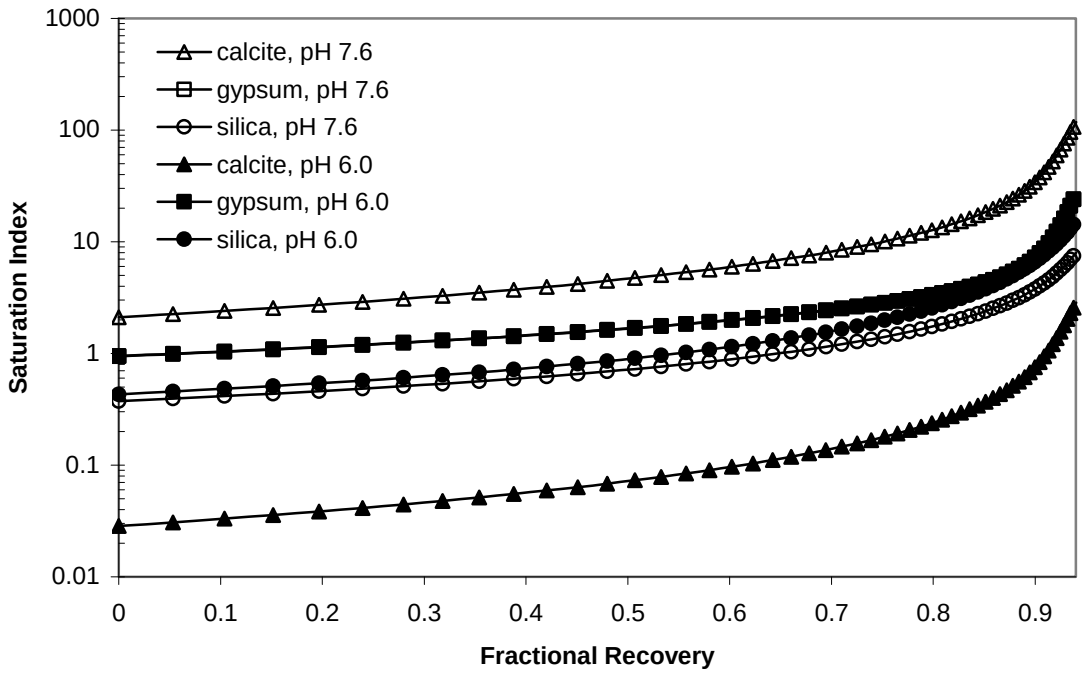

Figure 5-41. VGD field water saturation indices as a function of recovery (see Table 5-6)

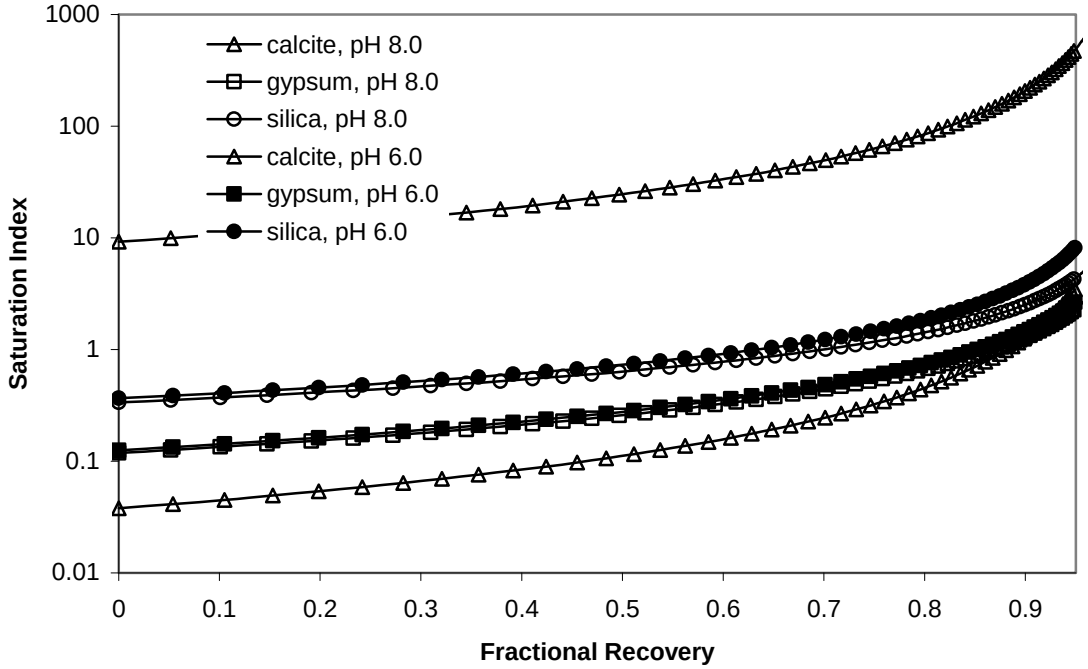

Figure 5-42. ERR field water saturation indices as a function of recovery (see Table 5-6)

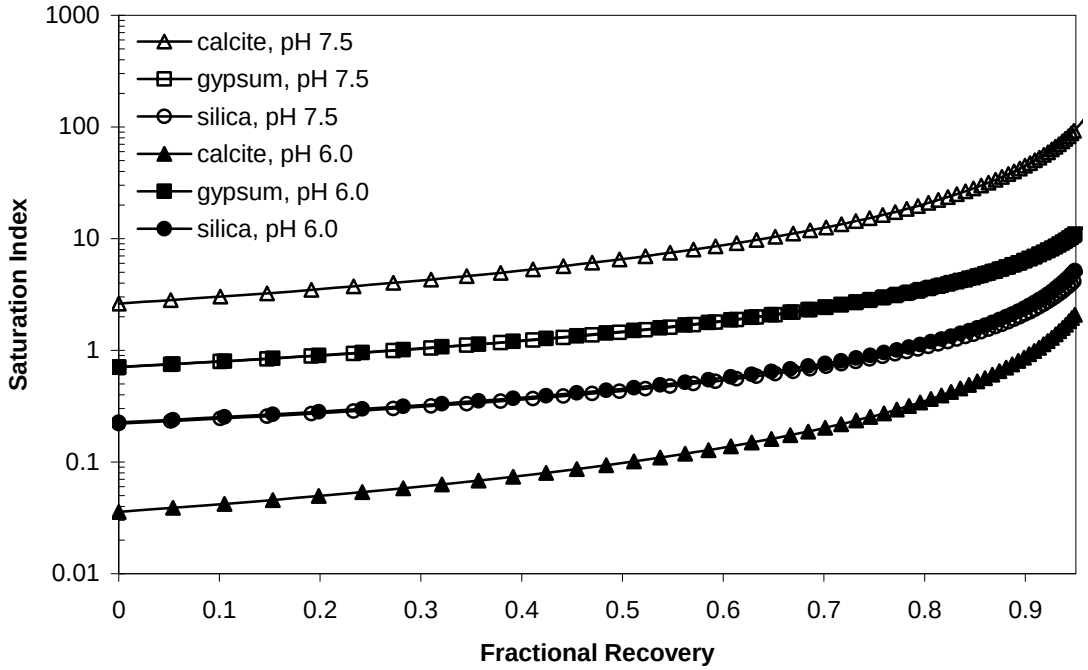

Figure 5-43. CNR field water saturation indices as a function of recovery (see Table 5-6)

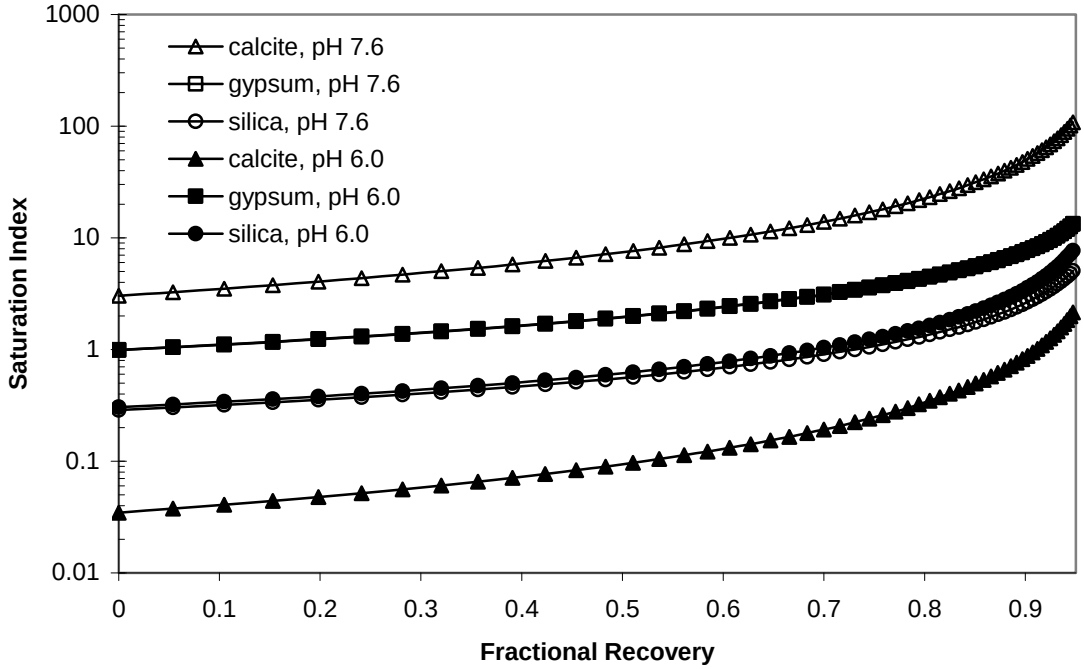

Figure 5-44. OAS field water saturation indices as a function of recovery (see Table 5-6)

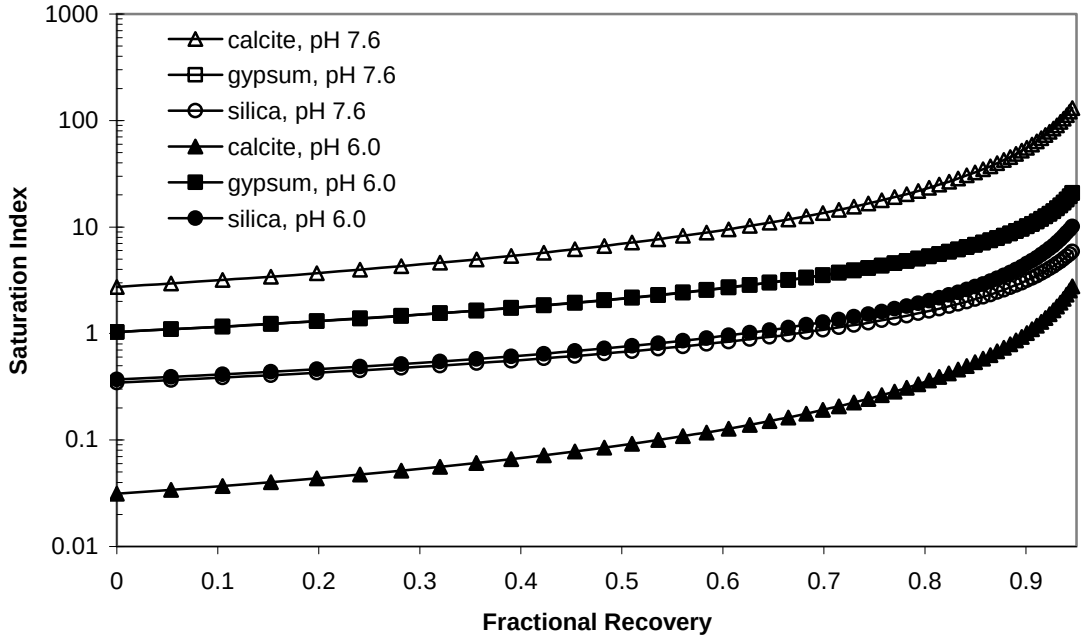

Figure 5-45. LNW field water saturation indices as a function of recovery (see Table 5-6)

The RO product water recovery limits were calculated with respect to potential scaling by gypsum, calcite, and silica for field water samples from each of the five sample locations (Table 5-2). Calcite and silica recovery limits were calculated at the natural pH of the field samples and at a reduced pH of about 6.0 so as to compare the recovery limits with and without pH adjustment. Additionally, the recovery limit associated gypsum for SI = 1 and SI = 2.3 were determined in order to compare the recovery limits with and without antiscalant addition. Two possible osmotic pressure recovery limits were also calculated as the recovery at which the osmotic pressure equals 600 and 1000 psi—two common maximum operating pressures for RO pressure vessels.

Table 5-7. Field water sample recovery limits

			Pressure Recovery Limits		**Scaling Recovery Limits**				
Site	**TDS, mg/L**	**Nat pH**	**π = 600 psi**	**π =1000 psi**	**Calcite (nat pH)**	**Calcite (pH 6)**	**Gypsum (pH 6)**	**Gypsum (pH 6)**	**Silica (pH 6)**
					SI = 1	SI = 1	SI = 1	SI = 2.3	SI = 1
VGD	28780	7.6	69.9%	81.4%	oversat.	91.1%	6.17%	67.0%	54.9%
ERR	4116	8.0	94.3%	96.5%	oversat.	88.2%	85.3%	94.0%	63.4%
CNR	6372	7.5	94.3%	96.5%	oversat.	91.0%	27.3%	68.2%	77.0%
OAS	11020	7.6	88.9%	93.1%	oversat.	91.1%	0.70%	57.9%	68.9%
LNW	11270	7.6	83.2%	89.6%	oversat.	90.0%	oversat.	53.6%	62.1%

Note: Bold values are the ultimate recovery limits with pH adjustment and antiscalant use**.**

Brackish water from each of the five locations is oversaturated with respect to calcite at the natural pH levels. Therefore, without pH adjustment, RO desalting of water at any of the five locations (Table 5-2) would not yield product water without risking scaling the membranes with calcite. When the pH is adjusted to 6.0 (e.g. by acid addition), the calcite scaling recovery limits increase to 88.2%–91.1% due to the elimination of calcite scaling. Since calcite scaling can be controlled by pH adjustment, gypsum scaling is the next important recovery limiting scalant. Without the use of antiscalants, gypsum scaling would limit the recovery for each location except for ERR which would still be limited by potential silica scaling (at pH = 6.0). It is noted that water at LNW is oversaturated with respect to gypsum. However, because gypsum scaling can be controlled with appropriate antiscalant addition up to $SI_G = 2.3$, the recovery limits could be greatly increased (with antiscalant use) to between 53.6% and 94.0%. Silica scaling would limit recovery to the range of 54.9%–77.0%. The recovery limits at osmotic pressures of 600 psi and 1000 psi are in the range of 69.9%–94.3% (600 psi) and 81.4%–96.5% (1000 psi), respectively. It is noted that even at the lower osmotic pressure limit of 600 psi, scaling remains the dominant factor that would limit recovery. Practical or economic considerations, however, may lead to a lower recovery limit depending on the maximum allowable operating pressure.

The ultimate recovery limits for each location (with antiscalant use and pH adjustment) are between 53.6% and 68.2%. Desalting for VGD and ERR source water would be limited by silica scaling to recoveries of 54.9% and 63.4%, respectively, while at CNR, OAS, and LNW desalting would be limited by gypsum scaling to recoveries of 68.2%, 57.9%, and 53.6%, respectively.

The analysis of the present study demonstrated that: (1) recovery limits can be estimated for field water sources prior to pilot studies; (2) potential recovery bottlenecks (e.g. scaling, osmotic pressure) can be anticipated and pilot study operations can be optimized for a particular water source and thus assist in the design of pilot studies; (3) pilot and full-scale RO plants should be designed to accommodate the expected range of feed water quality reducing the need for costly modifications after being built. It must be recognized, however, that the present study does not account for recovery limitations that may be imposed by colloidal fouling, organic fouling, or biofouling.

5.2 Diagnostic Flux Decline Experiments

Diagnostic flux decline experiments were performed on field water samples from the five selected locations in the San Joaquin Valley (see Table 5-2, §5.1.1) to assess the feasibility for RO desalination of water from these locations. The diagnostic experiments were performed for field water samples rather than model solutions to more closely represent natural conditions with respect to the source water quality. Three distinct experiments were performed for each field water sample (except for LNW field water for which only two of the experiments conducted are reported) by changing the initial conditions of the sample water, while leaving the operating conditions unchanged: (1) at the natural pH without any adjustment (pH 7.42 to pH 8.02), with adjustment to a low target of pH 6.0 (in practice the adjusted pH ranged from 5.27 to 6.48), and with adjustment to a low target of pH 6.0 with antiscalant addition (0.20 ppm PC-504). The operating conditions for the experiments were selected to impose an average CP such that over a 24-hr period substantial flux declines would be observed (see Table 5-7). The CP was controlled by adjusting the operating pressure and cross-flow rates which in turn change the permeate flux and mass transfer coefficient (see Eq 2-3).

The flux decline for each run was measured by plotting the relative flux (the flux at a given time divided by the initial flux) versus time. Although most of the runs were started at nearly the same initial flux (within 2%), and considering that in some cases the final flux decline was small (< 10%), the flux measurements were normalized (with respect to the initial flux) in order to make better comparisons among all of the runs. The percent flux decline, *FD*, is defined as:

$$FD = \left(1 - \frac{F_f}{F_i}\right) \cdot 100 \qquad (5\text{-}1)$$

where, F_f and F_i are the final and initial fluxes, respectively.

The initial average SI values for calcite, gypsum, and silica, at the membrane surface ($SI_{M,C}$, $SI_{M,G}$, and $SI_{M,S}$, respectively), were calculated by first estimating the average CP (CP_{avg}) for each run and then calculating the initial SI values at the new concentration by using CP_{avg} as a concentration factor (see Eq 3-1, §3.2). CP_{avg} was estimated by the finite element numerical model developed by Lyster and Cohen [26] which considers the fully coupled governing equations for fluid dynamics and mass transfer. A summary of the experimental conditions and the observed final 24-hour flux declines is provided below.

Table 5-8. Diagnostic flux decline experimental conditions and 24-hour flux decline

Site	Condition	TDS, mg/L	pH	x-flow, L/min	F_i, µm/s	P, psi	CP_{avg}	$SI_{M,C}$	$SI_{M,G}$	$SI_{M,S}$	FD	$R_{w,eqv}$
VGD	Nat. pH	28780	7.53	0.76	13.60	453	1.60	3.22	1.42	0.606	7.96 %	38%
VGD	Low pH	28780	5.56	0.76	13.54	432	1.59	0.0115	1.43	0.712	8.88 %	38%
VGD	Low pH+AS	28780	5.93	0.76	13.60	455.5	1.61	0.0447	1.44	0.720	9.36 %	38%
ERR	Low pH & AS	4116	6.00	0.76	24.45	276.1	2.12	0.128	0.301	0.787	7.54 %	53%
ERR	Low pH	4116	5.37	0.76	24.43	306.5	2.12	0.0105	0.307	0.786	11.6 %	53%
ERR	Nat. pH	4116	8.02	0.76	24.46	302.3	2.13	29.3	0.280	0.678	12.4 %	53%
CNR	Nat. pH	6375	7.50	0.76	24.41	277.7	2.11	7.37	1.53	0.464	6.37 %	53%
CNR	Low pH	6372	5.27	0.76	24.44	270.0	2.11	0.00613	1.55	0.487	11.0 %	53%
CNR	Low pH & AS	6372	6.00	0.76	24.42	290.9	2.12	0.111	1.55	0.487	6.73 %	53%
OAS	Low pH & AS	11020	5.94	0.76	24.36	349.0	2.11	0.862	2.10	0.660	7.89 %	53%
OAS	Low pH	11020	5.47	0.76	24.46	374	2.1	0.0140	2.10	0.657	47.4 %	53%
OAS	Nat. pH	11020	7.42	0.76	24.52	362.5	2.1	5.41	2.08	0.613	11.2 %	53%
LNW	Low pH	11270	6.48	1.0	18.88	283	1.8	0.368	1.94	0.679	14.2 %	45%
LNW	Nat. pH	11270	7.43	1.0	19.08	280.5	1.8	4.24	1.93	0.636	10.7 %	45%

Note: $SI_{M,C}$, $SI_{M,G}$, and $SI_{M,S}$ are the initial average values at the membrane surface; x-flow is the cross-flow velocity of the feed; P is the applied pressure; $R_{W,eqv}$ is the equivalent recovery (see Eq 3-2, §3.4).

The results summarized in Table 5-8 show that the saturation indices and 24-hr percent flux declines do not appear to correlate with TDS. The above is not surprising since the specific composition of the various ions determines the scaling propensity of the water. For each experiment, silica (for the different source water locations) was undersaturated at the membrane surface with $SI_{M,S}$ ranging from 0.46 (CNR) to 0.79 (ERR). For each sample at its natural pH condition, calcite was above saturation with $SI_{M,C}$ ranging from 3.22 (VGD) to 29.3 (ERR); after pH adjustment each sample was undersaturated with

respect to calcite with SI values ranging from 0.00613 (CNR) to 0.862 (OAS). Gypsum was oversaturated at the membrane surface in each water sample except for ERR where its SI was around 0.3.

For all of the field water except for VGD and ERR, there was significantly more flux decline at the lower pH than at the natural pH of the water samples. Although the saturation indices of calcite decreased by at least an order of magnitude and the saturation indices of gypsum and silica increased only slightly at the lower pH, there was more flux decline at the lower pH likely due to faster precipitation kinetics. It has been shown for waters containing both sulfate and bicarbonate, that bicarbonate can retard gypsum scaling by reducing the appearance and growth rate of crystals on the membrane surface. When both bicarbonate and antiscalants were present, they were shown to have acted synergistically to retard gypsum scaling. When considering the antagonistic kinetic effect, a greater flux decline would be expected at the lower pH because of the greatly reduced bicarbonate concentrations as seen for CNR, OAS, and LNW. The reduced flux declines observed for all of the experiments with antiscalant addition may be explained by the synergistic effects of the antiscalant and bicarbonate acting to retard gypsum scaling [30].

Equivalent recoveries can be calculated for each diagnostic experiment by using Equation 3-1. This yields the recovery at which an actual RO module would experience average concentration levels in its exit region equivalent to those near the membrane in the plate-and-frame system. The actual recoveries for the diagnostic tests were 0.21% for VGD; 0.38% for ERR, CNR, and OAS; and 0.22%–0.23% for LNW. The equivalent operating recoveries (accounting for CP) for the diagnostic experiments were 38% for VGD; 53% for ERR, CNR, and OAS; and 45% for LNW. These results indicate that with the use of antiscalants and pH adjustment (e.g. acid addition) an RO process could feasibly operate at least at the above recovery levels, if not higher, because there was no visible scale present on any of the membranes under these conditions and the flux declines at these conditions (<10%) was likely due to residual compaction only.

For the experiments performed with no antiscalant addition, scale was either visible in both the natural and pH adjusted cases (CNR, OAS, VGD, LNW) or in neither case (ERR). The ERR field water was the only sample undersaturated with respect to gypsum at the membrane surface for the present RO operating conditions. This indicates that without the use of antiscalants, whether or not pH adjustment is incorporated, the recovery of an RO process will be limited by scaling to well below the equivalent experimental recoveries of 53% (CNR, OAS), 38% (VGD), and 45% (LNW). For ERR, however, the recovery limit with respect to scaling will likely be at least 53%. Flux decline plots and photographs of the membrane coupons after the 24-hour flux decline runs are shown below.

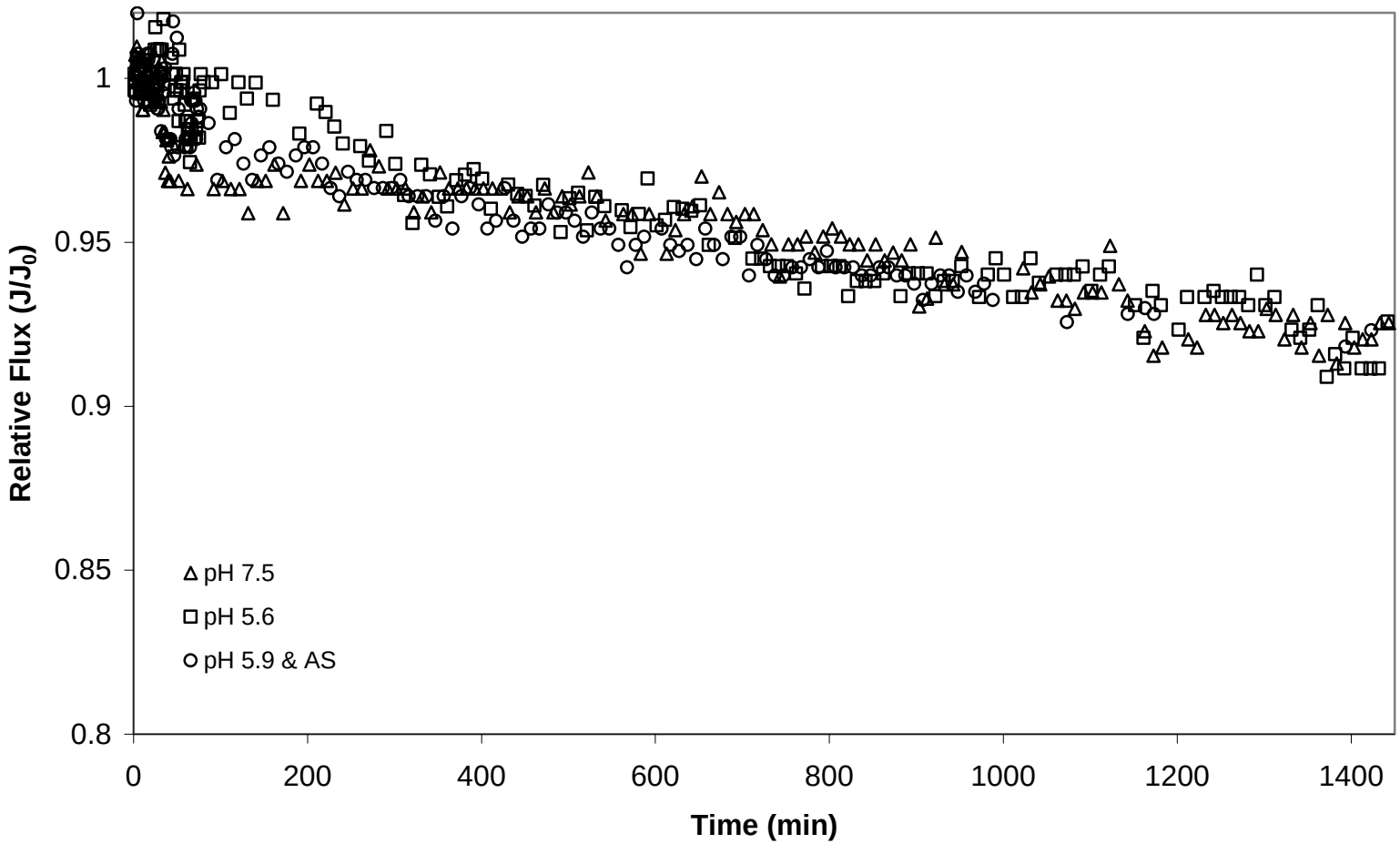

Figure 5-46. Relative permeate flux for diagnostic flux decline experiments for VGD field water sample at: (1) the native pH 7.5: 8.0% 24-hr flux decline, $SI_{G,M0}$ = 1.4, $SI_{C,M0}$ = 3.2, $SI_{S,M0}$ = 0.61; (2) pH 5.6: 8.9% 24-hr flux decline, $SI_{G,M0}$ = 1.4, $SI_{C,M0}$ = 0.012, $SI_{S,M0}$ = 0.71; and (3) pH 5.9 with 0.20 ppm AS: 9.4% 24-hr flux decline: $SI_{G,M0}$ = 1.4, $SI_{C,M0}$ = 0.045, $SI_{S,M0}$ = 0.72.

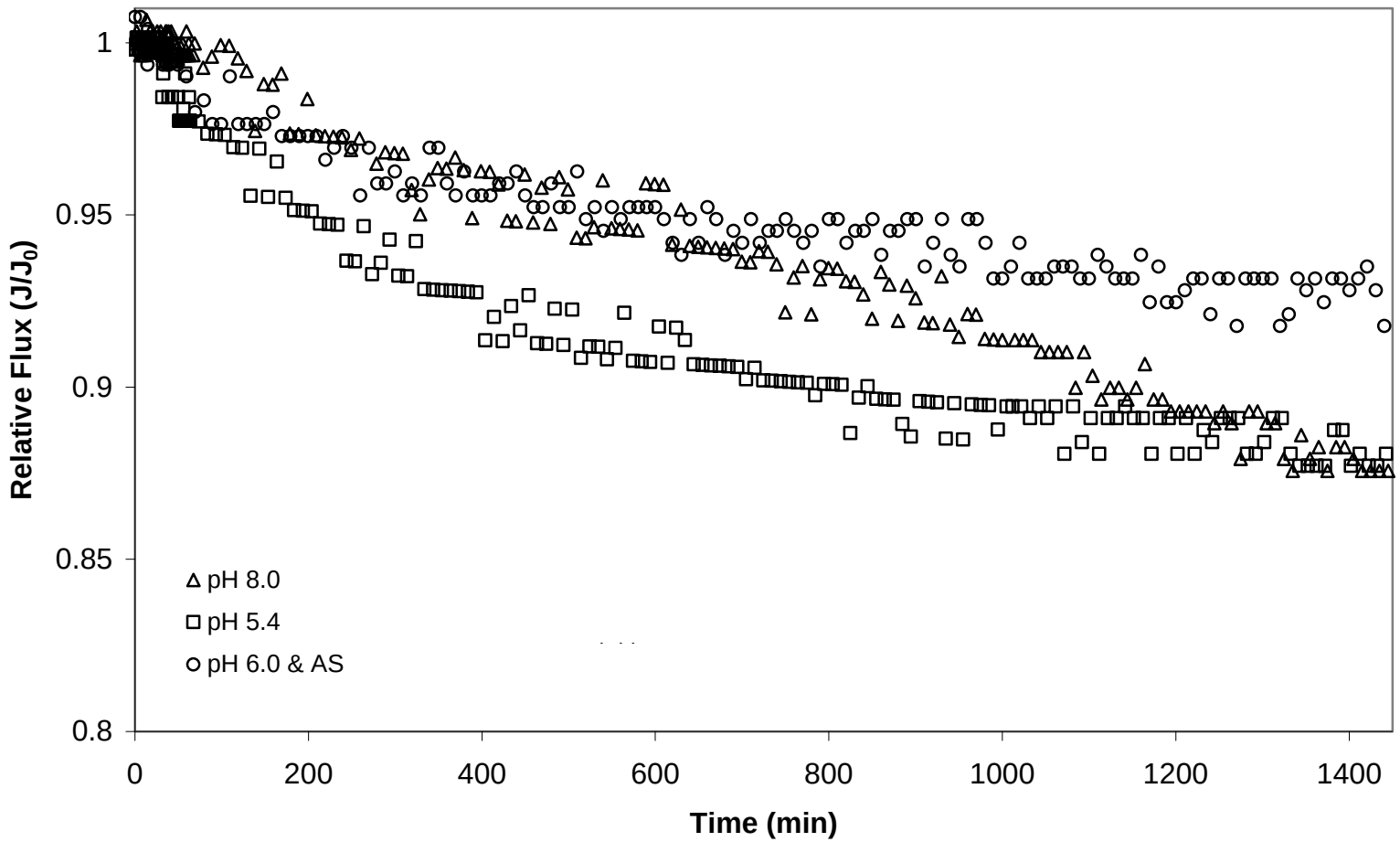

Figure 5-47. Relative permeate flux for diagnostic flux decline experiments for ERR field water sample at: (1) the native pH 8.0: 12.4% 24-hr flux decline, $SI_{G,M0}$ = 0.28, $SI_{C,M0}$ = 29, $SI_{S,M0}$ = 0.68; (2) pH 5.4: 11.6% 24-hr flux decline, $SI_{G,M0}$ = 0.31, $SI_{C,M0}$ = 0.011, $SI_{S,M0}$ = 0.79; and (3) pH 6.0 with 0.20 ppm AS: 7.5% 24-hr flux decline, $SI_{G,M0}$ = 0.30, $SI_{C,M0}$ = 0.13, $SI_{S,M0}$ = 0.79.

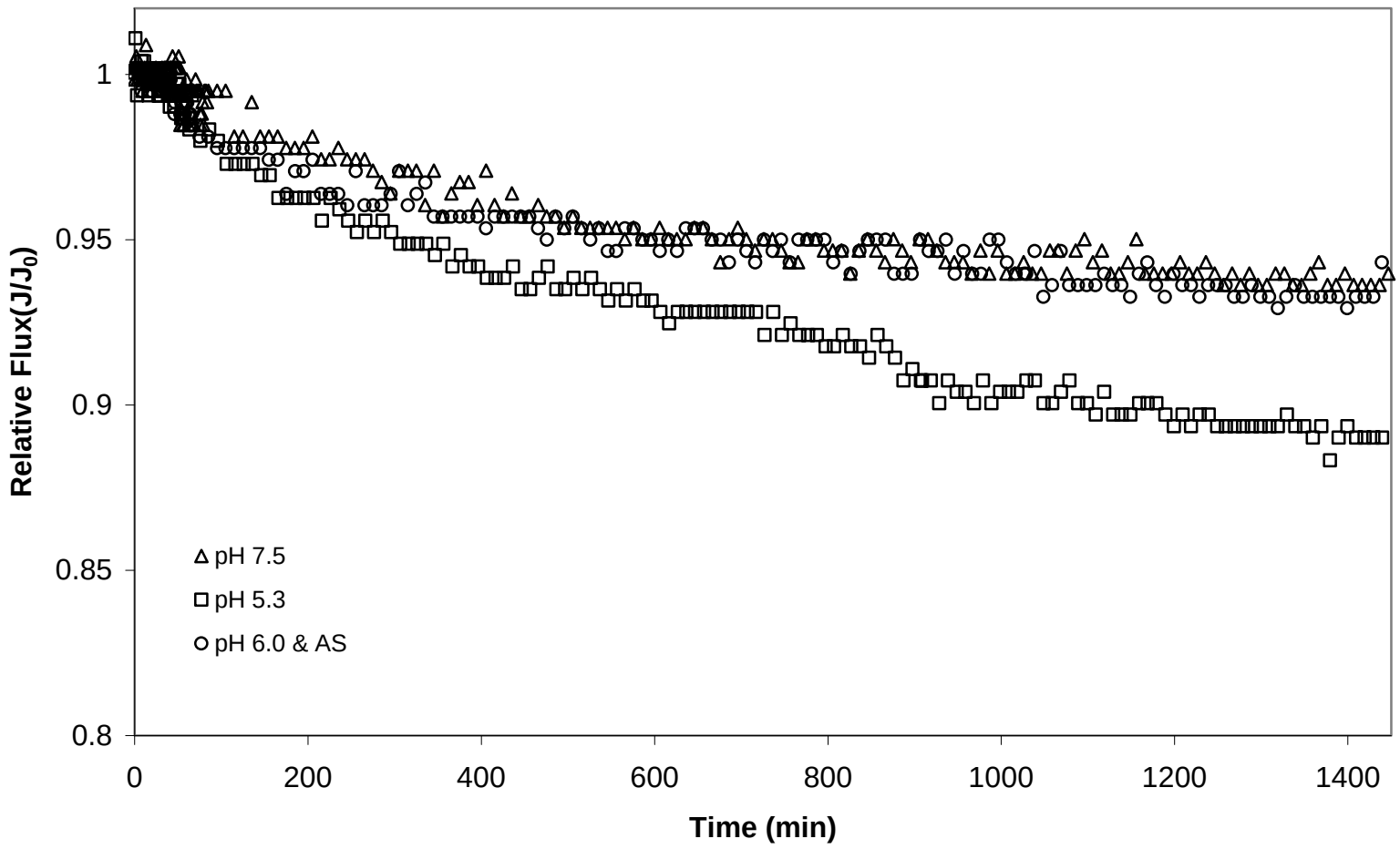

Figure 5-48. Relative permeate flux for diagnostic flux decline experiments for CNR field water sample at: (1) the native pH 7.5: 6.37% 24-hr flux decline, $SI_{G,M0}$ = 1.5, $SI_{C,M0}$ = 7.4, $SI_{S,M0}$ = 0.46; (2) pH 5.3: 11.0% 24-hr flux decline, $SI_{G,M0}$ = 1.5, $SI_{C,M0}$ = 0.0061 $SI_{S,M0}$ = 0.49; and (3) pH 6.0 with 0.20 ppm AS, 6.73% 24-hr flux decline, $SI_{G,M0}$ = 1.5 $SI_{C,M0}$ = 0.11, $SI_{S,M0}$ = 0.49.

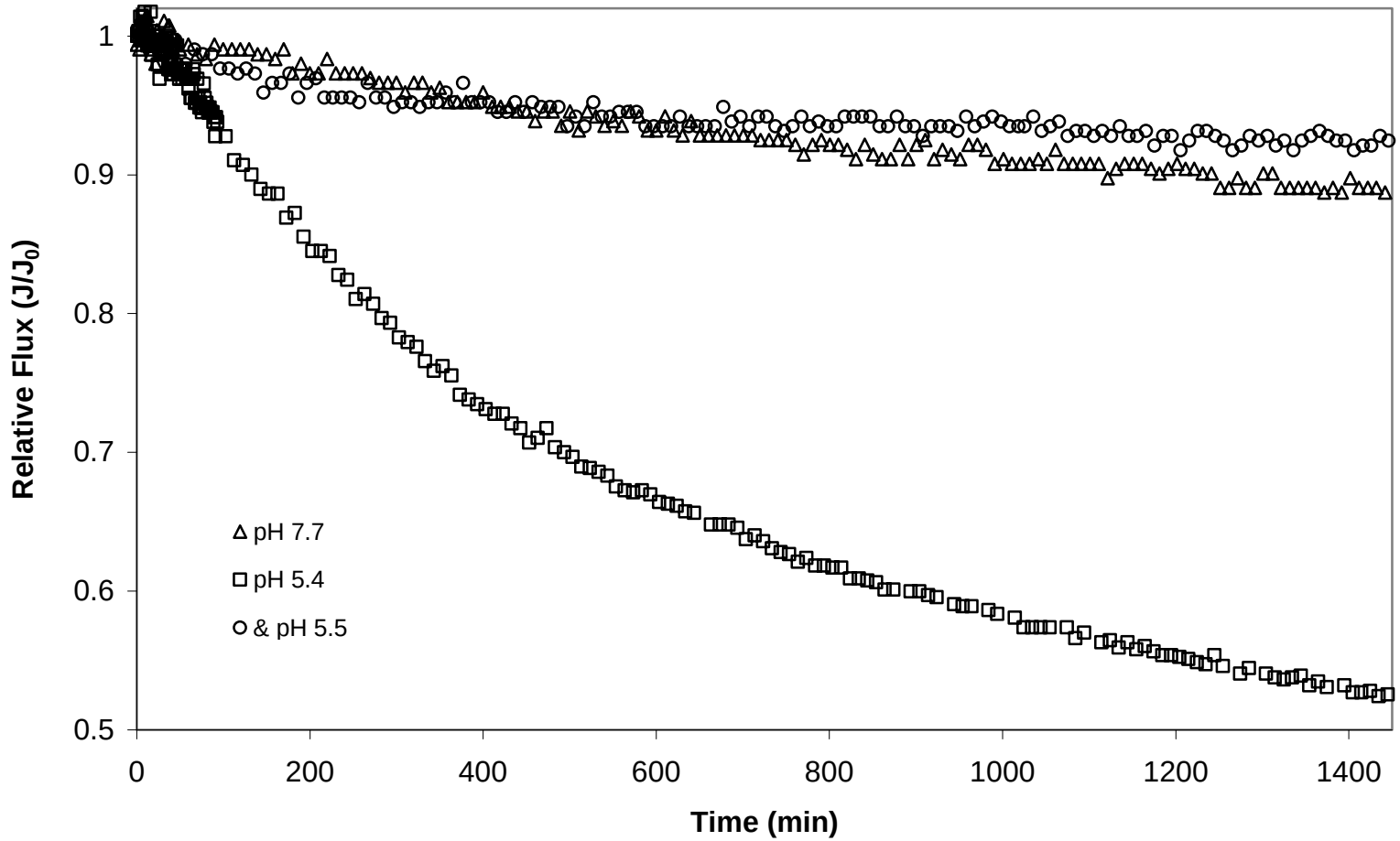

Figure 5-49. Relative permeate flux for diagnostic flux decline experiments for OAS field water sample at: (1) the native pH 7.4: 11.2% 24-hr flux decline, $SI_{G,M0}$ = 2.1, $SI_{C,M0}$ = 5.4, $SI_{S,M0}$ = 0.61; (2) pH 5.5: 47.4% 24-hr flux decline, $SI_{G,M0}$ = 2.1, $SI_{C,M0}$ = 0.014 $SI_{S,M0}$ = 0.66; and (3) pH 5.9 with 0.20 ppm AS: 7.89% 24-hr flux decline: $SI_{G,M0}$ = 2.1, $SI_{C,M0}$ = 0.86, $SI_{S,M0}$ = 0.66.

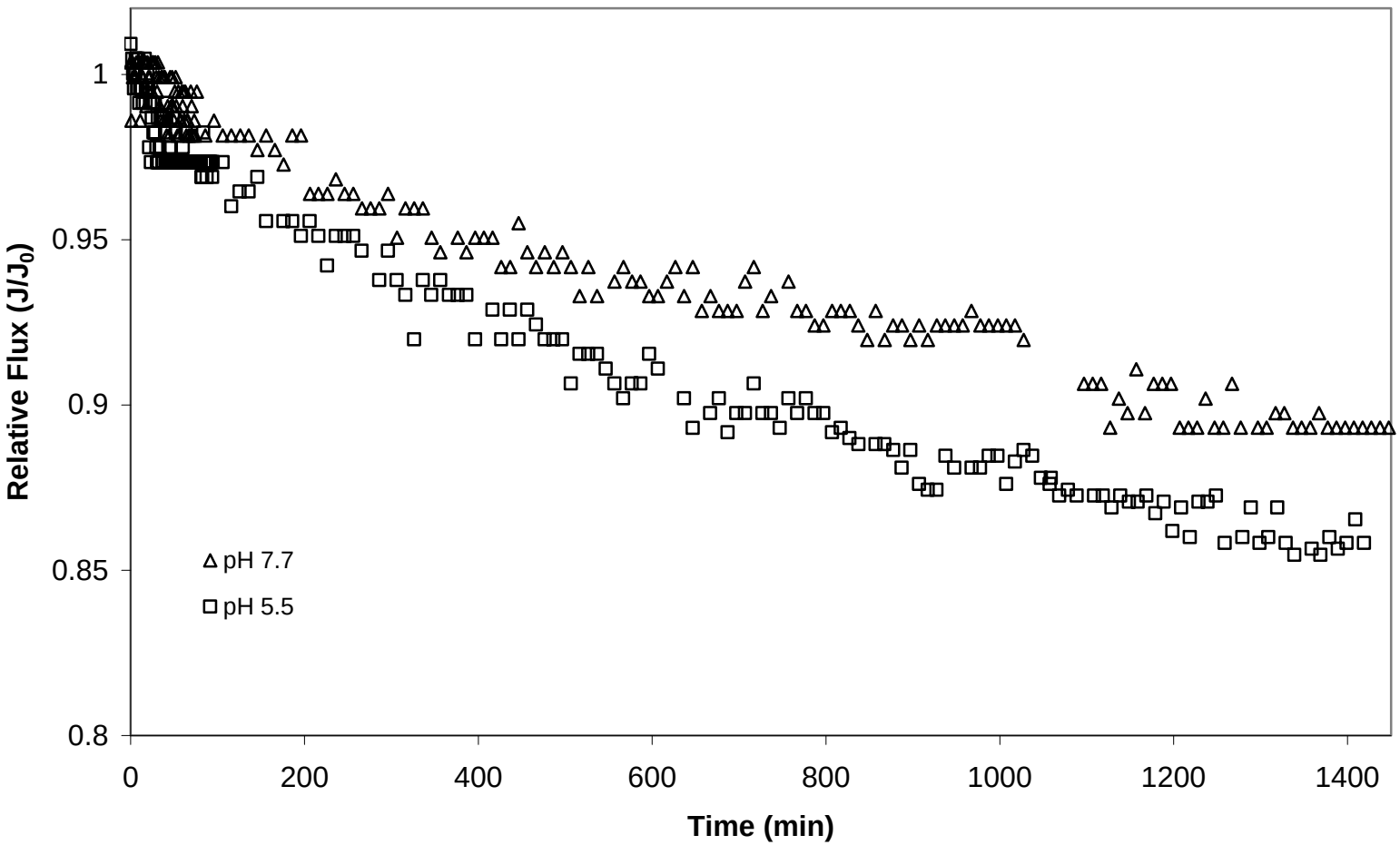

Figure 5-50. Relative permeate flux for diagnostic flux decline experiments for LNW field water sample at: (1) the native pH 7.4: 10.7% 24-hr flux decline, $SI_{G,M0}$ = 1.9, $SI_{C,M0}$ = 4.2, $SI_{S,M0}$ = 0.64; and (2) pH 6.4: 14.2% 24-hr flux decline, $SI_{G,M0}$ = 1.9, $SI_{C,M0}$ = 0.37, $SI_{S,M0}$ = 0.68.

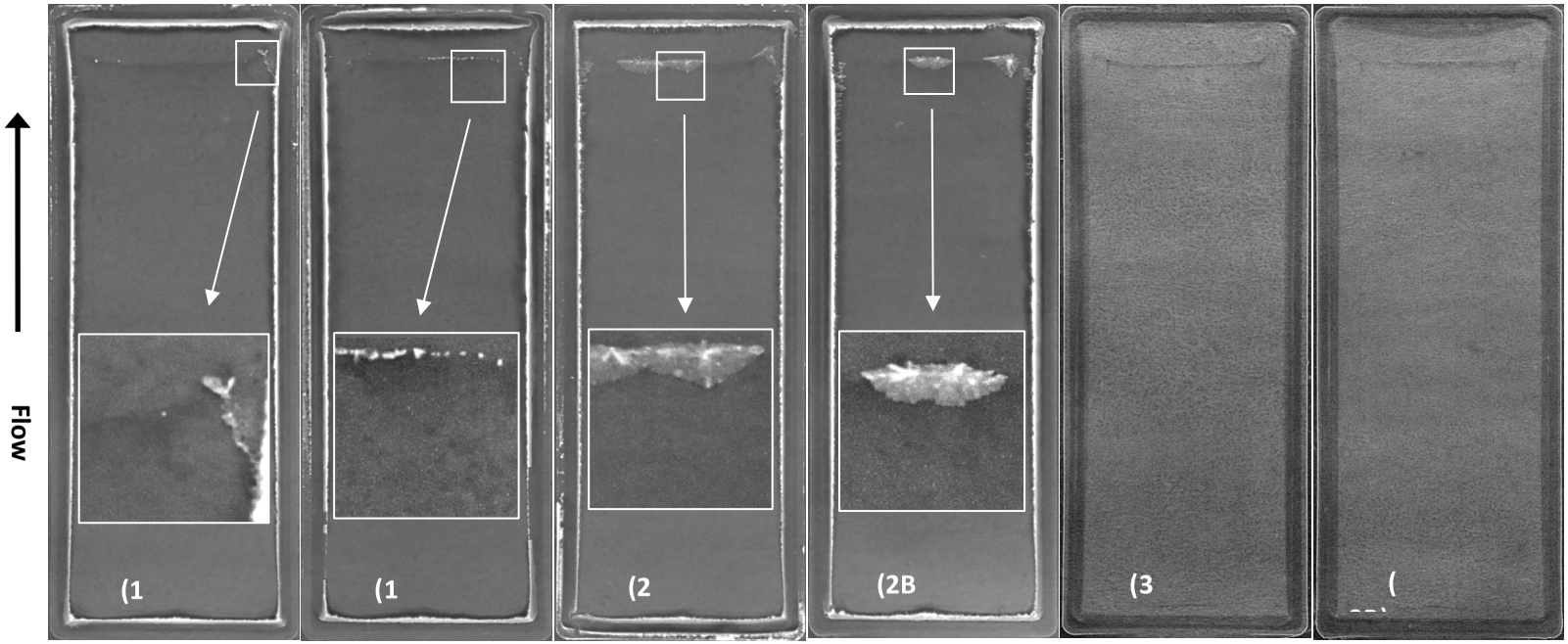

Figure 5-51. Membrane coupons after 24-hour flux decline run with CNR field water at (1), the natural pH 7.50 (2), pH 5.27, and (3) pH 6.00 with 0.20 ppm AS. Note: “A” and “B” indicate the test cell in which the coupon was placed

Figure 5-52. Membrane coupons after 24-hour flux decline run with ERR field water at (1) the natural pH 8.02, (2) pH 5.37, and (3).pH 6.00 with 0.20 ppm AS. Note: “A” and “B” indicate the test cell in which the coupon was placed

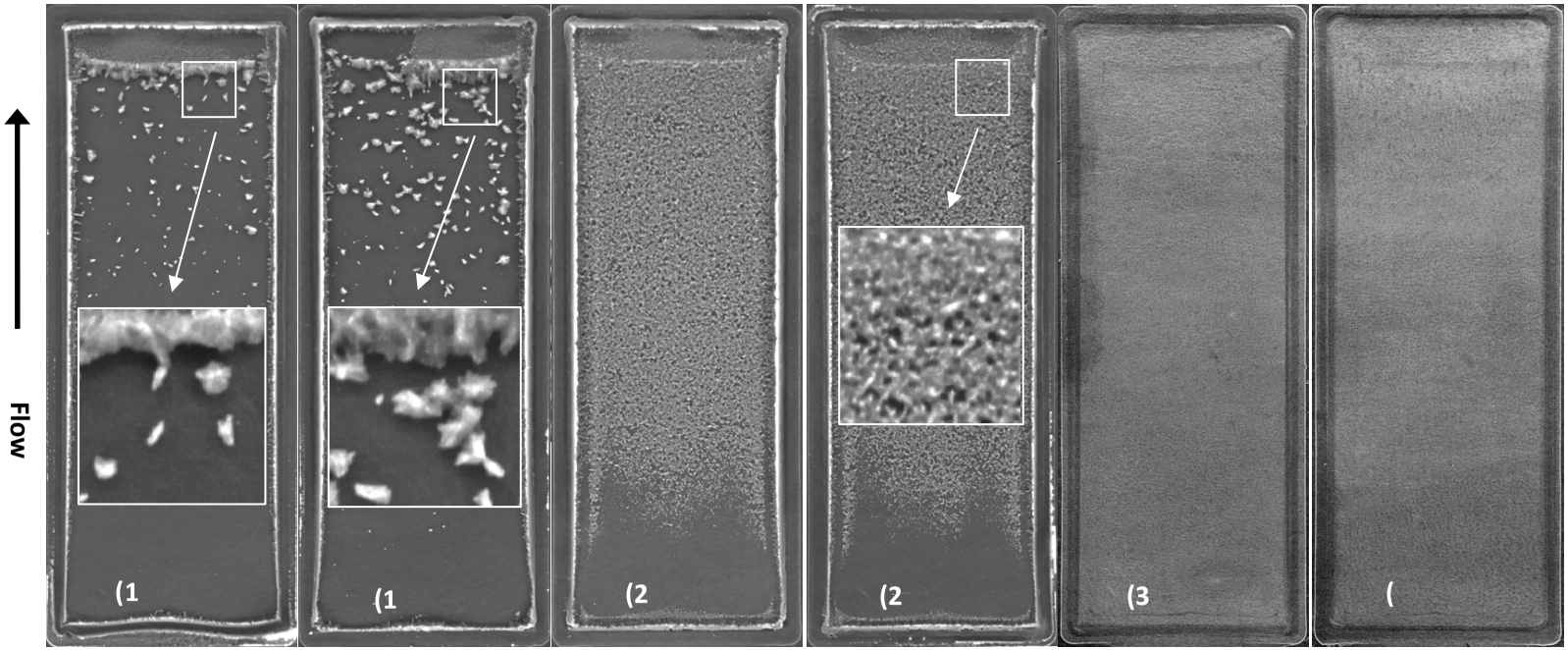

Figure 5-53. Membrane coupons after 24-hour flux decline run with OAS field water at (1) the natural pH 7.42, (2) low pH 5.47, and (3) pH 5.94 with 0.20 ppm AS. Note: “A” and “B” indicate the test cell in which the coupon was placed

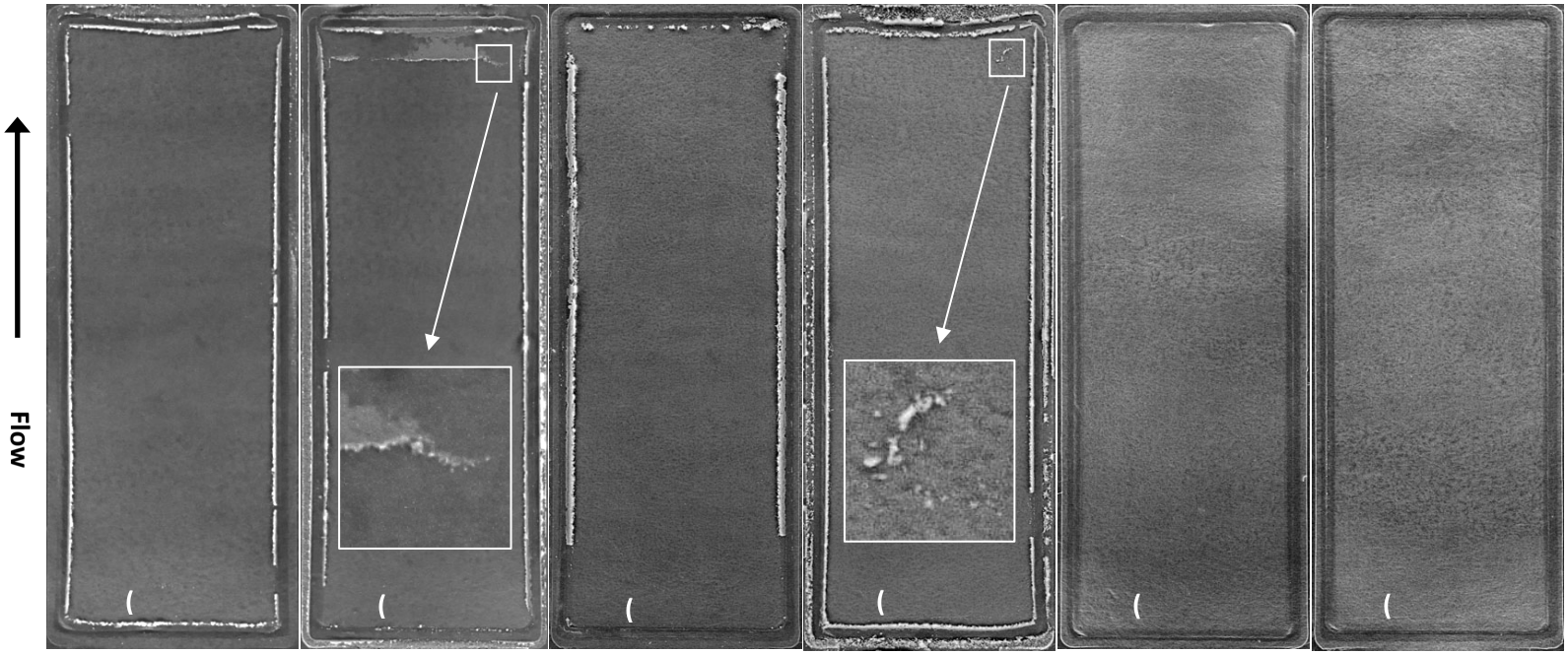

Figure 5-54. Membrane coupons after 24-hour flux decline run with VGD field water at (1)natural pH, 7.53 (2) pH 5.56, and (3) pH 5.93 with 0.20 ppm AS. Note: “A” and “B” indicate the test cell in which the coupon was placed

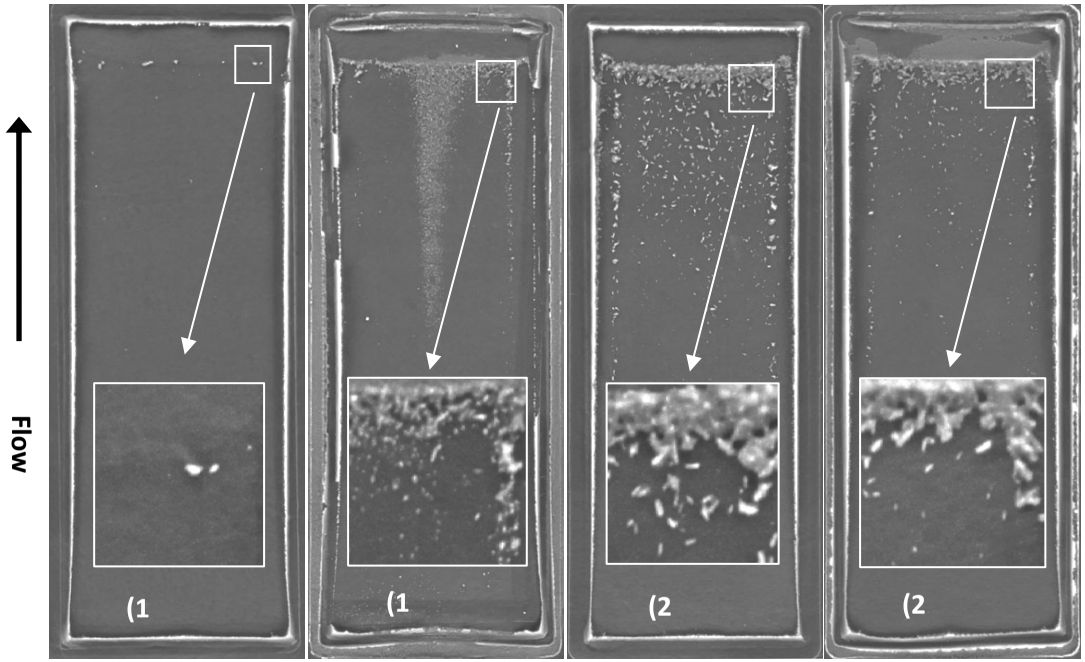

Figure 5-55. Membrane coupons after 24-hour flux decline run with LNW field water at: (1) the natural pH7.42, and (2) pH 6.48. Note: “A” and “B” indicate the test cell in which the coupon was placed

As can be seen in the membrane images (Figures 5-51–5-55) at least one of the three diagnostic runs for each field water sample displayed some degree of visible scaling after 24 hours, even though in some instances the scale only appears in the recirculation regions around the perimeter of the membrane coupons. It is noted that in recirculating regions in the present RO cell [26] the mass transfer coefficient for surface-bulk transport is significantly reduced thereby increasing the level of concentration polarization in these regions. Scale is visible only outside the recirculation regions within 24 hours when the initial average gypsum saturation index at the membrane surface, $SI_{M,G}$, is 1.55 or greater as can be seen for field water from CNR, LNW, and OAS. The degree to which the membrane coupons were visually scaled increased with increasing $SI_{M,G}$ both for membranes with and without visible scale in the recirculation regions and followed in order from least to most scale present: ERR, VGD, CNR, LNW, and OAS, with corresponding $SI_{M,G}$ values of 0.307, 1.43, 1.55, 1.94, and 2.10, respectively. None of the runs with antiscalant exhibited any degree of visible scaling.

At the reduced pH the flux decline after 24 hours increased with increasing initial $SI_{M,G}$ for each water source except for water from ERR (see Figures 5-46–5-50 and Table 5-7). The four runs that followed this trend were: VGD, CNR, LNW, and OAS with corresponding 24-hour flux declines of 8.88%, 11.0%, 14.2%, and 47.4%, respectively and $SI_{M,G}$ values of 1.43, 1.55, 1.94, and 2.10, respectively. ERR had a 24-hour flux decline of 11.6% and gypsum SI of 0.307. One possible reason that ERR did not follow the above trend is because of an unidentified component that gave the water sample a light yellow-brown translucent coloring which is thought to be responsible for staining the membrane as is visible in Figure 5-52.

At the natural pH the 24-hour flux decline is also observed to increase with increasing $SI_{M,G}$ for CNR, LNW, and OAS with flux declines of 6.37%, 10.7%, and 11.2% and $SI_{M,G}$ values of 1.53, 1.93, and 2.08, respectively (Figures 5-46–5-50 and Table 5-7). This trend was not observed for the two runs with the lowest $SI_{M,G}$ values, ERR and VGD which had flux declines of 12.4% and 7.96%, and $SI_{M,G}$ values of 0.280 and 1.42, respectively.

5.3 Biofouling Potential and Particulates

The biofouling potential was determined by performing a protein assay on each field water sample as an indirect measure of protein producing microbes present and by incubating each sample in a rich medium for 24 hours. A standard absorbance curve of known protein concentrations was produced using BSA. None of the field water samples had protein concentrations significantly greater than a blank sample of deionized water. There were also no detectable microbial colonies present for

any of the field water samples after incubation on rich substrates. Therefore, it is reasonable to assume that the AD water sources evaluated in this study are of low biofouling potential. Nonetheless, one would have to employ standard feed water pretreatment (e.g. media filtration) in order to remove microorganisms [12, 22, 23, 29]. Standard feed water pretreatment also removes particulate matter that would otherwise plug RO membranes and the filtration series utilized in the present study (5 µm followed by 0.2 µm) sufficed to prevent plugging.

6. CONCLUSIONS AND RECOMMENDATIONS

6.1 Conclusions

1. Agricultural drainage water in the San Joaquin Valley exhibits a large degree of both seasonal and geographical variation in water quality. The reported TDS levels at specific locations varied annually by 12% (LNW) to 52% (OAS) and the average annual TDS varied by as much as a factor of five from one location in the valley to another (23,480 mg/L at VGD compared to 4690 mg/L at ERR). Both the TDS and the composition of the water can change significantly with time. These variations must be considered when designing RO desalination plants by allowing for a wide range of operating conditions to have the flexibility to effectively manage mineral salt scaling at any foreseeable feed water quality. The above analysis also suggests that a distributed system of RO desalination facilities may be the preferred approach given the variability in water quality throughout the San Joaquin Valley.

2. pH adjustment in conjunction with antiscalant addition was found to be sufficient to prevent visible scale formation and significant flux decline (less than 10%) within the 24-hour test period. Given the relatively low antiscalant dosage used (0.20 ppm compared to 5 ppm or greater doses commonly used industrially) in the diagnostic runs, there is room for pH adjustment and antiscalant addition can be optimized for field scale agricultural drainage water desalination plants in the San Joaquin Valley.

3. Based on field water samples, with the use of pH adjustment and antiscalants, the recovery limits range from 53.6% to 68.2% with LNW, VGD, OAS, ERR, and CNR having recovery limits of

53.6%, 54.9%, 57.9%, 63.4%, and 68.2%, respectively. Considering that all of the field water samples have the potential to scale RO membranes at some critical recovery level, even with the use of pH adjustment and antiscalant addition, the feasibility of RO desalination would likely be dictated by economic and/or policy considerations.

4. The recovery limits determined from theoretical analysis of water quality measurements were consistent with the diagnostic flux decline tests. The latter tests indicated achievable recovery limits with the use pH adjustment and antiscalants that were greater than 38% for VGD; 53% for ERR, CNR, and OAS; and 45% for LNW.

5. In order to achieve enhanced recoveries greater than about 68% for the best case (CNR) and 54% for the worst case (LNW), demineralization of scale precursors must be incorporated into the RO process (e.g. removal of calcium and/or silica).

6. Although biofouling was not determined to be of significant concern for the source water locations evaluated in the present study, field studies over a reasonable period will be needed to assess the potential for biofouling during the different seasons.

6.2 Recommendations

1. The possibility of alleviating the recovery limit constraints via the use of flow-reversal should be explored as this approach would also lower the cost of water production by reducing the required antiscalant dosage.

2. An economic analysis of full-scale RO desalination plants in the SJV should be undertaken utilizing the results of the present study to establish overall design parameters. This evaluation should compare the costs of various RO process configurations as well as the potential use of inter-stage demineralization to achieve high recovery.

3. Pilot-scale studies are needed at selected locations to verify operational recovery limits and specific RO plant dynamic control strategies.

7. REFERENCES

1. *Evaluation of the 1990 Drainage Management Plan for the Westside San Joaquin Valley, California*. 2000, San Joaquin Valley Drainage Implementation Program and University of California Ad Hoc Coordination Committee.
2. *San Joaquin Valley Drainage Monitoring Program 2000*. 2003, State of California, Department of Water Resources.
3. Clinton Williams, M.A., *Agricultural Drainage in the San Joaquin Valley: A Gap Analysis*. 2002, San Joaquin Valley Drainage Implementation Program.
4. *Desalination Demonstration Report for Buena Vista Water Storage District.* 2003.
5. Gao, S., et al., *Chemical status of selenium in evaporation basins for disposal of agricultural drainage.* Chemosphere, 2007. **69**(4): p. 585-594.
6. Gorenflo, A., J.A. Redondo, and F. Reverberi, *Basic options and two case studies for retrofitting hollow fiber elements by spiral-wound RO technology.* Desalination, 2005. **178**(1-3): p. 247-260.
7. Al-Mobayed, A.S., F.M. Mubeen, and S. Balaji, *Comparison of the performance of hollow fine fiber and spiral-wound membranes in the Al-Jubail SWRO desalination plant.* Desalination, 2005. **178**(1-3): p. 273-286.
8. Polasek, V., S. Talo, and T. Sharif, *Conversion from hollow fiber to spiral technology in large seawater RO systems -- process design and economics.* Desalination, 2003. **156**(1-3): p. 239-247.
9. *Agritech Smartwater: Wellington Dam Water Recovery Project*. 2006 [cited 2007 October 15, 2007]; Available from: http://www.agritechsmartwater.com.au/agritech_smartwater_reverse_osmosis_process.htm.
10. Zydney, A.L., *Stagnant film model for concentration polarization in membrane systems.* Journal of Membrane Science, 1997. **130**(1-2): p. 275-281.
11. *Selection of Candidate Sumps to Determine Critical Membrane Desalination Process Requirements*. 2004, California Department of Water Resources.
12. ASTM-International, *ASTM D4189-07 Standard Test Method for Silt Density Index (SDI) of Water.* 2007. **11.01**.
13. Hydranautics, *LFC1 Membrane Element Spec Sheet*. 2003.
14. Andi Rahardianto, et al. *High recovery desalination of agricultural drainage water: integration of accelerated chemical precipitation with RO membrane desalination*. in *Proceedings of the AIChE Annual Conference*. 2005. Cincinnati, OH.
15. Brian C McCool, et al. *Technical and Economic Feasibility of Reverse Osmosis Reclamation of Agricultural Drainage Water in the San Joaquin Valley*. in *Proceedings of the AIChE Annual Conference*. 2006. San Francisco, CA.
16. Hasson, D., A. Drak, and R. Semiat, *Inception of CaSO4 scaling on RO membranes at various water recovery levels.* Desalination, 2001. **139**(1-3): p. 73-81.
17. Rahardianto, A., et al., *High recovery membrane desalting of low-salinity brackish water: Integration of accelerated precipitation softening with membrane RO.* Journal of Membrane Science, 2007. **289**(1-2): p. 123-137.
18. Uchymiak, M., et al., *A novel RO ex situ scale observation detector (EXSOD) for mineral scale characterization and early detection.* Journal of Membrane Science, 2007. **291**(1-2): p. 86-95.
19. Gabelich, C.J., et al., *High-recovery reverse osmosis desalination using intermediate chemical demineralization.* Journal of Membrane Science, 2007. **301**(1-2): p. 131-141.
20. Boerlage, S.F.E., et al., *The scaling potential of barium sulphate in reverse osmosis systems.* Journal of Membrane Science, 2002. **197**(1-2): p. 251-268.
21. Patzay, G., et al., *Modeling of scale formation and corrosion from geothermal water.* Electrochimica Acta, 1998. **43**(1-2): p. 137-147.

22. Flemming, H.C., et al., *Biofouling--the Achilles heel of membrane processes.* Desalination, 1997. **113**(2-3): p. 215-225.
23. Herzberg, M. and M. Elimelech, *Biofouling of reverse osmosis membranes: Role of biofilm-enhanced osmotic pressure.* Journal of Membrane Science, 2007. **295**(1-2): p. 11-20.
24. Hydranautics, *Chemical Pretreatment of RO/NF, Technical Application Bulletin No. 111 Rev. B*. 2003.
25. Ning, R.Y., *Discussion of silica speciation, fouling, control and maximum reduction.* Desalination, 2002. **151**: p. 67-73.
26. Lyster, E. and Y. Cohen, *Numerical study of concentration polarization in a rectangular reverse osmosis membrane channel: Permeate flux variation and hydrodynamic end effects.* Journal of Membrane Science, 2007. **303**(1-2): p. 140-153.
27. Rahardianto, A., et al., *Diagnostic characterization of gypsum scale formation and control in RO membrane desalination of brackish water.* Journal of Membrane Science, 2006. **279**(1-2): p. 655-668.
28. Boerlage, S.F.E., et al., *Stable barium sulphate supersaturation in reverse osmosis.* Journal of Membrane Science, 2000. **179**(1-2): p. 53-68.
29. Lee, R.-W., et al., *Low-pressure RO membrane desalination of agricultural drainage water.* Desalination, 2003. **155**(2): p. 109-120.
30. Andi Rahardianto, et al., *RO Desalination of Brackish Water: Kinetic Interactions in gypsum dominant scale formation and control.* Water Research, 2007. **Accepted**.
31. James Au, et al. *Kinetics of RO Membrane Scaling in the Presence of Antiscalants*. in *AIChE Annual Conference*. 2007. Salt Lake City, Utah.
32. Kurt Kovac, et al., *Drainage water samples and laboratory reports*, Brian C McCool and Y. Cohen, Editors. 2006-2007: Los Angeles, CA.
33. Shih, W.-Y., et al., *Morphometric characterization of calcium sulfate dihydrate (gypsum) scale on reverse osmosis membranes.* Journal of Membrane Science, 2005. **252**(1-2): p. 253-263.
34. Chong, T.H. and R. Sheikholeslami, *Thermodynamics and kinetics for mixed calcium carbonate and calcium sulfate precipitation.* Chemical Engineering Science, 2001. **56**(18): p. 5391-5400.
35. He, S., J.E. Oddo, and M.B. Tomson, *The Nucleation Kinetics of Barium Sulfate in NaCl Solutions up to 6 m and 90ºC.* Journal of Colloid and Interface Science, 1995. **174**(2): p. 319-326.